



Montanuniversität Leoben
Department Petroleum Engineering
Chair of Reservoir Engineering



Development of Integrated Production Model of WIDE Northern Oil Fields

MSc Thesis

Written by Peter Kronberger, BSc
MSc Student in Reservoir Engineering

Supervisor

Holger Ott,
Univ.-Prof. Dipl.-Phys. Dr.rer.nat.
Head of Chair of Reservoir Engineering

Peter Dabrowski, Stefan Salchenegger, Anna Langholf, Olawale Ibrahim Ajala, Manuel Zarfl, Torben Sander, Boris Roggelin

Wintershall Holding GmbH,

Barnstorf

August, 2016

Barnstorf, Germany

1 Proof Sheet for Thesis Submission

Name of MSc student: Peter Kronberger, BSc
Matriculation number: 1135254
Title of MSc Thesis: Development of Integrated Production Model of WIDE Northern Oil Fields

EIDESSTÄTTLICHE ERKLÄRUNG

„Ich erkläre an Eides statt, dass ich die vorliegende Arbeit selbständig und ohne fremde Hilfe verfasst, andere als die angegebenen Quellen und Hilfsmittel nicht benutzt und mich auch sonst keiner unerlaubten Hilfsmittel bedient habe.“

AFFIDAVIT

„I hereby certify that I am the sole author of this thesis. I certify that, to the best of my knowledge, my thesis does not infringe upon anyone’s copyright nor violate any proprietary rights and that any ideas, techniques, quotations or any other material from the work of other people included in my thesis, published or otherwise, are fully acknowledged in accordance with standard referencing practices.“

Germany, August 31, 2016

.....
Signature of MSc Student
Peter Kronberger, BSc

THE MSc THESIS HAS BEEN SUBMITTED ON,

.....
Administration of Department of Petroleum Engineering
Montanuniversität Leoben, Austria

2 Blocking Note

The following master thesis must not be read by a third party.

This Master's thesis includes internal and confidential information of Wintershall Holding GmbH. The full or partial disclosure of its content and any attached drawings or data is prohibited. No copies or transcripts, including digital ones, may be made.

Exceptions require the explicit permission of Wintershall Holding GmbH and the author, Peter Kronberger.

3 Acknowledgement

I would like to gratefully thank my advisors and mentors from Wintershall Peter Dabrowski, Stefan Salchenegger, Anna Langhof, Olawale Ibrahim Ajala, Manuel Zarfl, Torben Sander and Boris Roggelin, who always supported me with valuable information, proper techniques and had an open ear at any time in the development process of my thesis. Their help and guidance throughout the whole work meant a lot for me.

I would also thank Holger Ott, Univ.-Prof. Dipl.-Phys. Dr.rer.nat., who guided me from the very beginning continuously through the thesis. He always had time for me and supported me with precious hints and information to improve this thesis.

Last but not least, I am thankful to my family and friends for their patience, when I was overwhelmed with the work of the thesis.

Table of Content

1	Proof Sheet for Thesis Submission	- 2 -
2	Blocking Note	- 3 -
3	Acknowledgement.....	- 4 -
4	Abstract	- 8 -
5	Kurzfassung	- 9 -
6	Introduction.....	- 10 -
7	History	- 12 -
7.1	Aldorf	- 12 -
7.2	Bockstedt	- 12 -
7.3	Dueste	- 12 -
8	Data Management Structure.....	- 14 -
9	The Back – Allocation Scheme.....	- 16 -
10	Modeling Surface Networks with GAP	- 20 -
10.1	Production System	- 22 -
10.2	Injection System.....	- 23 -
11	Modeling Lift Performance with PROSPER.....	- 25 -
11.1	Production Wells.....	- 25 -
11.1.1	Artificial Lift System Generation	- 26 -
11.1.1.1	Sucker Rod Pumps	- 26 -
11.1.1.2	Progressive Cavity Pumps	- 27 -
11.1.1.3	Electrical Submersible Pumps.....	- 28 -
12	Injection Wells.....	- 30 -
13	Creation of Aldorf Reservoir Model	- 34 -
13.1	Aldorf PVT	- 37 -
13.2	Relative Permeability Curves	- 38 -
13.3	History Matching.....	- 40 -
14	Bockstedt MBAL Model Implementation	- 48 -
15	Dueste Eclipse Model	- 52 -
16	Modeling of Surface Facilities	- 53 -
16.1	Multiphase Pump.....	- 53 -
16.2	Injection Pumps	- 53 -
17	Creation of an Integrated Model with RESOLVE	- 54 -
17.1	Implementation of Application Objects.....	- 55 -
17.1.1	GAP Production and Injection Network	- 55 -
17.1.2	Eclipse Reservoir Simulator for Dueste	- 56 -

17.1.3	Microsoft Excel for Data Transfer Control	- 59 -
18	Data Transfer Overview.....	- 60 -
19	Verification Simulation Runs	- 63 -
19.1	Dueste	- 63 -
19.2	Aldorf	- 65 -
19.3	Bockstedt	- 68 -
19.4	Full Field	- 71 -
20	Full Field Forecasts	- 83 -
20.1	Scenario 1.....	- 83 -
20.2	Scenario 2.....	- 86 -
20.3	Scenario 3.....	- 91 -
20.4	Comparison of Forecast Scenarios.....	- 94 -
21	Areas of Improvement	- 96 -
22	Conclusion and Recommendation.....	- 97 -
23	Nomenclature.....	- 100 -
24	References.....	- 102 -
25	List of Figures.....	- 104 -
26	List of Tables	- 109 -
27	Appendix A	- 111 -
27.1	Well allocation per re-defined compartment in Aldorf	- 111 -
27.2	Aldorf Reservoir and Production Properties.....	- 112 -
27.2.1	PVT Cell Experiment from Aldorf 002 on the 16.06.1953	- 112 -
27.2.1.1	Solution Gas Oil Ratio	- 113 -
27.2.2	Vasquez and Beggs Correlation.....	- 113 -
27.2.2.1	Oil FVF – Saturated	- 113 -
27.2.2.2	Oil FVF - Undersaturated	- 114 -
27.2.3	Layers Petro Physical Parameters	- 114 -
27.2.4	Brine Viscosity Correlation	- 115 -
27.2.5	Parameters for IPR generation in Aldorf.....	- 116 -
27.2.6	PVT Matching in PROSPER field Aldorf.....	- 117 -
28	Appendix B.....	- 118 -
28.1.1	PVT Cell Experiment from Dueste 008 on the 17.02.1955.....	- 118 -
28.1.2	Logs Dueste field	- 119 -
28.1.3	PVT Matching in PROSPER field Dueste	- 124 -
29	Appendix C.....	- 125 -
29.1.1	PVT Cell Experiment from Bockstedt 035 on the 15.03.1961	- 125 -

29.1.2	PVT Matching in PROSPER field Bockstedt.....	- 126 -
29.1.3	Parameters for IPR generation in Bockstedt.....	- 127 -
30	Appendix D	- 128 -
30.1	Simplified Water Saturation Over Time Derivation (Dake, 1978).....	- 128 -
31	Appendix E.....	- 130 -
32	Appendix F.....	- 132 -
32.1	Module for Pipeline Parameter Update	- 132 -
32.2	Module for Full Field Validation Run Output.....	- 134 -

4 Abstract

The three fields Aldorf, Bockstedt and Dueste are producing since almost 65 years into one processing plant in Barnstorf, where the oil production is measured and – based on irregular field measurements – back-allocated to the individual wells. This allocation was perceived to be an error prone activity, as deviations of 30% were observed in 2014.

Therefore, in order to enable cross-checking the data from PDMS and improve the current data situation, the development of an integrated network for the back-allocation of the data began. The integrated model considers not only the irregular liquid rate and water cut measurements, but also important pump characteristic parameters.

The mainly used software were MBAL, GAP, PROSPER and RESOLVE from Petroleum Experts as well as an Eclipse reservoir model.

At first the whole pipeline network was built in GAP, and PROSPER models were created for each individual well. The reservoir representation for Dueste was provided by an Eclipse model. The Bockstedt reservoir is represented by two MBAL models, because of its complexity. Both had to be properly adjusted and finally connected to the GAP systems. The Aldorf field had no representative MBAL or Eclipse model. Therefore, it was re-analyzed, set up as an MBAL model and finally history matched. For a faster data transfer of results and input parameters, various Microsoft Excel macros with an OpenServer connection were created. Ultimately, all modelled tools were put together in RESOLVE and properly adjusted to each other to achieve consistency. Relative permeability curves, designed with a Brooks Corey model for each production well, were used as tuning parameters to get satisfying fits of the rates. Furthermore, mainly near wellbore permeability changes and skin adjustments were performed to match the injection rates.

The fully integrated model showed good results for the back-allocated liquid rates per field after a verification simulation. The achieved deviations between the model and the PDMS by the end of 2015 were 3.0% for Aldorf, 2.7% for Bockstedt and for Dueste 2.4%. Compared to the sum per field of the well testing units, the differences in Aldorf were -16.2%, -9.3% in Bockstedt and -6.5% in Dueste. Furthermore, three short-term forecast scenarios until the end of 2020 were created to show the predictive functionality of the model.

The verification runs showed the over-estimating of the field measurements quite clearly. It was found out that on a field and compartment level more precise matches were achieved than on the individual well basis and that the relative permeability curves are very sensitive as the average water cut over all three fields is with 96% already at an extremely high stage. Keeping in mind that two fields are based on multi-tank material balance, the results achieved provide a reasonable cross-checking tool for the PDMS and for creating various prediction scenarios for sensitivity studies.

5 Kurzfassung

Die drei Erdölfelder Aldorf, Bockstedt und Dueste produzieren seit beinahe 65 Jahre in eine Aufbereitungsanlage im Betrieb Barnstorf, wo die Ölproduktion gemessen und auf Basis von unregelmäßigen Messungen in den Feldern auf die einzelnen Bohrungen zurückgerechnet wird. In dieser Rückrechnung wurden massive Abweichungen von 30% im Jahr 2014 beobachtet.

Deshalb wurde die Entwicklung eines integrierten Netzwerkes für die Rückrechnung begonnen um eine Überkreuzprüfung der Daten des PDMS und eine Verbesserung der Datensituation zu erlangen. Das Modell berücksichtigt neben den unregelmäßigen Messungen der Flüssigkeitsraten und Wasseranteile auch wichtige pumpspezifische Parameter.

Für diesen Zweck wurden die Softwaretools MBAL, GAP, PROSPER und RESOLVE von Petroleum Experts, sowie der Eclipse Simulator benutzt.

Zu Beginn wurde das Leitungsnetzwerk mit GAP und PROSPER Modelle für jede Bohrung erstellt. Die Darstellung der Lagerstätte in Dueste wurde durch ein Eclipse Modell zur Verfügung gestellt. Aufgrund der Komplexität des Feldes Bockstedt wurden zwei MBAL Modelle, welche zur Verfügung gestellt wurden, angewendet. Diese wurden angepasst in das GAP System eingebunden werden. Die Aldorf Lagerstätte besaß weder ein MBAL noch ein Eclipse Modell. Deshalb wurde das Feld neu analysiert, ein MBAL Modell aufgesetzt und letztlich ein History Matching durchgeführt. Um einen schnelleren Datentransfer der Resultate und Input Parameter zu gewährleisten wurden verschiedenen Microsoft Excel Makros mit OpenServer Verbindungen erstellt. Letztlich wurden alle Tools in RESOLVE zusammengeführt und angepasst. Die mit einem Brooks Corey Modell erstellten Relative Permeabilitätskurven für die Produktionsbohrungen wurden als Tuningparameter benutzt um Übereinstimmungen der Raten zu erreichen. Größtenteils wurde die Permeabilität in der Nähe der Bohrung verändert sowie der Skin Faktor angepasst um mit den gemessenen Injektionsraten Übereinstimmungen zu finden.

Das integrierte Modell zeigte gute Resultate für die Rückrechnung der Flüssigkeitsraten für die einzelnen Felder in den Überprüfungssimulationen. Die Abweichungen Ende 2015 zwischen dem Modell und den rückgerechneten Werten des PDMS betragen für Aldorf 3.0%, für Bockstedt 2.7% und für Dueste 2.4%. Verglichen mit den aufsummierten Werten der Feldmessungen pro Feld betragen die Unterschiede für Aldorf -16.2%, für Bockstedt -9.3% und für Düste -6.5%. Auch drei kurzfristige Prognosen bis Ende 2020 wurden simuliert um die vorhersagende Funktionalität des Modells aufzuzeigen.

Die Überprüfungssimulationen zeigten die Überschätzung der Feldmessungen klar auf. Auf Feld- und Kompartimentebene konnten genauere Übereinstimmungen als auf Bohrungsebene erreicht werden. Sehr sensitiv reagierten die Relativ Permeabilitätskurven auf Veränderungen, da auch der durchschnittliche Wasseranteil über alle Felder bereits bei 96% liegt. Beachtet man, dass zwei Lagerstätten auf Materialbilanzen basieren, so sind die erreichten Resultate sehr zufriedenstellend und ermöglichen eine vernünftige Überkreuzprüfung des PDMS sowie die Erstellung von verschiedenen Feldstudien.

6 Introduction

The three oil fields Aldorf, Bockstedt and Dueste are producing into one common processing plant at WIDE Barnstorf where the oil production is measured and back allocated to each individual well in the field. This calculation is currently performed with the production data monitoring system (PDMS) using well checker, which are well testing units for liquid rate measurements, and irregular water cut measurements but without considering important well information like well head pressure, pump speed, surface stroke length or temperatures. Therefore, it can be observed that the back-allocated data in the PDMS show a great range of uncertainty, which makes further processing and analyzing studies more error-prone.

The development of an integrated network for the back-allocation of the data would improve the current data situation significantly. It would enable cross-checking the data from the PDMS and would give a better understanding of the behavior from a macroscopic point of view of the fields and in a next step of each individual well. Beside more precise full field forecasts, because of a reduced range of uncertainty, it will help to react faster and more efficient on changes in the fields – subsurface as well as surface.

Petroleum Experts integrated production monitoring (IPM) software package enables the integration of all fields and processing facilities into a common system, which can also be linked to external applications such as reservoir simulation programs for a fully integrated model to optimize field production. Setting up such a system enables integrated production forecasting including subsurface simulation results and surface facilities limitations. In order to reach that, the existing data must be gathered from different data systems such as FIX (which is currently migrated to a new version called IFIX), which data is saved in the ACRON database. Moreover, field analyses such as well checker and water cut measurements, saved in reports and the PDMS and Finder database. These data have to be validated, properly processed and integrated into the new model. This set up of a new fully integrated model will include the entire Petroleum Experts IPM suite, Schlumberger Eclipse 100 reservoir simulator and Microsoft Excel.

The surface, be it the production or injection network will be modeled based on the latest maps and pipeline data with the GAP software tool. After creating the individual pipeline segments and surface facilities like wellheads and compressors operating in the field, the next step will be to design the lift performance curves for each individual wellbore in the field with PROSPER. The design in PROSPER will require PVT data, deviation survey, downhole equipment and property data of the reservoir near the wellbore area. It is of great importance to collect these data accurately from the individual sources, be it from fluid experiments for the PVT data or log data for near wellbore parameters such as net to gross ratio for the IPR curve. An Eclipse model for the Dueste reservoir that is already history matched will be provided for this thesis. The Bockstedt Eclipse model is currently in the history matching process, so therefore no satisfying Eclipse model for this field is available for this thesis by now. From previous studies of the Bockstedt field, material balance models with MBAL were generated. These Bockstedt MBAL models will be quality checked and evaluated whether a direct implementation is possible or adjustments are necessary. The Aldorf field has no representation of the reservoir yet, be it an Eclipse

or MBAL model. A part of this thesis is to build and history match an MBAL multi tank model for this field from the beginning of pressure data acquisition and the creation of a PVT model. The challenges of setting up a simple representation of the complex Aldorf reservoir in MBAL will be discussed in this thesis.

Finally, after creating, modelling and adjusting these pieces with the various software tools it is necessary to connect all together and therefore the IPM software tool RESOLVE will be used. GAP already provides a seamless implementation of MBAL models and lift curves from PROSPER for the wells, but RESOLVE will act as the main controlling software over the three fields and also as a connection tool for the Dueste Eclipse model and their corresponding wellbores. Furthermore, Microsoft Excel will be used at different stages in the model as an interface between simulation data output, for quality checks of runs and moreover to provide a faster data transfer into the model for instance loading all parameters in the pipeline segments.

The ultimate goals of this thesis are therefore the creation of a fully integrated field model for Aldorf, Dueste and Bockstedt to firstly get a tool for cross checking of the back-allocated PDMS data with the underlying well checker measurements and show the uncertainty of these systems. Moreover, the model should improve the whole data situation and perform forecasts over the whole system more precisely.

An achievement to be gained is the simulation of pressure losses in the pipeline networks to investigate possible bottlenecks in the system and create a system for proactive interventions. A major achievement with the model will be the study of different scenarios and interactions in the field. It will be possible to disable specific injection or production wells, which represents workover operations and to investigate such shutdowns on the field behavior. These analyses would not be possible just on a microscopic wellbore level. It will be possible to represent pipeline failures or blocked pipes, because of failed pigging jobs for instance, where just some parts of a field or even a whole field will be shut down.

The thesis will describe the workflow of creating and adjusting the fully integrated field model for Aldorf, Bockstedt and Dueste, the approach of reaching the underlying goals such as getting a comparison between the databases such as PDMS and the field measurements and achieving more precise full field forecasts for operative planning with uncertainty reductions. Furthermore, premature recognition of bottlenecks can be possible after sufficient adjustment and learning with the network. Strengths, but also occurring problems and weaknesses of such a modelling approach will be discussed and analyzed systematically.

7 History

The fields Aldorf, Dueste and Bockstedt are located in the near neighborhood of the processing plant in Barnstorf. The field Aldorf is approximately 2 km north of the plant in Barnstorf and Bockstedt is located further 4 km to the north of Aldorf. The field Dueste is on the east side of Barnstorf. All three fields are approximately in the same range according to their OOIP and peak reservoir parameters like their porosity and net pay. The permeability of Aldorf is an exception, because it is two order of magnitudes less than the one in Bockstedt and Dueste. All three fields are almost for 65 years in production.

7.1 Aldorf

The field Aldorf was discovered in 1952 with the Aldorf 001 well. The structure is a local high with pinchouts and fault patterns to the northeast with only two reservoirs present, whereas to the southwest up to six different reservoir levels could be recognized in former studies. The main reservoir rock in the southern part is the Dogger sandstone at 1090 m with thickness ranging from 1.0 to 25.0 m. The truncation line forms the eastern boundary of the field. The production wells in the northeast compartment show a great connectivity, which shows that the water breakthrough from the injection to the production well location took place very early. The original oil in place was estimated with 6.0 MM tones, whereas the current recovery factor (31.12.2013) is reported with 40.85% with a specific gravity of the oil between 0.86 to 0.9 g/cm³. In the Aldorf field were 126 wells drilled from these are currently 11 in production and 4 act as injection wells, where the main recovery mechanism is since early days water flooding. Currently, the average water cut in Aldorf is according to the PDMS at 96%. The long production history of the field lead to the point that the reservoir pressure dropped already below its natural flowing capacity and artificial lifting systems such as sucker rod and progressive cavity pumps were installed.

7.2 Bockstedt

Bockstedt was discovered in 1954 by the wellbore Bockstedt 002. The structure of the field is an anticline with a structurally high northeast thrust. The reservoir rock is the upper Valendis sandstone at 1260 m with a thickness ranging from 2.0 to 35.0 m. Due to massive faulting Bockstedt can be separated into several compartments especially in the northern region, where restricted or no communication between the blocks exists. The original oil in place is 6.392 MM tones with a current recovery factor (31.12.2013) of 56.1% tones with a specific gravity of around 0.88 g/cm³. There are 87 drilled wells in Bockstedt where 17 are active producers and 6 as injection wells. Electrical submersible, progressive cavity and sucker rod pumps were installed as artificial lifting systems after natural flow was not guaranteed anymore. The average water cut in the field is 94% according to the PDMS.

7.3 Dueste

This field was discovered in the year 1954 with the well Dueste 008. Structurally Dueste is the northern edge of a huge anticline with many faults that divide the field into several compartments. Not only the various compartments, but also the many different layers make this field a great challenge. The main reservoir rock is similar to the one in the field Bockstedt - the upper Valendis sandstone at 750 m with a thickness range from 2.0 to 20.0 m. The primary depletion was expansion drive, where some parts,

especially in the south of the field, are connected to a big aquifer. This enormous underlying aquifer is expected to act in the Bockstedt field, mainly in the southern part, too. In 1961, the reservoir pressure dropped below the lifting capacity and secondary depletion using water flooding and artificial lifting systems such as sucker rod pumps and progressive cavity pumps have been undertaken. The original oil in place was reported with 5.241 MM tones, whereas the current recovery factor (31.12.2013) is estimated with 34.37% with a specific gravity of 0.87 g/cm³. Dueste has 115 drilled wells out of these are currently 14 in production and 10 act as injectors. The average water cut in the field is with 97% already at a high level.

Table 1 shows a comparison of the field parameters of Aldorf, Bockstedt and Dueste

	Aldorf	Bockstedt	Dueste
First oil	1952	1954	1954
OOIP [MM. t]	6	6.392	5.241
Net Pay [m]	1.0 – 25.0	2.0 – 35.0	2.0 – 20.0
Permeability [mD]	< 750	< 7,000	< 4,000
Porosity [-]	< 0.26	< 0.20	< 0.25
WC [%]	96	94	97
Recovery factor [%]	40.9	56.1	34.4

The Table 1 gives a first overview and comparison of the individual fields, which will be discussed and analyzed in the following chapters. The fields were all discovered approximately 65 years ago and their OOIP ranging from 5.241 to 6.392 MM tones are in the same order of magnitude. The values for permeability and porosity listed in Table 1 are the maximum occurring ones in each field. This should not deceive, as the fields Bockstedt and Dueste are very different in their structure, compartment distribution, interaction and number of layers and production behavior. The long lifetime of the fields led to these high water cuts as can be seen. A minor indicator of the difference in reservoir characteristics and the great structural complexity in Dueste is the recovery factor, which is for the Dueste field lower than compared to Aldorf or even Bockstedt. After a first investigation and insight into the individual reservoirs and their characteristics the uncertainty, validity and processing of the various underlying data will be studied in the following chapter.

8 Data Management Structure

The data reporting system consists of several processing levels, from a real time high frequency system to a low frequency one, which is based on a monthly interval.

The direct connection to the installed measurement tools at the wellsites are given by the IFIX monitoring system. There are several pump performance parameters and pressure gauges broadcasted for production wells and further rate measurements for injection wells. This is the high frequency real time system based on seconds for operators, which also gives alarms if values exceed or fall below certain thresholds.

The next system in the data processing chain is the ACRON management system, which actually saves the data from the IFIX monitoring system. The data in the production data management system (PDMS) is back allocated from liquid level measurements in the tanks behind the separator (Figure 1), as there are no rate measurements installed for each individual production well. It can be further seen in Figure 1 that just the oil and water is measured directly behind the separator on a daily basis, but not the gas phase. The gas is together with additionally bought one mixed and used in the processing plant. It can be already assumed that the recorded gas in the PDMS is a highly uncertain property. The back-allocation itself is based on infrequent, so-called well checker measurements, which were performed directly on the well side to get information about the liquid rate. Further water cut measurements are performed at the well side to evaluate the oil rate too.

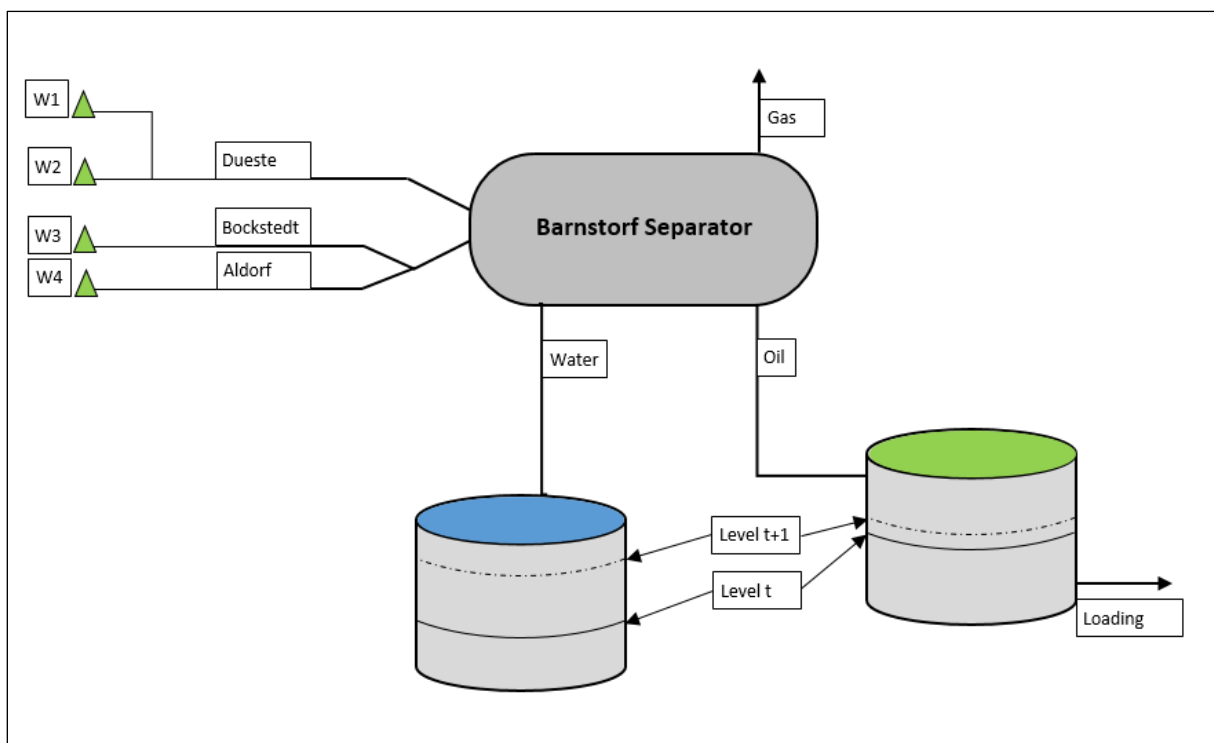


Figure 1 shows the basic scheme of the back-allocation in Barnstorf. The liquid levels in the tanks are measured every day at 6 am to get the production from the previous day. These daily-calculated quantities are then back allocated to each individual well in the field based on the well checker measurements. The brine will be pumped back to the fields through the injection wells and the separated oil is transported away with the railway. As can be further seen the gas is not measured directly behind the separator

Initially the Finder Oracle database was build up for geological data, because of its popularity and easy handling it steadily grew, production data and various field information was started to be stored in this structure as a monthly back-up too. It became a massive data storage with a lot of information. With increasing amounts of data, struggles with the structure started to appear, because continuous maintenance was not given a high priority in all stages of its usage and therefore some data are often redundant, outdated or complex to extract. Data maintenance and consistency as well as redundancy are key factors for improvements at each stage of data processing whether ACRON, PDMS or Finder.

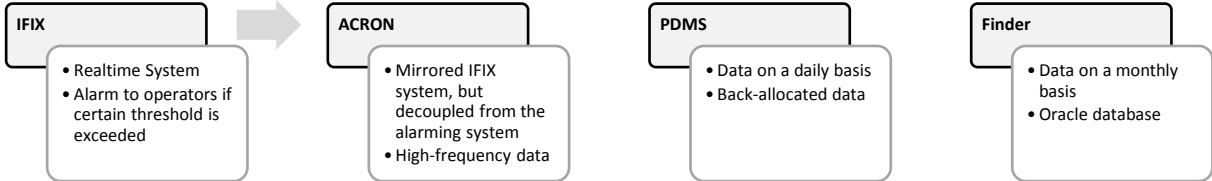


Figure 2 illustrates the data processing and database systems. There are three main databases the ACRON, PDMS and Finder and one operating system the IFIX. The IFIX is for operators and broadcasts real time values from the gauges at the well side and further alerts if limits are reached. This high frequency data is then saved in the ACRON database. Furthermore, the back allocated production data is saved on a daily basis in the PDMS. As a back-up tool the Finder database stores various information, be it production data or of other relevant origin, on a monthly basis.

The main issue and source of error is the back-allocation of rates to each individual well. The discrepancy of the daily-allocated PDMS rates and the values, which were measured in the field on a not continuous basis, can be up to more than 30%. These errors in the back-allocation can further be recognized in selected water cut entries, which sometimes exceed 100% and are therefore not realistic at all. Beside this error in the calculation scheme, further influences like environmental factors that influence the back-allocation and precipitations in pipelines, which are in some segments increased than in others. The uncertainty of the liquid level measurements behind the separator plays a significant role, which is further based on the degree of foaming, distortions at the phase interfaces and precision of the calibration.

9 The Back – Allocation Scheme

The error in the back-allocation process can be quantified when comparing the average daily-allocated oil rates with the oil rates estimated from the well checker and water cut measurements. These well checker measurements are performed not continuously, but every few months per well. The well checker actions are on the one hand the basis for the back – allocation in the PDMS, and show on the other hand when summing up the rates the huge uncertainty of this distribution action. It has to be mentioned that the well checker measurements itself are prone for errors too, as the simultaneously performed water cut measurements are. Influencing factors are for example the opening speed of the valve or time given for the phase separation. Furthermore, when keeping in mind that the water cut of most of the wells is above 90% the oil rim after separation will be very thin, so a good experience is needed to measure these rates properly. In the following Table 2, there are the rates for each field in a row and the measurement system per column from the year 2014. Moreover, the field as well as the measured amount per field is allocated to each active well. It can be realized that the well checker in combination with the water cut measurements show in every field higher amounts of oil than from the summed back-allocation in the PDMS. This deviation of the amounts, even per field, is not in an acceptable range.

Table 2 Comparison of oil rates in Sm³/d per field between the PDMS and well checker measurements in 2014. The well checker measurements highly overestimate the rates.

	PDMS	Well Checker
	<i>[Sm³/d]</i>	<i>[Sm³/d]</i>
Aldorf	15.43	24.45
Bockstedt	41.41	61.60
Dueste	16.62	25.92

When taking the well checker and water cut measurements as a basis and having a look at the deviation it can be realized that, the deviation for the oil rates ranges from 37% for Aldorf, over 32% for Bockstedt to 36% for Dueste.

Beside the overall oil rates of the fields, the liquid rates per well as well as their water cuts where further investigated. To do so, threshold values were estimated to better estimate underlying trends. These limits where defined based on the average values per field from the PDMS as can be seen in Table 3. It can be observed that the average water cuts per field are already on very high levels, for instance with 93.3% in the Aldorf field, which is not a surprise when keeping in mind that each field is in production since almost 65 years. However, although one can recognize that the lowest average water cut is in the Bockstedt field with 72.0%. This is true when applying the arithmetic mean without weighting the rates per well and as can be seen the standard deviation in the Bockstedt field is with 30.2% very high. Due to that deviation and hence the arithmetic mean is quite sensitive to outliers, these lowered average water cut values can be observed. The same effect, but not as severe as in Bockstedt, is the deviation in the field Dueste. Not just the average water cuts, but also the average

liquid rates per field from the PDMS system where analyzed. As it can be seen with the water cuts, the deviation is also very high for the average liquid rates. This data interpretation allowed defining threshold values. Therefore, a high water cut is set to be 90% or higher and high rates as 80 m³/d or higher.

Table 3 shows average water cuts (WC) and liquid rates per field as well as their minimum and maximum values and the standard deviation per property for the year 2014 from the PDMS. Furthermore, the number of encountered production wells for these calculations can be seen at the bottom line.

	Aldorf	Bockstedt	Dueste
Average water cut [%]	93.3	72.0	84.5
Minimum water cut [%]	82.1	1.1	11.0
Maximum water cut [%]	98.7	98.5	98.4
Standard deviation [%]	5.1	30.2	22.7
Average liquid rate [m³/d]	37.5	58.8	42.4
Minimum liquid rate [m³/d]	15.3	1.1	1.0
Maximum liquid rate [m³/d]	97.3	237.2	138.1
Standard deviation [m³/d]	26.6	65.5	40.7
Active producers encountered	11	14	16

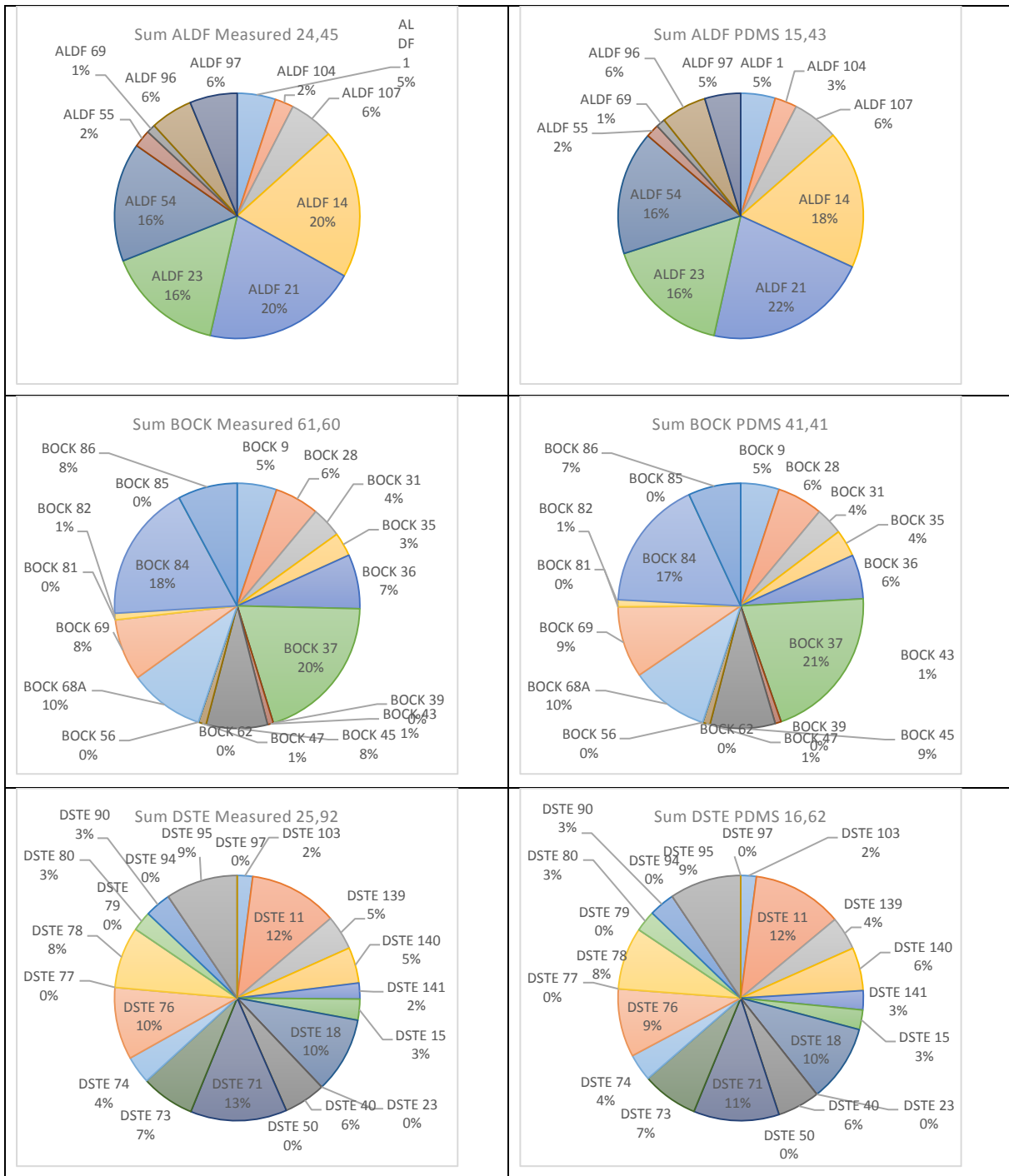


Figure 3 shows pie charts, which compare the well checker rates (left column) with the PDMS rates (right column) per field and the distribution of the rates for each production well. It can be observed that the error per well for the oil rate between the PDMS and the well checker measurements is not high for any individual well (maximum of 3%).

The next step after defining threshold values was to investigate the deviation on a well level with the aim to recognize trends in the error. It is important to know, also on a later stage of simulation, whether the error increases with lower rates or maybe higher water cuts. For this purpose, a classification of the active production wells was performed as can be seen in Table 4. One well was selected for each of the four cases for better illustration.

Table 4 shows the classification matrix for active producers. It was separated between high and low water cuts and liquid rates over all fields. The limit for the water cut as previously defined is set to 90% and for the liquid rate to 80 m³/d.

	Low average WC [%]	High average WC [%]
Low average liquid rate [m³/d]	BOCK 31	DSTE 15
High average liquid rate [m³/d]	BOCK 68a	DSTE 40

Table 5 lists the average water cut (WC) and average liquid rate per chosen well

Well	Average WC [%]	Average liquid rate [m³/d]
BOCK 31	38.6	2.5
DSTE 15	97.0	23.6
BOCK 68a	74.0	23.4
DSTE 40	98.4	87.9

It can be observed that Bockstedt 068a, which is intended to have a high average liquid rate previously defined as 80 m³/d, is not in that range. There was no active wellbore found with rates higher than the defined threshold and a water cut lower as previously set. A compromise was chosen and the next best well for that position was selected.

As a result, it was found out that the influence of the liquid rate to the back-allocation error is by far not as strong as the magnitude of the water cut. The lower the water cut of a well the higher the deviation between the PDMS values and the measured values will be. This can be explained as that the back-allocation system uses a weighted arithmetic mean based on the rates and further accounts the downtimes of the production wells. Most wells have a water cut greater than 90% and outliers with a lower actual water cut will hence be miscalculated. This can be clearly seen in the diagrams with the selected wells in Appendix E, which directly compares the water cuts and liquid rates from the PDMS with the well checker measurements from 01.04.2014 to 31.12.2014.

In the wells Dueste 040 and Dueste 015, because of the massive water cut, the error between the measured and the back-allocation is very low, although Dueste 040 has almost a factor of four higher rates than Dueste 015. Having a look at the diagram of Bockstedt 031 the deviation between the PDMS and the measured values is much greater. A further unacceptable issue is the fact that some back-allocation actions in the PDMS are not in a physical range anymore. This can be seen when water cut values tend to exceed 100%. This effect of such unrealistic water cuts can be observed in the charts in

Appendix E in November 2014. Those extreme and unrealistic calculation errors are not on a regular basis, but they have to be removed, as they distort the whole data interpretation workflow.

10 Modeling Surface Networks with GAP

As a first step and basis in creating an integrated model of Aldorf, Bockstedt and Dueste the pipeline network for the production as well as the injection system was built in GAP. GAP is the 'General Allocation Package', which allows modeling, solving and optimizing production as well as injection networks for multiphase flows. The software tool is able to, on the one hand to handle different fluid types such as oils, gases and waters of different composition and on the other hand, directly connect with external tools such as PROSPER for modelling wellbores or MBAL to properly represent the reservoir. Moreover, GAP allows to determine the whole system at a defined point in time as a simple network solve, where underlying models such as MBAL are not directly taken into account. The possibility to run forecasts in GAP to understand the future development of the system is also given. The starting point for this approach was on the one hand the latest map of the pipeline networks created by engineers in Wintershall and on the other hand two Excel files. One for the production and the other for the injection system – that give a great overview of each pipeline segment and its individual specifications such as the length, diameter and materials. One important assumption for modelling made is that the ground elevation of the whole pipeline network is constant with 1 m below the surface. This includes that there are not any elevation changes. This can be accepted as valid, because the underlying geography in this area is very planar. Furthermore, exceptions of this assumption like river crossovers or underpasses could easily be adapted, because a connection to an Excel macro (Appendix F) was set up with IPM OpenServer. The OpenServer is a tool, which allows other external applications like Microsoft Excel to read, write and execute functions in all IPM software tools. Therefore, a nearly seamless data transfer between the IPM suite and external applications, simulators and databases can be performed. In the created Excel macro, it is possible to adjust each pipeline parameter individually for every segment in the field. The main pipe properties that can be set are the length of the segment, the inside diameter, the roughness and as already mentioned the TVD. Moreover, the attached nodes have to be defined whether being down- or upstream. The correlation for the flow calculations are – as recommended by Petroleum Experts – performed by GAP internal correlations. It is necessary to define environmental parameters to complete the input data for a pipeline segment such as the surrounding temperature, the overall heat transfer coefficient, which will also be transferred to the pipeline properties if not defined differently and the oil, gas and water heat capacities. If 'Pressure Only' calculations are performed for the pipeline network, these previously listed environmental parameters are not of relevance. As soon as the network will be solved for both temperature and pressure, these

set of parameters will be of equal importance. Initially these parameters have their default values (Table 6) as set by Petroleum Experts. As the RESOLVE simulation takes control, they will be updated continuously at each RESOLVE timestep.

Table 6 Initial 'Environment Parameters' as set by Petroleum Experts for temperature calculations in the pipeline segments.

Parameter	Value
Surrounding Temperature [°C]	10
Overall Heat Transfer Coefficient [W/m²/K]	45.43
Oil Heat Capacity [KJ/kg/K]	2.22
Gas Heat Capacity [KJ/kg/K]	2.24
Water Heat Capacity [KJ/kg/K]	4.19

As a second assumption, the pipe inside diameter was set to its maximum diameter, which assumes that no precipitations occurred during the lifetime of the pipelines. This assumption can be made on a first approach, because of the pigging of the pipelines on a continuous basis over the years. Although pigs have been running and therefore cleaning is performed, the initially set parameters are altered for sure. As already mentioned exceptions can easily adjusted via the Excel macro. The latter assumption that no precipitation occurred – will also influence, for instance, the roughness, as precipitations will crucially alter the inner surface of the pipe.

Summing up, there is no doubt that the listed pipeline parameters and their adjustments have an influence on the production and injection rates. The uncertainty of the production data (Table 2) is so severe and significant, that the sensitivity for the pipeline input parameters is in such a small range that they would be almost negligible. Therefore, sensitivities of temperature effects and friction pressure drops in the pipelines will be treated with minor priority in this thesis.

After creating the pipeline segments and adjusting their properties with the Excel macro all existing wellheads and their type of pump was pre-set and connected to the corresponding pipeline segment (Figure 5). Furthermore, a grouping of the wellheads in the system was performed. This gives on the one hand a first overview of wellbores that are somehow connected from a geologically as well as production point of view and on the other hand, it will allow a better and more precise production analysis among the compartments at a later stage. The map, as can be seen in Figure 4, accounts for the production as well as the injection pipeline systems. It is the underlying map and used as a backup

to the Excel files to measure certain distances for the GAP systems when no other specific information concerning a pipeline segment was available.

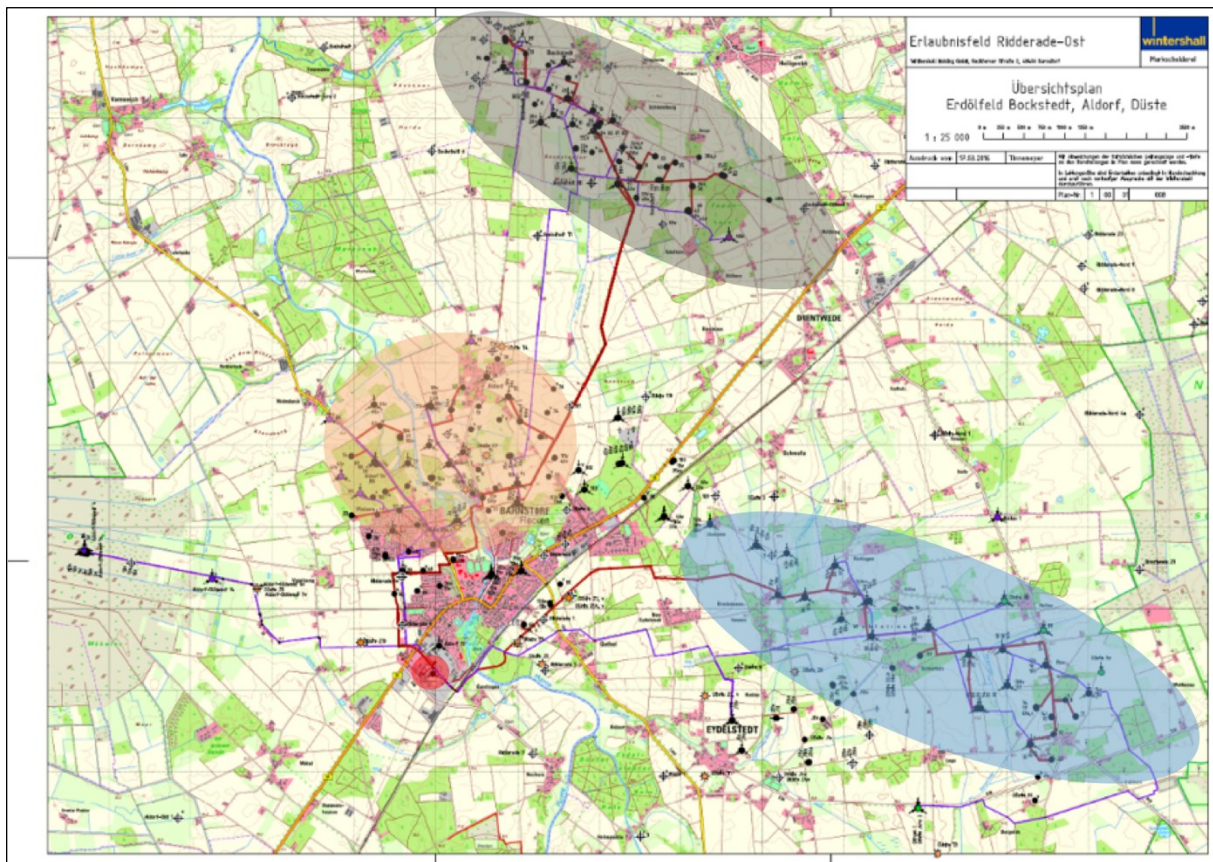


Figure 4 shows a map of the production (red pipelines) and injection (blue pipelines) system connecting Aldorf (orange), Düste (blue) and Bockstedt (black) fields with the processing plant in Barnstorf (red circle)

10.1 Production System

There are approximately 35 km of pipelines, when summing up each individual segment in the production system, which connects the fields Aldorf, Düste and Bockstedt with the processing plant in Barnstorf. There were 69 pipe segments defined throughout all three fields, whereas 19 are referred to Aldorf, 23 to Bockstedt and 27 to the Düste field. This separation was necessary as there are in some regions changing inside diameters, pipeline materials, which have different roughnesses and splits in the system. This split up of the pipeline system in GAP and allocation of the segments can be seen in Figure 5. Furthermore, major surface facilities like the multiphase pump at the Bockstedt field, the artificial lifting system, whether the well is active or disabled as well as to which compartment, a well-bore belongs, are included and visible in the GAP network.

The multiphase pump was, because of design reasons of the application, modelled as a compressor, because in the compressor tool it is possible to insert pressure differentials without any pump performance charts as a fixed delta pressure. Along with this setting, it was possible to insert an initial pump displacement pressure of 8.0 bar. This value was taken from the ACRON-Reporter from Friday, 20.05.2016.

Figure 5 shows the production surface network as it is modeled with the GAP software tool. On the south, the processing plant in Barnstorf can be seen as a red separator symbol. Following against the flow in the pipeline from the separator a node is reached. This node separates the Dueste pipeline system from the northern network, which represents Aldorf and Bockstedt. All green triangles represent production wellheads, whereas the symbols in the triangle give an indication of which kind of pump is installed. The green underlying circle segment shapes correspond to tanks from the individual MBALs. Arrows in the pipelines represent the flow direction, as can be seen they are directed to the processing plant. Moreover, grey symbols are currently disabled elements, which are not in production anymore, and not yet abandoned too or tanks, which were used experimentally as an auxiliary tool for modeling purposes.

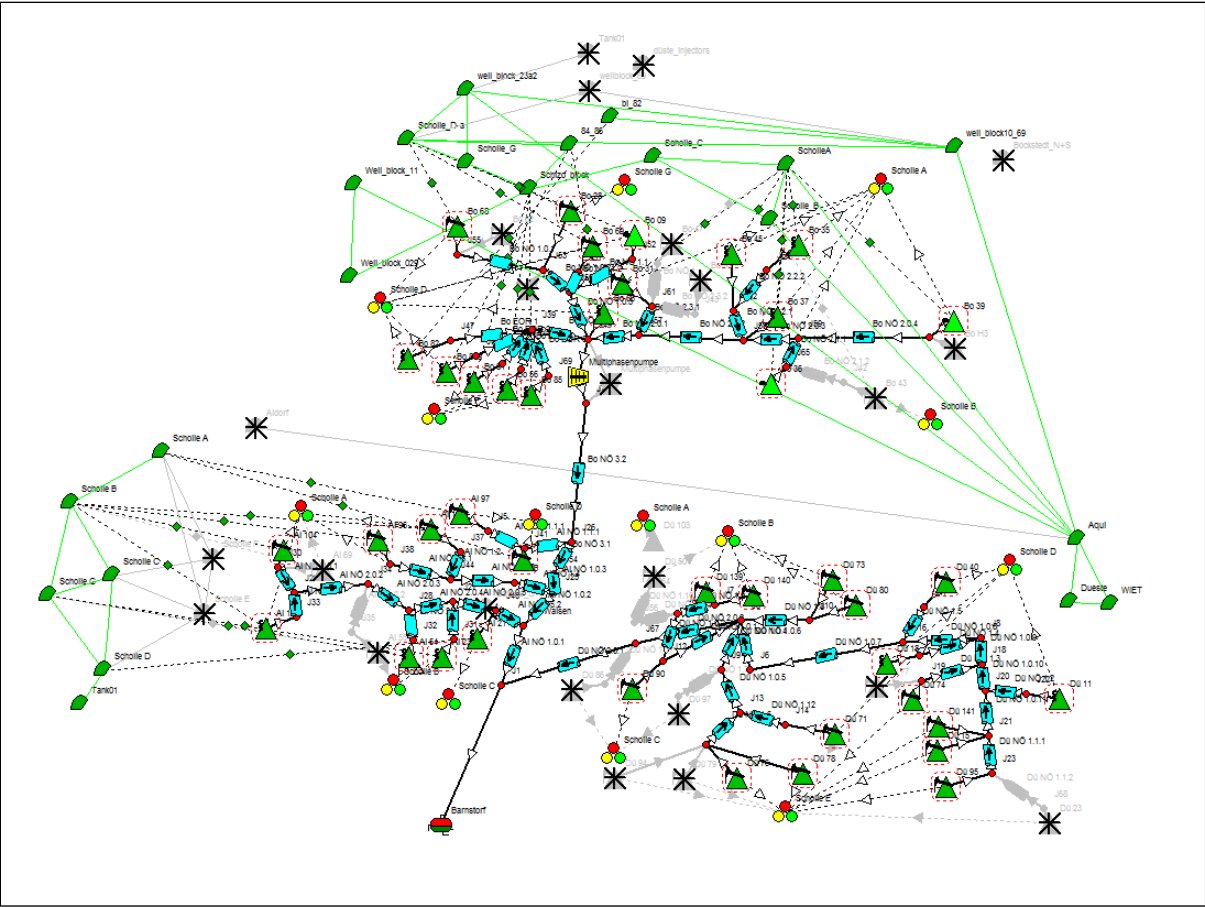


Figure 5 illustrates the surface network of the production system in GAP. The northern part represents Bockstedt, with the multiphase pump installed as a compressor. All green triangles represent production wellheads, whereas the various symbols in the triangles represent the pump type. Arrows in the pipelines indicate flow direction. Green segment symbols represent tanks from the underlying MBAL models. All grey symbols are currently disabled elements. The most southern facility (indicated in red) represents the processing plant in Barnstorf.

10.2 Injection System

The overall structure of the injection system is designed like the production system in GAP. The injection system is not as huge as the production system, but there are approximately 32 km of pipelines installed for a sufficient water supply to all injectors. It is, as previously the production system, allocated into 33 parts. Aldorf accounts for 8 segments, Bockstedt for 12 and Dueste for 13. Figure 6 shows

the corresponding injection system in GAP to the production system from Figure 5. The processing plant in Barnstorf is not represented with a separator symbol anymore therefore; the symbol represents an injection manifold. The flow arrows in the pipeline segments moving away from the plant as the water is injected. The green circle segments have the same underlying MBAL models as in the GAP production system to get a closed circulation. In this case, the blue-mirrored triangles represent injection wellheads. In the near vicinity of the injection manifold 'Barnstorf' there is a compressor symbol visible. This compressor is necessary for modelling purposes, because the calculated pressure from the production system is transferred directly via a Microsoft Excel file to the injection system. Therefore, this compressor, which can be seen as pressure pumps, is necessary; otherwise, the injection pressure would be the same as the separator pressure.

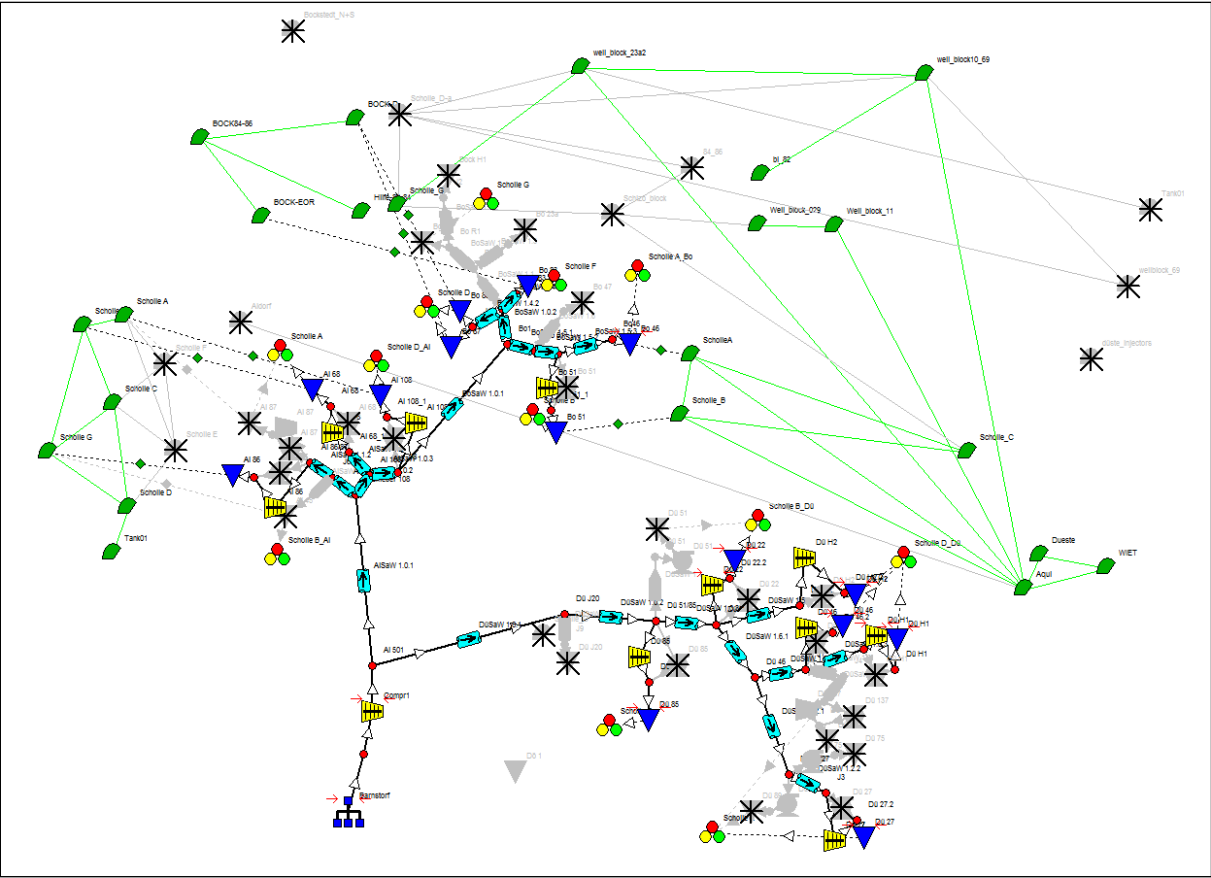


Figure 6 shows the surface network of the injection system in GAP. Blue-mirrored triangles represent injection wellheads and the green segments show the MBAL tanks. The most southern facility represents the injection manifold at the processing plant in Barnstorf. Green circle segment symbols represent underlying MBAL tanks. All grey facilities are currently disabled elements.

11 Modeling Lift Performance with PROSPER

By now, the surface pipeline network and the facilities in the production as well as injection system are designed and initial values are inserted. As the next step, it was necessary to create and further adjust each individual wellbore, their properties and artificial lifting system or injection performance. The IPM tool PROSPER performs this wellbore modelling. The ultimate goal for each individual wellbore is the generation of realistic lift performance, where properly adjusted fluid characteristics as PVT and inflow performances from the reservoir as IPR are of great importance. Therefore, it is necessary to insert as realistic PVTs, deviation survey, equipment and inflow performance data as possible for a valid PROSPER model. The usual and by Petroleum Experts predefined workflow is to start inserting field and general data such as the characteristics of the wellbore, its artificial lifting system, fluid descriptions, user information and field information.

As a next and extremely important step, the input of proper PVT data was necessary. For this case, the initial PVT from previously performed flash experiments were taken into account. At this point, it has to be mentioned, that this analysis is also included in the already created Eclipse model for Dueste. This will later be of great importance when setting up the RESOLVE to achieve proper PVT transfer consistency. The lack of precise data and further because of modelling simplicity, a main assumption was that one PVT model per field was created, although it is known that production comes from more than one layer in each of the fields. Therefore, it is very likely to have more than one fluid type per field too. The next step before the creation of the IPR and further matching the VLP was to insert equipment and deviation survey data. Deviation data is not saved in the Finder database as a continuous property, so it was necessary to create and adapt an Excel interpolating tool to get the right TVD for a certain MD. After the interpolation the data was extracted for every wellbore and inserted in 100 m steps of the TVD in PROSPER. Furthermore, the casing and tubing data were copied from a downhole wellbore picture from the company's internal database. The properties for the artificial lifting systems were also found in the local disk in various equipment and workover reports. After inserting all known wellbore, equipment and pump related parameters, it was able to start designing the inflow from the reservoir.

11.1 Production Wells

There are various kinds of production wells in the three fields present, which greatly differ in performance such as liquid rates, water cuts, well integrity and inflow performance on the one hand and hence characteristics and facilities like installed pump type on the other hand. Most pumps in the field are sucker rod pumps but also progressive cavity pumps and three electrical submersible pumps can be found. The variety between the wellbores and its underlying production performance made it necessary and very important to study and model each wellbore individually. The PVT data per field was set up from previously performed experiments. Those experimental PVT parameters for the Dueste field are taken from an PVT cell experiment from 17.02.1955 as can be seen in Appendix B. The same parameters were also determined experimentally in Aldorf in 16.06.1953 as can be seen in Appendix A and Bockstedt as listed in Appendix C. As the solubility (R_s), the formation volume factor of oil (B_o) and the oil viscosity (μ_o) tables were inserted, it was able to match these parameters and the bubble

point pressure properly. The Dueste as well as the Aldorf and Bockstedt oil viscosity shows with the Beggs et al correlation the best match. Properties such as R_s , B_o and p_b are better matched with Glasø in Dueste and Bockstedt and Vasquez and Beggs in Aldorf. The IPR data section was in the set up procedure the next step, for which a Darcy inflow model was chosen in PROSPER to be as comparable to the inflow performance calculation performed by Eclipse, which is of great importance to achieve a consistent data transfer when connecting with the reservoir simulator, as possible. Input parameters such as reservoir pressure, drainage area, permeability and net pay were extracted from the near well-bore area of the underlying Eclipse model (Appendix B), for the same consistency and transfer reason as mentioned. The initial settings for the Aldorf wells IPR generation can be seen in Appendix A and for Bockstedt in Appendix C. After generating the IPRs, it was able to create and adjust the VLPs with data from the ACRON database for the top node pressure. Well checker rates were used as a starting point to match an as adequate intersection point between the IPR and VLP as possible. Trying to match the rates more precisely, the volumetric pump efficiency factor for sucker rod pumps and pump wear factor for progressive cavity pumps and electrical submersible pumps was used, because this factor is an empirical parameter dependent on paraffin precipitation, wear and pump efficiency itself to name a few and therefore not defined yet.

11.1.1 Artificial Lift System Generation

As the fields are very advanced in their production life the reservoir pressure already reached a point where naturally flowing is not possible anymore. For counteracting production losses and still maintaining an intersection between IPR and VLP, secondary recovery and artificial lift systems were introduced to the fields. As there are various pumps with different specifications active in the three fields, it was important to get an understanding of the characteristics and modelling peculiarities of the different kinds of pumps. The most common artificial lift system throughout the fields is the sucker rod pump, but there are also 15 progressive cavity pumps and 3 electric submersible pumps in operation. The approach of modelling each pump type in PROSPER is outlined in the following section.

11.1.1.1 Sucker Rod Pumps

There are approximately 22 sucker rod pumps in operation in Aldorf, Bockstedt and Dueste. Whereby mainly two types are used in the fields. The first one is a 2 3/8" x 1 3/4" in dimension and the second one is 3 1/2" x 2 3/4". The first diameter references to the outside diameter (OD) of the pump body and the second one defines the OD of the plunger acting in there. Further settings that have to be made to specify the sucker rod pump in PROSPER are the pump depth, the surface stroke length and the pump speed. Since the solubility of the fields is low, problems with associated gas was not reported and is not common. The described parameters such as stroke length were found in daily reports. One very sensitive parameter, which is still unknown, is the pump volumetric efficiency factor. This empirical property was adjusted with the generated inflow performance relationship and the well checker measurement. During the adjusting procedure, it could be observed that this efficiency factor is in a range between 30 and 70%. Such low values can be explained with inefficiencies due to paraffin precipitations and hence bonding in the pump or loss of integrity. The volumetric pump efficiency factor is defined as:

$$\text{Effective Pump Performance} = \text{Ideal Pump Performance} * \frac{\text{Volumetric Pump Efficiency}}{100\%}$$

After matching the latest well checker measurement with the pump volumetric efficiency factor a set of vertical lift performance curves for later prediction runs was generated with the VLP calculation tool in PROSPER. The following parameters were chosen as sensitivity parameters, whereas their range differ from wellbore to wellbore: Pumping speed, GOR, water cut and top node pressure. For each parameter the maximum of 10 cases was inserted, which led to a set of 10,000 VLP cases per well that had to be exported from PROSPER and subsequently imported to the corresponding well in GAP.

11.1.1.2 Progressive Cavity Pumps

In wellbores with yet higher inflow performance, progressive cavity pumps are installed. The operation for this type of pump is possible in 15 wellbores in the field currently. A summary of individual wellbores with an active PCP, their model and starting date can be seen in the summary in Table 7. There are in general three different PCP Netzsch pump types installed in the field. Pumps with 4", 3 1/2" and 2 7/8" pump OD. Modelling a PCP differs from creating a sucker rod pump in PROSPER, as it is necessary to first fully define the pump and its specifications such as the performance chart in the internal artificial lift database of the software. The pump data as well as the performance data are provided by Netzsch the various pump types were assigned in the PROSPER internal database.

Table 7 summarizes the progressive cavity pumps in the field in operation

Wellbore	Pump model	Active since
Aldorf 014	NTZ 350*200 ST 16.4	02.07.2014
Aldorf 021	NTZ 400*200 DT 66	25.02.2015
Aldorf 023	NTZ 278*200 DT 20	24.11.2014
Aldorf 054	NTZ 400*200 DT 66	03.11.2014
Bockstedt 035	NTZ 400*200 DT 66	10.12.2014
Bockstedt 037	NTZ 278*200 DT 20	25.02.2015
Bockstedt 045	NTZ 400*200 DT 66	10.07.2014
Bockstedt 056	NTZ 400*200 DT 66	09.07.2014
Bockstedt 081	NTZ 278*200 DT 20	17.09.2012
Bockstedt 082	NTZ 278*200 ST 10	16.12.2014
Bockstedt 084a	NTZ 350*180 ST 16.4	26.04.2012
Bockstedt 085	NTZ 400*200 DT 66	05.02.2014
Bockstedt 086	NTZ 350*200 ST 16.4	12.02.2014
Dueste 011	NTZ 400*100 DT 66	07.12.2009
Dueste 018	NTZ 400*180 DT 83	22.08.2014

An example of the approach how the PCP model was assigned in PROSPER can be seen for Aldorf 014 in the Figure 7, where first, the data was inserted in the database and as a next step, it was able to generate the PCP performance chart in PROSPER.

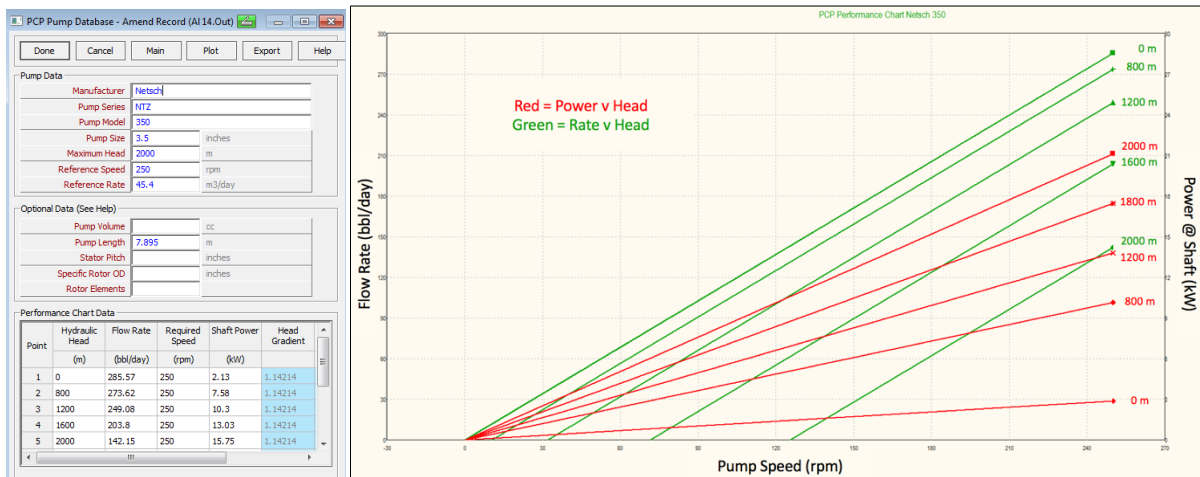


Figure 7 shows on the left the input screen for defining a PCP in the PROSPER internal database. After defining the pump specifications, it was able to generate the performance chart for the pump (right).

Previously, for precisely adjusting a SRP model, PROSPER provides the pump volumetric efficiency factor. However, this factor is not yet available for PCPs; instead, a so-called pump wear factor is available, which is used to apply deviations such from the performance curves, because of wear or other inefficiencies. This factor is defined as:

$$\text{Effective Pump Performance} = \text{Database Pump Performance} * (1.0 - \text{Pump Wear Factor})$$

The pump wear factor was then used like the pump volumetric efficiency factor for the sucker rod pumps to adjust the rates to the latest well checker measurement.

Furthermore, the VLPs for forecasting were generated, whereas the sensitivity variables are the top node pressure, water cut, GOR and pump speed. The approach for generating the VLP cases was like previously described in the sucker rod pump. A set of 10 values per sensitivity variable were individually specified, which also led to an amount of 10,000 VLPs per wellbore. These lift curves were then further exported and then assigned to the associated wellbore in the GAP network.

11.1.1.3 Electrical Submersible Pumps

Currently there are three ESPs in the field present, whereas all three of them are installed in the north in Bockstedt. The generation of the PROSPER file for an ESP pump can be compared to the one from a PCP. Petroleum Experts already provides in the internal database for the artificial lift systems a great variety of ESPs. Therefore, it was not necessary to fully implement the pump performance from the very beginning as it was for the PCPs. Based on the manuals of the pumps and operating reports the input data for the individual ESPs were defined in PROSPER. In between these pump data there is also the possibility to insert a pump wear factor as defined in the PCP section. The provided pump data as well as the huge already existing database of ESPs allowed a fast and sufficient initial data input.

After defining the pump and its performance data, the IPR and VLP intersection was matched in the system analysis section. An acceptable fit then allowed generating the set of VLPs. The main sensitivity

parameters were the top node pressure, the water cut, the gas to oil ratio and different to the PCP the operating frequency. Each of the sensitivity parameters were addressed with 10 equally spaced values. The minimum and maximum was defined individually based on the wellbore and pump performance, characteristic and recommendations from Petroleum Experts handbook. Like in the previous sections, after the generation of the 10,000 VLP cases the set was exported for and further imported in GAP to the corresponding wellbore.

It is important to be aware of the consistency between the used lift performance correlation in PROSPER and the one applied in GAP. If the correlation is, because of some reasons, changed in the PROSPER file it is necessary to newly import the whole *tpd file in GAP. It will not be sufficient to re-create the lift performance curves in GAP. Figure 8 and Figure 9 show the recommended ranges from Petroleum Experts from the GAP user manual, which were used as a basis. (GAP Technical User Manual, 2015)

	From	To	Number of Points	Distribution of Points	Comments
Liquid Rate	From low value (say 100 stb/d)	AOF (Absolute Open Hole Flow of well)	20	Geometric Spacing	
Top Node Pressure	From separator pressure value (for example, 100 psig)	Reservoir Pressure	10	Linear Spacing	The Top Node Pressure corresponds to the Well Head Pressure.
Water Cut	0 %	90% or 95 % or 99 %	10	Linear Spacing	
GOR	A value less than Solution GOR	25000 scf/stb	10	Geometric Spacing	The Solution GOR should be entered for one of the values to avoid unnecessary interpolation. The value less than Solution GOR corresponds to the reduction in GOR when Reservoir Pressure just falls below the bubble point.

Figure 8 shows the recommended sensitivity variables and ranges for a naturally flowing oil well.

	Variable	Values	Comments
Gas Lifted Wells	GLR Injected or	0, 100, 200, 400, 800, 1600, 3200, 6400, 12800, 25600 (in scf/stb)	Using the GLR Injected as a variable will ensure that the VLP curves will always interpolate for the Gas Lift Gas Rate. This is the recommended method.
	Gas Lift Gas Rate (not recommended)		Enter the range of values that could be injected in the well
ESP wells	Frequency of Operation		Depending on the Variable Frequency Drive Option, enter the range of values for the frequency of motor operation. These generally range from 40 to 70 Hz.
PCP Well	Motor RPM		The Motor rpm corresponds to the Pump Speed.
Jet Pump Well	Power Fluid Rate		
HSP Well	Pump Rotational Speed		
CBM Well	Liquid Level		The maximum depth of the liquid level cannot exceed the depth of the pump

Figure 9 shows the recommended sensitivity parameters and ranges for various artificial lifting systems.

12 Injection Wells

Modeling an injection well in PROSPER differs, because of various reason, from the modelling approach of a production well. First, the PVT model per field does not has to be as accurate as for an oil well, because the only phase an injection well deals with is the water phase. Therefore, the only input PVT parameter that needs to be defined for a water injector in PROSPER is the salinity of the phase. Furthermore, it has to be mentioned that this parameter will be later estimated from RESOLVE and transferred to PROSPER. Being aware of this calculation workflow and knowing that there are different salinities during production, because of the various compartments and layers per field one pre-defined average salinity value of 150,000 ppm was chosen for initialization. This assumption can be made, as the injection performance is not greatly sensitive to the salinity. Far higher dependent parameters are the condition of the wellbore itself such as the integrity, or the near wellbore properties like the skin factor, permeability and reservoir pressure. The skin factor is a very uncertain property regarding the water injectors in the fields, because beside expected, but not fully known paraffin precipitations in some injectors, the mechanical skin in the wellbore itself is for some wellbores estimated to be massive. In fact, because there are fewer interventions or tests performed in injection wells the size and individual composition of the skin is not known.

After inserting the average salinity value, the next step was to define the deviation survey and down-hole equipment data. The approach of this step was the same as for a production well. The only entry that has to be further defined was the injected fluid temperature, which was set throughout the field with 15 °C. For the IPR generation, the Jones model was selected and not the thermally induced fracture model as recommended by Petroleum Expert. This step was selected, because for the thermally induced fracture model too few parameters for a proper design were known. As mentioned previously, already the skin factor is a highly uncertain parameter and this model would require even further precise thermo-mechanical parameters for a reasonable design. On the other hand, it would be important

to simulate and understand the creation of fractures coupled to thermal effects to optimize the performance of the injection wells and the reservoir itself more properly. The Jones IPR model is based on the Darcy equation, which is extended with further reservoir properties for the estimation of the 'a' and 'b' parameters as can be seen in the following definition:

$$(P_r - P_{wf}) = a \cdot Q^2 + b \cdot Q$$

Q is the rate at a test point in time for the corresponding well flowing pressure P_{wf} . The laminar flow parameter 'b' and the non-Darcy turbulence coefficient 'a' were then estimated with the test data. The average reservoir pressure P_r was firstly taken from the underlying reservoir compartment of the MBAL tank in Aldorf or Bockstedt or extracted from the Eclipse Dueste model. The main issue was finding test data for defining the two parameters 'a' and 'b'. In most of the water injection wells in the fields there are no downhole gauges installed, therefore it was necessary to find another way to get a match. The fact that no well flowing tests or ones, which are already extremely old and not representative anymore, lead to a less accurate method, but still reasonable for finding the right trend. The wellhead pressures as well as the water injection rates per wellbore are saved in the ACRON database. These two corresponding values were then extracted for three representative times in the past until 01.01.2014 were no operational interruption and therefore a steady injection performance for a minimum of two weeks was guaranteed. The gradient function in PROSPER was then used to back-calculate a pressure value for the P_{wf} out of the wellhead pressure. Keeping in mind that this action is quite uncertain, because of various unknowns. Great influence on the calculations are the deviation survey and the equipment data as the depth and the dimensions of the wellbore are significant for the flow conditions. Moreover, the integrity of the wellbore itself has a high influence, as any leakage in the tubing or packer will severely alter the pressure and flow regime in the tubing as for example increased precipitation near a leakage might occur. All these uncertainties have to be kept in mind when performing the gradient traverse functionality. In the gradient tool of PROSPER the selected wellhead pressure and rate were inserted as required. After performing the calculation, the estimated pressure is found as a result in the result table at the bottom measured depth per well. The calculated P_{wf} as well as the injection rate are then further inserted beside other reservoir parameters, which were extracted from the near wellbore area of the Eclipse model, the MBAL or log data. Furthermore, the skin factor was defined too, which allowed to account for the previously defined pressure drops such as junk in the wellbore. The fact that the skin factor for injection wells is a very uncertain property, because it accounts for any type of pressure drawdown lead to skin factors from 5 to up to 80. Such high values are physically not realistic, but from a modelling point of view to match the injection rates, especially in the Dueste field, necessary. As mentioned the PROSPER IPRs in the Dueste field are later overwritten by the Eclipse model. Moreover, it has to be noted these relationships are on the edge of their applicability as the rates are very low and the integrity in selected wells is bad. An example of a matched IPR for an injection well can be seen in Figure 10.

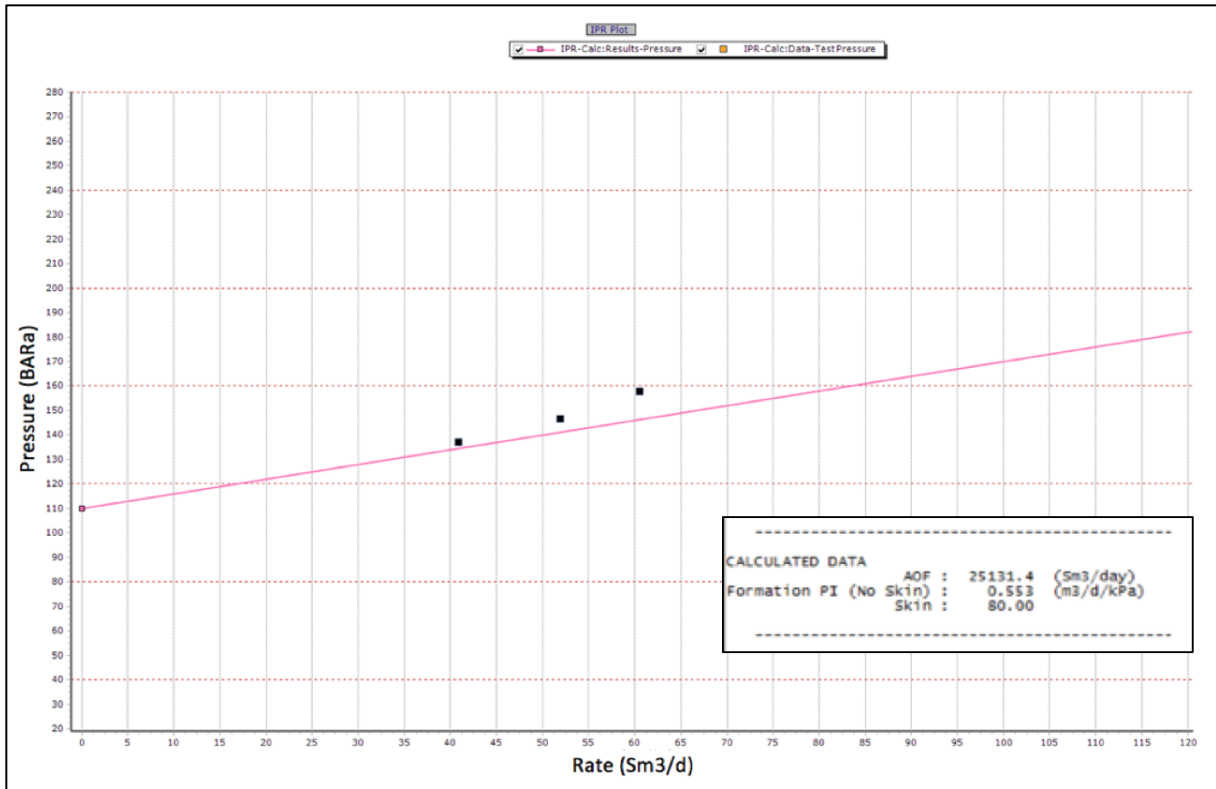


Figure 10 shows an example of a matched IPR for a water injection well of Dueste 085. It was necessary to zoom in to the low rate region as it is on the edge of the relationship.

The edge of the applicability of the underlying Jones relationship has a further impact as it was necessary extremely zooming in to the low rate region of the plot to be able to adjust the curve. Moreover, this means that just minor adjustments for this region will have huge impacts of the curve at higher rates. The fact that no water injection well will exceed an injection rate of 400 m³/d and the main matter is a fit to purpose model for cross-checking data and prediction, the negligence of a proper fit for high injection rates is valid. Beside the skin factor the reservoir pressure per well was also slightly adjusted for minor vertical shifts of the IPR curve. The inflow performance relationship is, not as known from production wells, increasing with increased rates. This is a reasonable behavior because the higher the injection rate, the higher will be the well flowing pressure as the reservoir will not be able to instantly absorb the increased rates. A result of the continuously growing IPR curve is that there will not be any intersection with the x-axis, which means there is no physically realistic absolute open flow. This effect can be seen in the data summary on the right of Figure 10 as the AOF is with 25,131.4 Sm³/d just a theoretical value.

For every injection well a validation of the match was performed in the system sensitivity analysis section of PROSPER. A top node pressure from the ACRON database, but differently to the already selected ones for matching purposes was selected. Then a calculation of the system was performed to get the VLP/IPR intersection and therefore the injection rate for the inserted top node pressure. If the deviation between the calculated rate and the one saved in the ACRON database appeared to be too high the IPR adjustment was revised. The threshold for the maximum deviation of the data was set to 20%, because on the one hand the data from the ACRON itself is known to be slightly error prone and

on the other hand as listed above there are many influencing factors with a high uncertainty. An even closer match would therefore not add further value to the result.

The last step in the PROSPER modelling approach was to create VLPs for prediction purposes, therefore sensitivity cases like previously elucidated for the production wells were created. Differently to the production wells, there are now three sensitivity variables defined in the injection part. The first parameter is the top node pressure, whereas the sensitivity range is dependent on the individual injection well as their wellhead pressures range from atmospheric conditions, because the hydrostatic pressure is for some injection wells sufficient, up to more than 100 bar. This range is also recommended by Petroleum Experts as can be seen in Figure 11. The other two sensitivity parameters are the liquid rate, where the injection rates from ACRON were taken as a basis and the flowing wellhead temperature.

After exporting the simulated cases and inserting these into the corresponding injection wells in the GAP injection network the IPRs, VLPs for the Aldorf and Bockstedt field were calculated, and for Dueste the IPRs were set to lookup tables and only the VLPs were taken from PROSPER.

	From	To	Number of Points	Distribution of Points	Comments
Liquid Rate	From low value (say 100 stb/d)	Refer Comments on Right	20	Geometric Spacing	The maximum available rate is dependant on the equipment present and the field itself
Top Node Pressure	0psig	Injection manifold pressure	10	Linear Spacing	The maximum pressure should be the maximum injection manifold pressure
FWHT					The temperature range is dependent on the temperature at the injection manifold and the surrounding temperature in the pipelines.

Figure 11 shows the possible sensitivity variables and their ranges for water injection wells as recommended by Petroleum Experts.

13 Creation of Aldorf Reservoir Model

The field Aldorf, located right in the north from the processing plant in Barnstorf, is with a start of production in 1952 the oldest known field of the three oil fields in investigation. Nevertheless, there is no existing static as well as dynamic reservoir model. The field Aldorf was, and currently is, mainly analyzed with production and injection data from PDMS. Dynamic pressure data is gained with measurements of the liquid level during short shut in periods of the pump. It is possible to investigate four compartments with these fluid column measurements and dynamic pressure balancing. These four main compartments can be seen in Table 8.

Table 8 lists the four main compartments in Aldorf and their active wells. Blue marked ones represent the injection wells; the others are production wells.

Aldorf			
A	B	C	D
Aldorf 014	Aldorf 023	Aldorf 021	Aldorf 001
Aldorf 096	Aldorf 054		Aldorf 097
Aldorf 104	Aldorf 045		Aldorf 108
Aldorf 107			
Aldorf 068			
Aldorf 087			

It is necessary to provide some type of reservoir model in the full field model, be it a dynamic flow model with Eclipse, a material balance model with MBAL or a simple tank in GAP, which represents a pressure dependent decline curve. The first approach for getting a trend was to create a pressure dependent decline curve. For this purpose, the cumulative production from 1965, where the first decline was recognizable, until now was estimated. To get viable reservoir pressure data, research in the company’s internal archive shows that there were many build up tests conducted between 1961 and 1990, but never digitalized. In fact, it was just necessary to get an overall trend, so one average pressure per year was taken and plotted against the corresponding cumulative production. These data were inserted as a tank in the GAP model and connected to the individual wells. It can be quickly observed that this approach for prediction purposes was not successful for more than one reason. Firstly, the Aldorf field is in production for 64 years with a current overall recovery factor of almost 41%, which is at the very end of the field life. Extremely low pressures as well as huge water cuts are not seldom, and therefore most of the internal correlations in GAP are not applicable anymore and will fail at these conditions. Secondly, which is also a result of the already long production history, is that small pressure deviations in the pressure dependent decline curve model can already lead to economic and technical production limits of the field. That means, simple putting average pressure values is not possible as the pressure range and the resulting uncertainty would be too high. Thirdly, the field Aldorf consists of various compartments with huge pressure differences of up to 60 bars. It is not possible to ignore these compartments for reason of simplicity, as mentioned previously the pressure range and hence the error would be too high.

Another problem that was not addressed until now is that the production in Aldorf comes from at least four layers, which are different in their characteristics as their fluids coming out of the individual layers are too. Some wells even produce or previously produced out of six layers, which makes the situation even more complicated. One big issue is that these individual layers, where not analyzed explicitly and a production logging tool operation in each currently producing wellbore would be necessary to better study the behavior. However, these operations will not be performed, as it is not economic at this stage in time. For the following approach, it was decided that all possible information, geologically with the latest interpretations of faults in the map as well as dynamically to use all reservoir pressures previously performed, are being consulted. Therefore, all shut in pressure tests from 24.10.1961 to 17.02.1992 were digitalized to get a proper pressure history of the Aldorf field. Furthermore, to make these pressures comparable all pressure points were corrected to the company internal reference depth of 1090 m. This depth was defined in 1953 when the very first fluid sample was taken in Aldorf 002 for analysis. For a proper correction, the ground elevations in reference to the sea level were extracted from the Finder database of each tested well. The given gauge depth and specific gravity of the fluid during pressure testing and the ground elevation allowed to calculate the pressure for comparison to the common reference depth of 1090 m. Therefore, the following formula was applied to get the corrected pressure data:

$$P_{corrected} = P_{measured@Gauge} - (D_{ground\ elevation} - D_{reference} + D_{gauge@sealevel}) \cdot \rho \cdot g \cdot 10^{-5}$$

The different definitions of the depth in the formula above can be seen in Figure 12. The density is calculated with the measured specific gravity of the fluid during testing multiplied by 1000 kg/m³. The gravity constant g was set to 9.81 m/s².

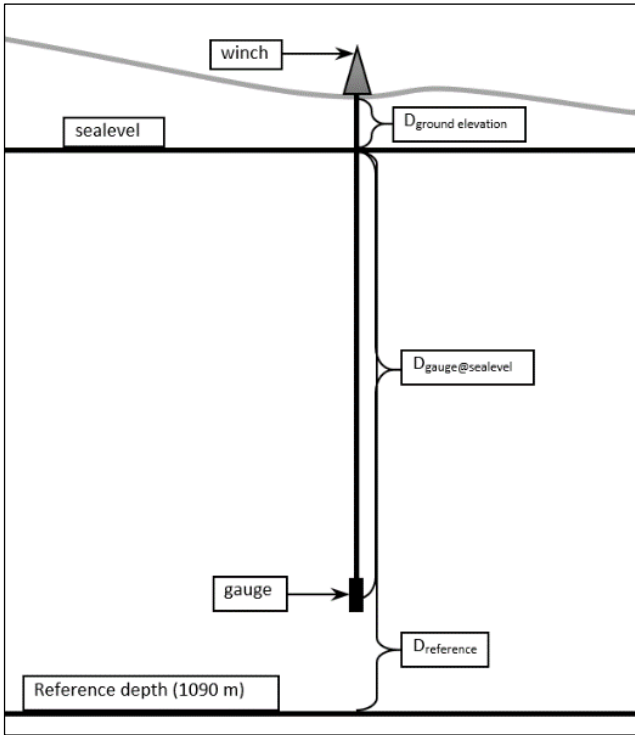


Figure 12 illustrates the different depth definitions. The reference depth in Aldorf of 1090 m can be seen at the bottom. This depth is further used to calculate all historical pressure points to a common depth.

After performing all pressure corrections the historical data was plotted and analyzed as can be seen in Figure 13. Whereas the different colors in the plots already define the re-defined compartments as can be seen in Figure 14. The pressure data was not corrected and therefore it has to be mentioned that outliers can still influence the trends. Furthermore, systematical errors should be kept in mind, because some selected wells were used on a yearly basis for testing and others were never included. If such a regularly used well has unknown peculiarities such as inflow problems, lays in a highly fractured region, which is not known or in an abnormal pressure area, would influence the whole re-interpretation process.

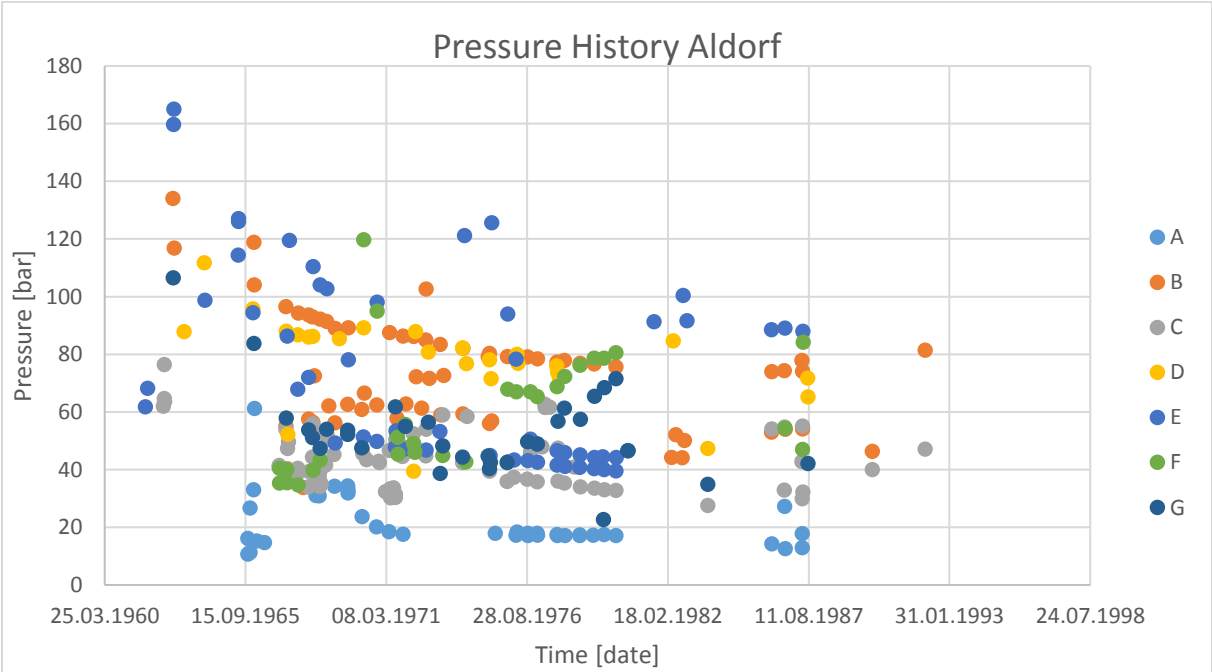


Figure 13 illustrates the pressure history of field Aldorf (referenced to 1090 m). The different colors represent the different compartments as can be seen in Figure 14.

At first, the compartments were defined by just dividing the pressures into ranges. The lowest range includes all pressures below 20 bar. The first intermediate range was defined from 20 to 60 bar and the second intermediate range from 60 to 80 bar. All pressures higher than 80 bar were then put in the last and therefore highest range. This allocation allowed already a rough estimation of trends. The next step was to divide these trends locally, whereas the highest influence for the decision to separate one compartment into another was the geological maps with the latest faults indicated (Figure 14). The northern part was clear to distinguish, because between compartment A and compartment B are pressure differences of 60 bar, although they are located beside each other and not clearly separated with a reported sealing fault. Far clearer, from a geological fault interpretation point of view, was the separation of all other compartments, because their borders proceed along the interpreted faults as can be seen in Figure 14. However, the pressure differences were not as high as between compartment A and B and sometimes even in a very narrow range as can be seen in Table 14.

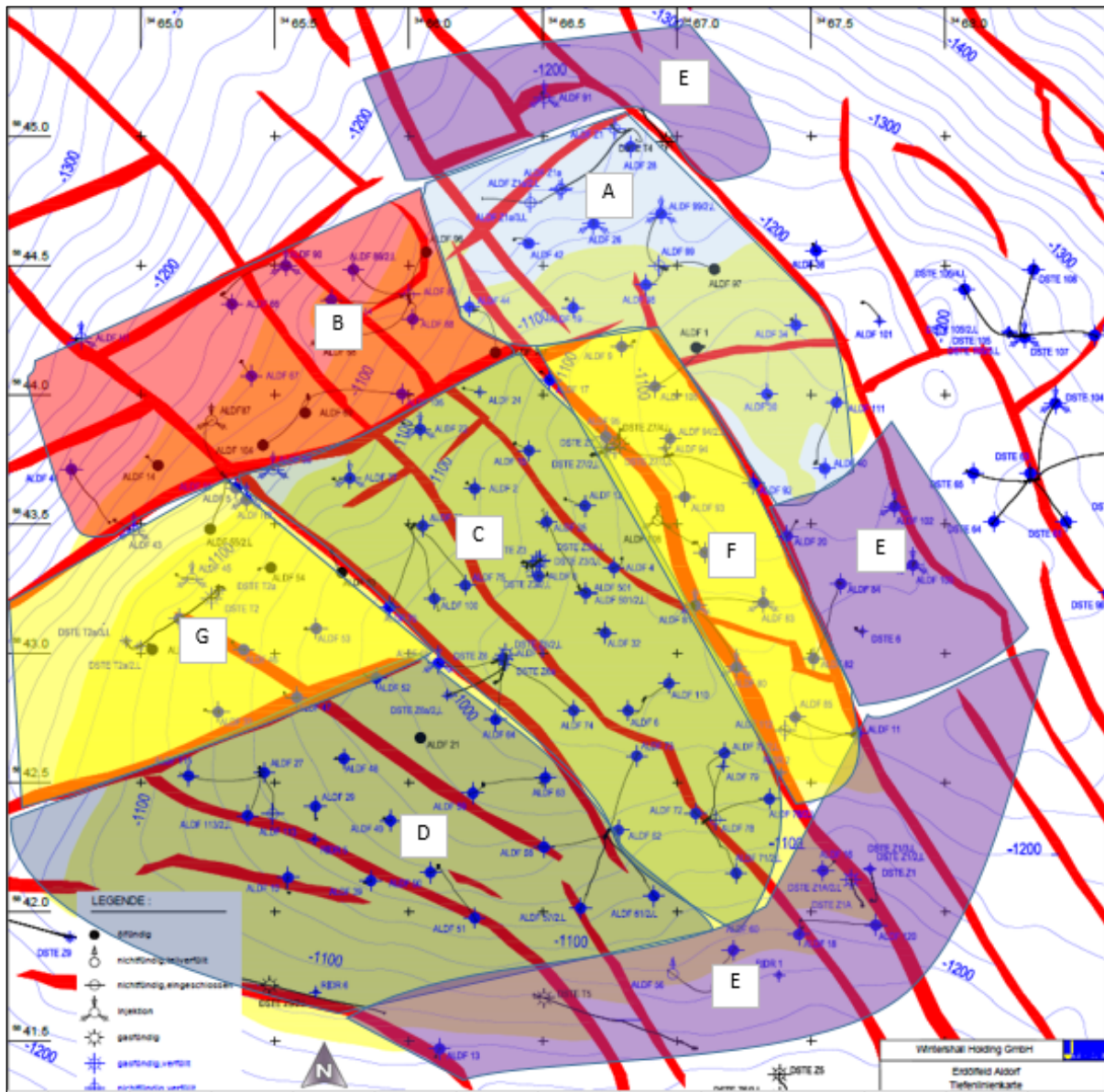


Figure 14 illustrates the re-defined compartments based on the digitalized shut-in pressure history in the field Aldorf. The pressure difference between compartment A and B was with almost 60 bar quite significant, whereas the other ones were not that clear and therefore mainly separated between already interpreted faults. Compartment E include pressure tests near the oil water contact and is therefore not locally defined as the others are.

It can be seen that the wells in the originally defined compartments (Table 8) are in the re-defined ones. For history matching reasons in MBAL, all wellbores were further sorted since the start of production in the field Aldorf according to their compartments as can be seen in Appendix A.

13.1 Aldorf PVT

For practical and simplicity reasons it was decided to create one simple PVT model for all compartments and layers in the Aldorf field. The bubble point pressure, solubility as well as the viscosity of the oil were gained from an PVT cell experiment from 06.07.1953. The formation volume factor for oil for the unsaturated and saturated region was then further calculated with the Vasquez and Beggs general correlation. Viscosity and R_s values were with best fitting polynomial functions in Excel interpolated.

For the viscosity a polynomial of fourth degree, for the saturated region of the viscosity a polynomial of second degree and for the viscosity in the unsaturated region a linear interpolation was chosen.

13.2 Relative Permeability Curves

The long lifetime of the field results in water cuts, which are already at a very high stage, therefore it is important to have accurate relative permeability curves especially for high water saturations. A time dependent water saturation was calculated (Appendix E) from the oil production, connate water saturation and oil in place, which was extracted from the Finder database.

$$S_w(t) = S_{wc} + (1 - S_{wc}) \cdot \frac{\sum Q_o}{OIP}$$

The connate water saturation is assumed constant in all previously defined compartments with 0.4. This value is based on initially performed petro physical studies from the early field life. The cumulative oil production per compartment was then further calculated from the oil rates per well saved in the Finder database.

The oil initially in place per compartment was back-allocated by dividing the current cumulative oil produced per compartment with the cumulative produced oil of the whole field. The cumulative values for produced oil, water and gas and the cumulative injection as well as the allocated amount can be seen in Table 9.

$$OIP_{compartment} = OIP \cdot \frac{Q_o \text{ compartment}}{Q_o \text{ total}}$$

Table 9 shows the amounts produced per compartment for oil, gas and water, which was estimated from the wellbores previously defined in the individual compartment. Furthermore, the back-allocated amounts of field Aldorf for MBAL input are noted.

	A	B	C	D	E	F	G
Oil [m³]	310246.9	437589.9	1074546	359043.3	96904.8	172796	368623.3
Gas [m³]	12793818	12603605	44762010	16591129	2605010	7867294	12896958
Water [m³]	836255	2245098	3468637	3047283	755457	642025	2835419
Inj. Water [m³]	21891	3140069	3578173	3283565	98151	1336760	2138858
Allocation [%]	11	15.5	38.1	12.7	3.4	6.1	13
Absolute [m³]	770184	1086312	2667549	891321	240565	428964	915103

This input data allowed to first calculate the water saturation for each timestep in each compartment for Aldorf as a next step it was possible to estimate the oil saturation with the following simple relationship:

$$S_o = 1 - S_w$$

This assumption is valid because the initial R_s is with $28.42 \text{ m}^3/\text{m}^3$ extremely low and therefore the gas phase is neglected for modelling the relative permeability curves. The relative permeability of oil and water were then obtained by applying the Brooks-Corey relative permeability models (Brooks & Corey, 1964):

$$k_{ro} = k_{ro,max} \cdot \left(\frac{S_o - S_{or}}{1 - S_{or} - S_{wc}} \right)^{n_o}$$

$$k_{rw} = k_{rw,max} \cdot \left(\frac{S_w - S_{wc}}{1 - S_{or} - S_{wc}} \right)^{n_w}$$

The connate water saturation was, as previously mentioned, assumed with 0.4 and the residual oil saturation was estimated previously with 0.15. Therefore the unknowns, and hence to match parameters, are the maximal relative permeability of oil and water ($k_{ro,max}$ and $k_{rw,max}$) and the exponents n_o and n_w . These values were then estimated by first plotting the fractional flow by its basic definition:

$$f_w = \frac{q_w}{q_t} = \frac{q_w}{q_w + q_o}$$

After plotting these fraction against the previously obtained $S_w(t)$ it was possible to investigate the fractional flow curve. This action was performed for each of the seven compartments in the field Alldorf. The defined aim is to achieve a good match for the four unknowns in the Brooks-Corey model for every single compartment. This is possible by plotting the Buckley-Leverett fractional flow, whereas the gravity and capillary pressure is neglected. This assumption can be made, because of the low-density difference between the water and the oil. With this previously defined assumption, the fractional flow definition reduces to the following term:

$$f_{w,BL} = \frac{1}{1 + \frac{\mu_w}{\mu_o} \frac{k_{ro}}{k_{rw}}}$$

The viscosity of the brine was estimated using correlation charts (Appendix A), whereas first the brine viscosity was estimated at atmospheric pressure, but at reservoir temperature and further corrected to the reservoir pressure. The viscosity of the oil was already known from the PVT cell experiment. By plotting this curve together with the previously estimated f_w it was able to adjust the unknowns.

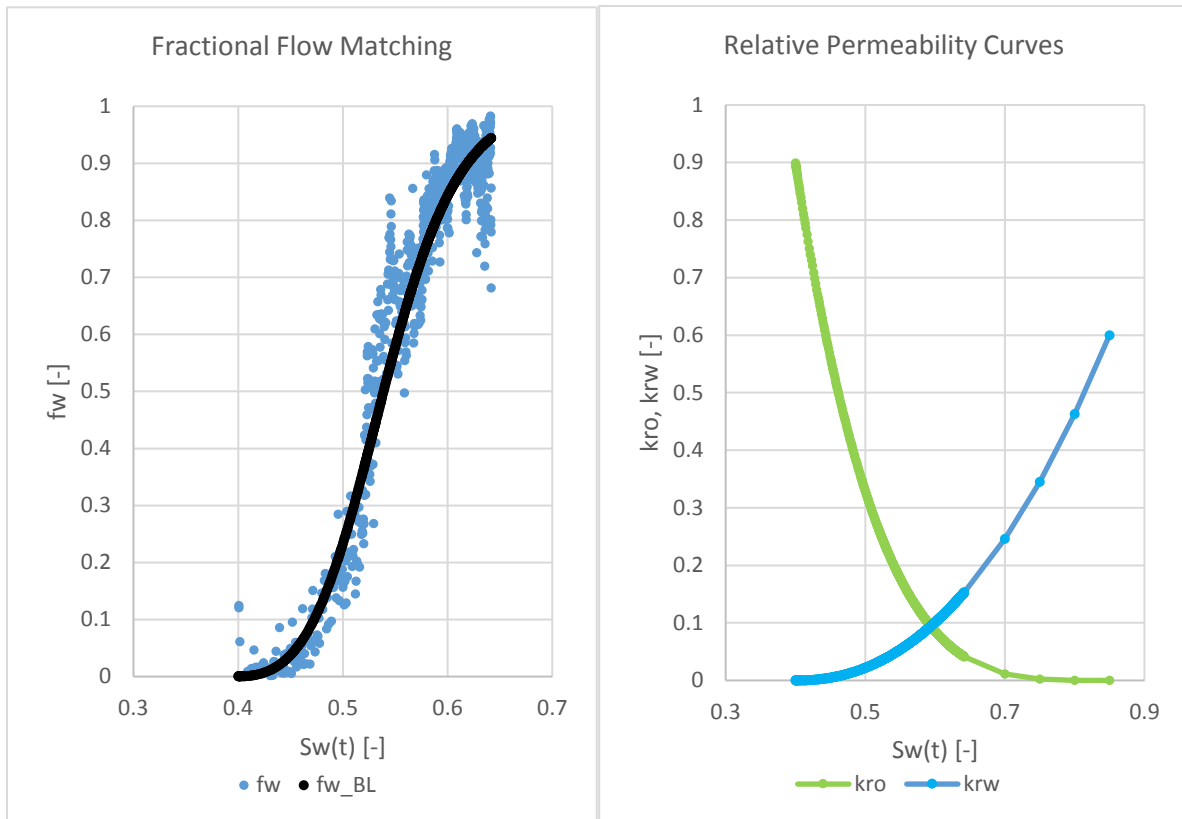


Figure 15 illustrates an example (compartment A): Fractional flow matching based on cumulative oil production (left); Relative permeability curves of oil and water based on the Brooks-Corey model (right)

The two previous diagrams (Figure 15) show an example of the matching procedure for the Brooks-Corey parameter in compartment A. As mentioned, it is very important to match the shape of the fractional flow curve especially at high water saturations, because of the already high water cuts in the production wells. A summary of all adjusted parameters for the compartments can be seen in Table 10:

Table 10 shows the summary table of Brooks-Corey parameters estimated for each compartment in Aldorf

Compartment	$k_{ro,max}$	$k_{rw,max}$	n_o	n_w
A	0.9	0.6	4.0	2.2
B	0.85	0.55	3.6	1.0
C	0.9	0.6	4.0	1.9
D	0.7	0.6	4.0	1.0
E	0.7	0.6	4.0	1.0
F	0.7	0.6	3.5	2.0
G	0.8	0.6	3.5	1.0

13.3 History Matching

After finishing the data preparation such as the digitalization of the pressure data and all pre-setting activities like the generation of the simple PVT model and the relative permeability curves, one tank

for each re-defined compartment was created in MBAL. Adjacent compartments as can be seen in Figure 14, which were represented by tanks in MBAL, were further connected through transmissibilities to allow possible communication for history matching purposes. The initial settings for each tank were kept the same as represented in Table 11.

Table 11 lists the initial settings for every MBAL tank in Aldorf.

Tank Type	Oil
Temperature [°C]	53
Initial pressure [bar]	116
Porosity [-]	0.16
Connate water saturation [-]	0.4

The properties of the individual layers and the measurements performed to estimate the above values could be seen in Appendix A.

The study of the long production history as well as the pressure history gave a quite clear indication of an active aquifer in the Aldorf field. Furthermore, because of geological reasons it can be estimated that in the southwestern part the aquifer will become stronger as the local high located in the north-eastern part. Moreover, the layers have been reported to be thicker in the southwestern part of the field; therefore, stronger aquifer inflow is expected. For the aquifer, the radial version of the Hurst-van Everdingen-Modified model was chosen. This decision was made, as it is the most representative yet known aquifer model and recommended by Petroleum Experts. Although there were not wells drilled in the aquifer and therefore no measured properties available it was able to perform a history match. The Hurst-van Everdingen-Modified model, based on the diffusivity equation, requires the reservoir thickness, reservoir radius, encroachment angle, outer to inner radius ratio, and aquifer permeability as input parameters (Van Everdingen & Hurst, 1949, December 1). It was able to get initial values for the reservoir thickness as they were estimated from core and log analysis in the early field life. First values for reservoir radius and encroachment angle were estimated from the geological map for each compartment. The two latter ones were set by an educated guess, which is based on a study performed for the Valendis pool (Lübber & Nolte, Dezember 1978) for the first few runs. The production and injection history as well as the reservoir pressures per tank were then extracted from the Finder database and from the Excel file of the digitalized pressures. Already before performing the first history matching runs compartment F and E were disabled. This decision was made on the one hand to make the history matching faster and on the other hand easier, because less parameters have to be adjusted. As can be seen in Table 9 the shares of compartment E and F are with 3.4% and 6.1% minor to the total OIP. A further reason to accept this simplification is that there are no production or injection wells active anymore.

The order of the described tanks in the MBAL model as well as one further auxiliary tank called 'Tank01' can be seen in Figure 16. The idea of Tank01 came up, when no proper match for compartment D was realizable. After revising the input data, especially for the one tank where a sufficient match could not

be performed, which represents compartment D, a geological explanation could be found. The reason is that the injection well Aldorf 031 is located on the most southwestern area of the Aldorf field. Between this injector and the main field, a fault was interpreted as can be seen in Figure 17. The fact that this injector is responsible for almost all the injected water in that compartment it would not be able to simply neglect it, because it would disturb the production – injection balance too much. Therefore, the decision was made to introduce a separate tank with the same initial properties as the tank for representing compartment D has, except the fact that the fluid type is water and not oil. This has been done, because it is assumed that the region Aldorf 031 has been injecting, lays already in the aquifer. The transmissibility 'Trans13' then allowed to better control the impact of the injected rates on compartment D. This setting with seven transmissibilities and six tanks was then used to achieve a proper match.

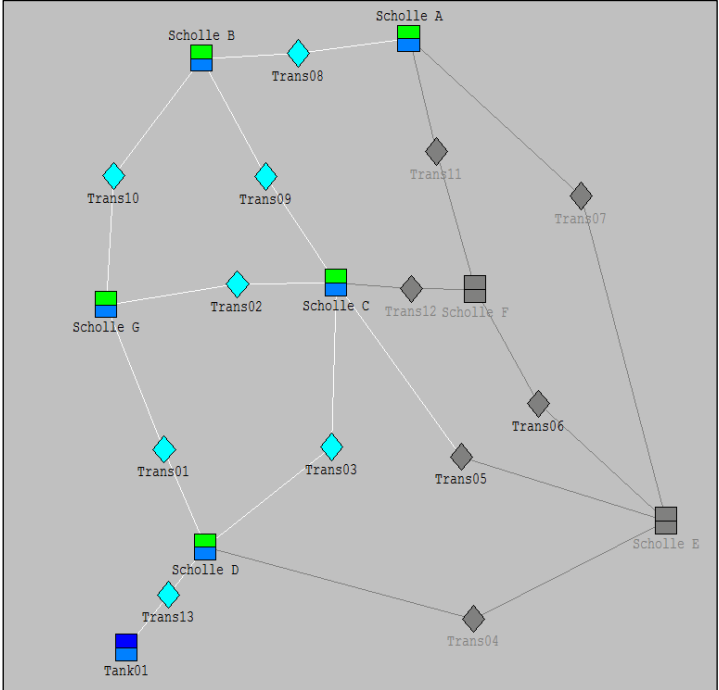


Figure 16 illustrates the underlying MBAL model of the Aldorf field with the six active tanks and seven active transmissivities. It can be seen that all tanks, except 'Tank01' are divided into green and blue color code. This represents an oil tank with an underlying aquifer. Tank01 has two different intensities of blue, which represents a water tank with an underlying aquifer too. The rhombus symbols connecting the individual tanks represent the transmissibilities in the MBAL model. Grey tanks and transmissibilities are disabled in the model.

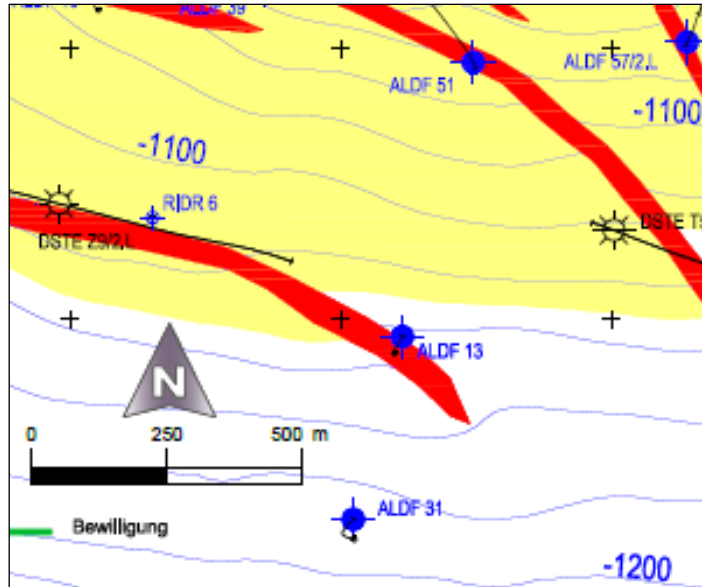


Figure 17 represents the location of injection well Aldorf 031 in the near vicinity of an interpreted fault, which separates the injector from the main field.

During the matching procedure it was worked out that beside the transmissibilities, the outer to inner radius ratio and the reservoir thickness were the most sensitive parameters during the history matching. This is because the range for the reservoir thickness is not as wide, due to given logs, as for other aquifer model input parameters like the encroachment angle or the aquifer permeability. Therefore, it was tried to avoid too massive manipulations of reservoir thickness. The best results for the transmissibilities as defined in Figure 16 can be seen in Table 12.

Table 12 shows the resulting transmissibility values for the Aldorf field after history matching.

Name	Value
	$[m^3/hour * mPa.s/bar]$
Trans01	10
Trans02	1
Trans03	15
Trans08	40
Trans09	0.3176
Trans10	300
Trans13	20

The communication between compartment B and G is strong as can be also seen in Figure 13 as the ranges and trends are almost the same. Not as expected is transmissibility 'Trans08', which represents the connection between the high-pressure compartment B and the low pressures in A. This increase of the transmissibility had to be performed, because the aquifer is assumed not to be as strong as in the other compartments, because of the location in the north. Despite this lower aquifer interaction, pressure support was needed and therefore communication to compartment A was increased. The

result of all other transmissibilities are in the range as expected. The results of the aquifer model parameters in each compartment after the history matching can be seen in Table 13. The initially expected trend from a strong active aquifer in the southwest to a much weaker influence in the northeast can also be seen.

Table 13 illustrates the parameters of the aquifer model in each compartment after the history matching.

Parameter	A	B	C	D	G	Tank01
Reservoir Thickness [m]	10	15	25	60	30	30
Reservoir Radius [m]	300	300	600	700	400	200
Outer/Inner Radius ratio [-]	1	7	5	7	8	25
Encroachment Angle [°]	180	120	200	180	200	180
Aquifer Permeability [md]	200	600	2000	1500	600	2000

The history-matched pressures for the individual compartments can be seen in Figure 18 and Figure 19. The separation into two diagrams was introduced for readability reasons. The history match, as the whole MBAL model, is a fit to purpose performance. As the ultimate goal of the model is to provide full field prediction runs, the focus was to get the right trend for the latest simulation times and not necessarily for the very early times. It can be seen that the fit of the trend and range of pressure is for all compartments successful, except in compartment C an increase in the simulated pressure and therefore a deviation from the falling trend is observed. Nevertheless, this is not yet a main concern, as there are no active wells in that compartment. It has to be mentioned that massive outliers were excluded from the calculation. The average pressures, the minimum, the maximum as well as the standard deviation for the uncorrected pressure data per compartment can be seen in Table 14. At this point, a further reason for the exclusion beside their minor contribution to the original oil in place can be seen as their standard deviation (σ) is with 32 bar and 20 bar for compartment E and F extremely large. This high standard deviation of 32 bar in compartment E can be explained as already mentioned, it differs locally from the other ones. It is the area at the rim laying already in the aquifer's transition zone. The area extents from the north of the low-pressure compartment A and takes its way over the eastern margin down to the very southern part. This wide area of influence explains the exceptional high standard deviation compared to the other compartments.

Table 14 Summary of uncorrected pressure data per compartment

Compartment	No. of measurement	P_{avg} [bar]	P_{min} [bar]	P_{max} [bar]	σ [bar]
A	38	21	10	61	9
B	64	74	33	135	19
C	84	44	28	76	10
D	26	78	39	111	15
E	56	73	40	165	32
F	30	59	34	119	20
G	33	53	22	106	14

The sudden pressure increase in the early 1960s in compartment B and in the 1961s in compartment G, as can be observed in Figure 18, can be explained as the first water flooding operation, which started there for pressure stabilization. Moreover, as marked yellow in Figure 18, there is a clear pressure trend visible in compartment B, which is 20 bar higher than the simulated one from 1967 to 1987. However, this yellow marked trend is from one wellbore, the Aldorf H001, which is located in the north at the near vicinity of the oil water contact, where increased pressure is estimated. The decline in compartment A behaves, because of the minor aquifer support, as expected and is therefore extremely steep at the beginning. Nevertheless, the current pressures in compartment A of around 10 bars match good with the yet active production wells operating in this compartment, which are Aldorf 001 and Aldorf 097. As can be seen in Figure 19 the simulated pressure decline fits well with the historical data. In 1987, the decline stopped and a constant pressure behavior of 65 bar adjusted. The change from the declining trend to a constant pressure trend can be explained because of two actions. The first and major one can be seen in Figure 20 as the oil production decreased rapidly in 1987. Because of this production decrease, the pressure decline is attenuated. A second effect that comes along is the strong support from the active aquifer and an even further pressure support from the Aldorf 031 water injection well, which is represented by Tank01. The sum of these effects result in the constant pressure performance of 65 bar, which is when having a look at the production well Aldorf 021, which is still active in that compartment, a realistic value.

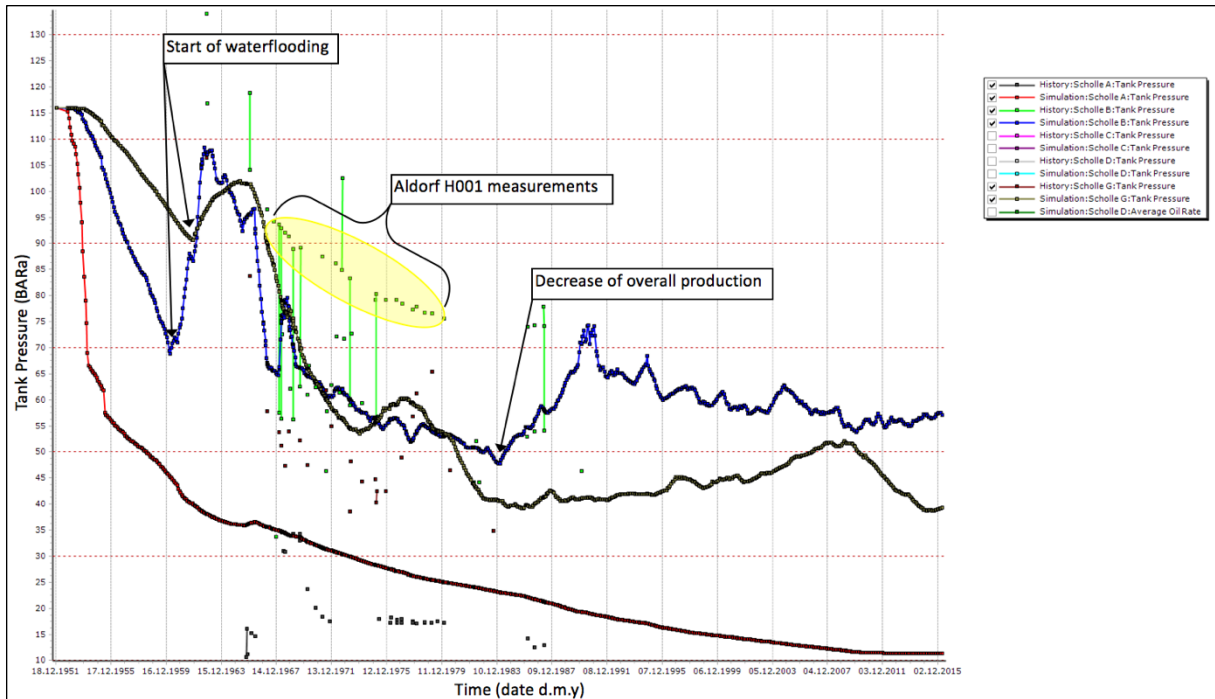


Figure 18 shows the history matched pressure result for compartment A, B and G. In compartment A a steep pressure decline at the early life can be observed, which is quickly attenuated and stabilizes at around 10 to 15 bar. Compartment B and G show in the 1960s an increase in pressure, which can be explained with establishing the waterflooding operations. A further significant pressure increase in 1980 can be explained with an overall reduction in liquid production. Furthermore, yellow marked are the pressure measurements performed in Aldorf H001 as they are not in the normal range of compartment A.

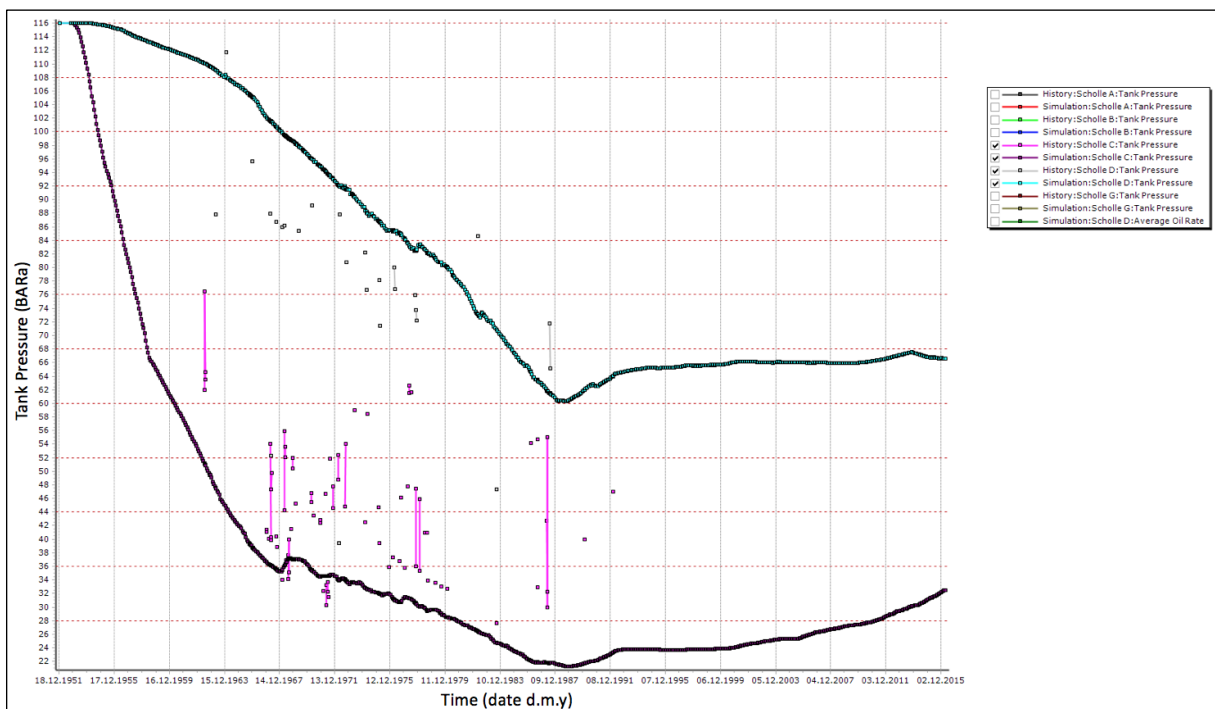


Figure 19 shows the history matched pressure result for compartment C and D. It can be seen that the pressure in compartment C slowly starts to increase, which is a result of the reduced overall production. The pressure increase is not yet alarming as there are no active wells in that compartment. A further result is the stop of decline in compartment D in 1987.

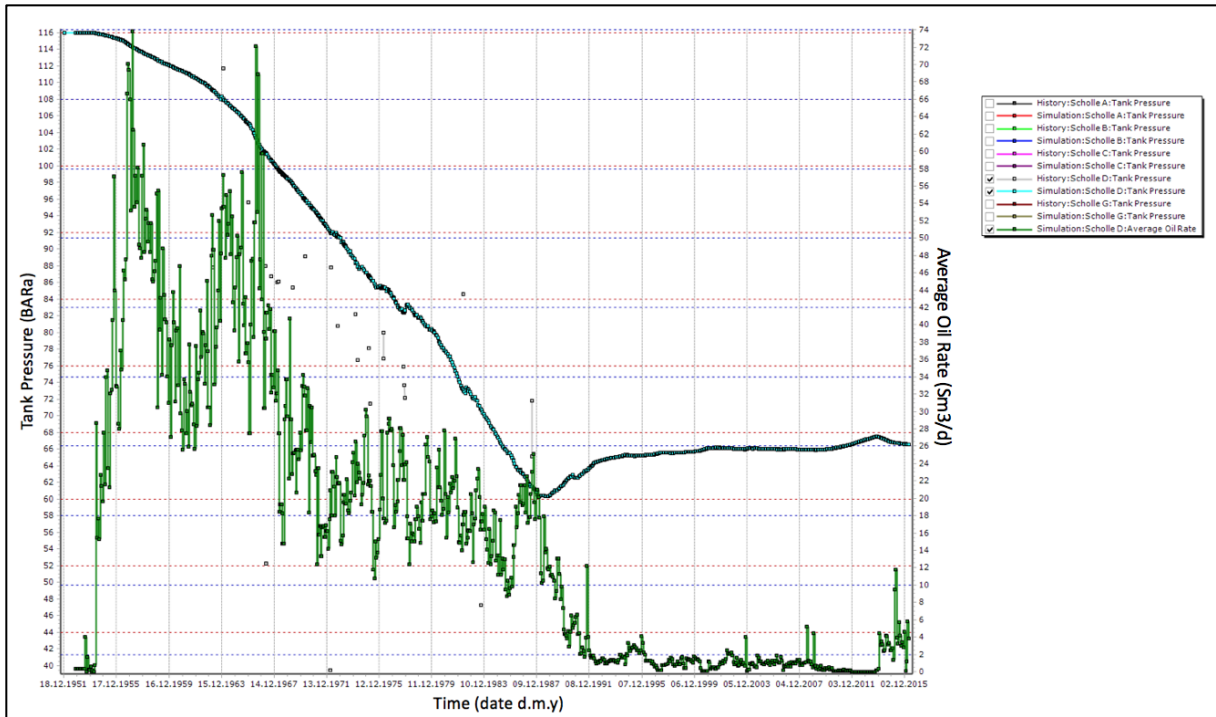


Figure 20 shows the simulated pressure decline and oil production compartment D. It can be observed that the oil production decreased in the 1987s, which further resulted in a stop of the pressure decline in the corresponding tank D.

14 Bockstedt MBAL Model Implementation

Several options have been provided for representing the Bockstedt reservoir in the full field model. The first one is an Eclipse model of Bockstedt, which is based on a newly shot seismic in 2013 and therefore the most valuable representation of the Bockstedt reservoir at this stage in time. The second option would be an already existing MBAL model in which the tanks are mainly built on a compartment level. These compartments are based on observed production and pressure responses of the individual wells in the field.

The northern part in the Bockstedt field is known to be more compartmentalized than the southern one. A smaller MBAL model of the northern Bockstedt field, which represents the compartments D, 84/86 and EOR has previously been generated and provided for this thesis.

The Eclipse model of Bockstedt was not chosen for the implementation in the full field model, because it is not yet fully history matched and therefore not representative enough as the uncertainty would be too high. At a later stage in time, when the history matching process of the Eclipse model is finished it would be recommended to implement it properly into the full field model like the Dueste Eclipse model as described in the chapter 'Implementation of Application Objects' in RESOLVE.

Therefore, the existing MBAL model was firstly implement within the GAP system, but after the first validation run as can be read in the 'Bockstedt' part in the chapter 'Verification Simulation Runs' the smaller tanks, especially in the north reacted very sensitive. This outcome led to the decision to disable these small sensitive tanks and implement the smaller MBAL model, which represents the compartments D, 84/86 and EOR. Moreover, because of the disabling of the northern tanks in the existing MBAL model it was necessary to re-history match the model. However, although the disabled tanks provide some pressure support, they are so small that on the one hand, almost no manipulation has been necessary and on the other hand, the matching procedure has been easier to perform, because less influencing parameters are enabled. These two underlying MBAL models can be seen in Figure 21 and Figure 22.

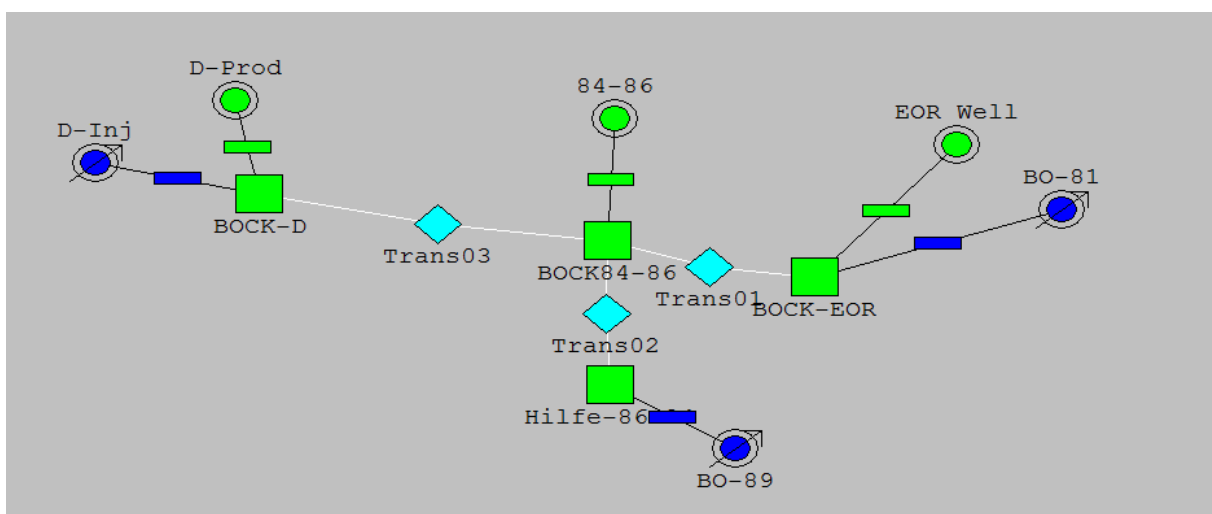


Figure 21 represents the northern part of the Bockstedt field in MBAL. The green squares show the three compartments, which were created for this study. Furthermore, one auxiliary tank 'Hilfe-86' was implemented. The circles represent wells, whereas

green ones are production wells and blue ones for representing injectors. It can be seen that no aquifer model was activated in this representation, as there is no influence encountered.

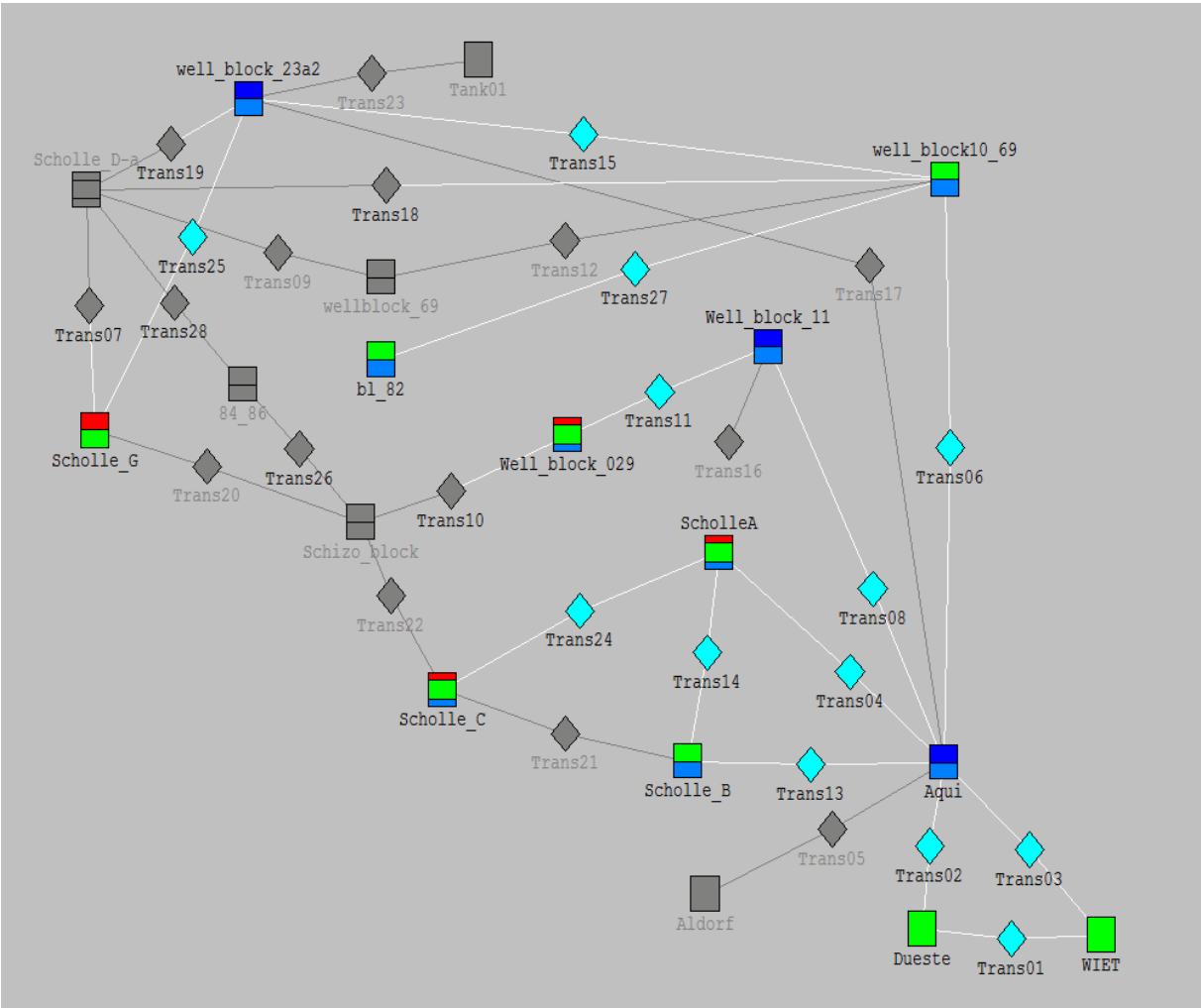


Figure 22 illustrates the southern part of the Bockstedt field in MBAL, whereas the grey tanks and transmissibilities represent disabled items, which were replaced by an extra MBAL model as can be seen in Figure 21. The southern part of the Bockstedt field experiences influence from an aquifer (Lübben & Nolte, Dezember 1978), therefore chosen aquifer models were inserted at specific locations in the MBAL model. The red shaded parts represent gas caps in specific tanks.

Both models were created independently from each other, therefore some input parameters slightly differ from each other, as the PVTs do too. However, the matched correlations are the same, whereas Glasø is the closest match for R_s , B_o and Beggs et al the best for μ_o . The three slightly different matches for R_s , B_o and μ_o versus the pressure for the PROSPER files, the Bockstedt north MBAL and south MBAL can be seen from Figure 23 to Figure 28 and in Appendix C.

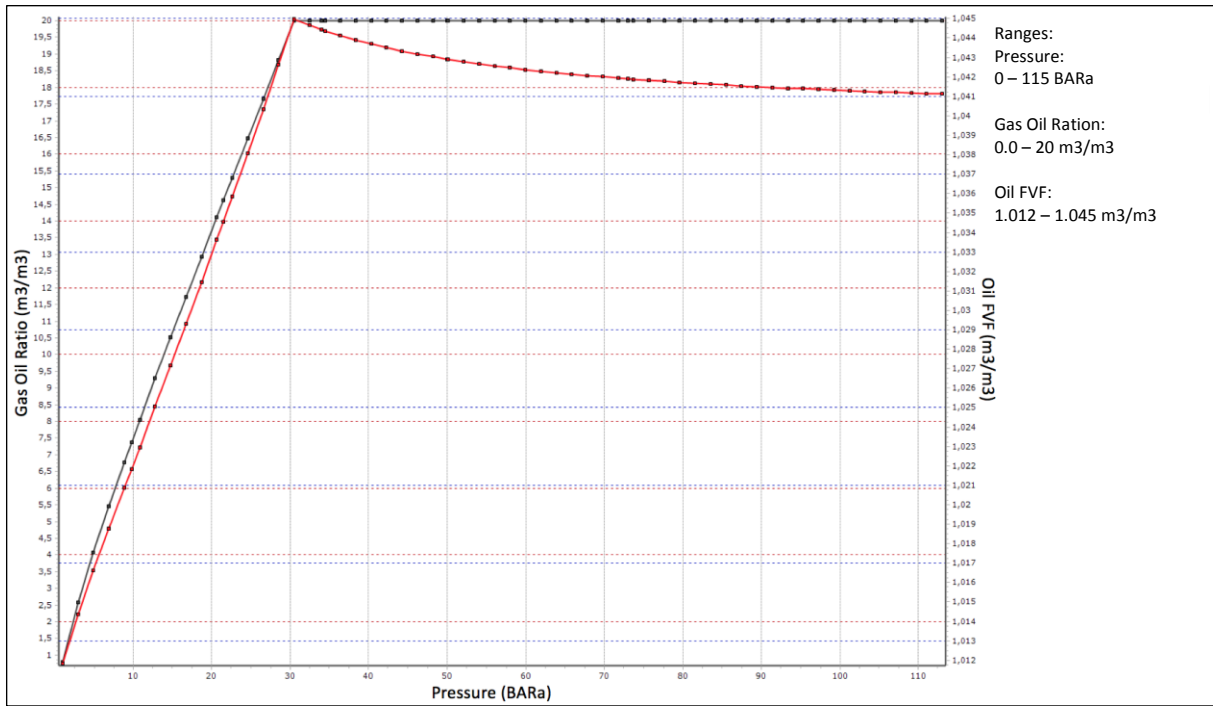


Figure 23 shows the R_s and B_o for the Bockstedt north MBAL model, which were correlated with Glasø.

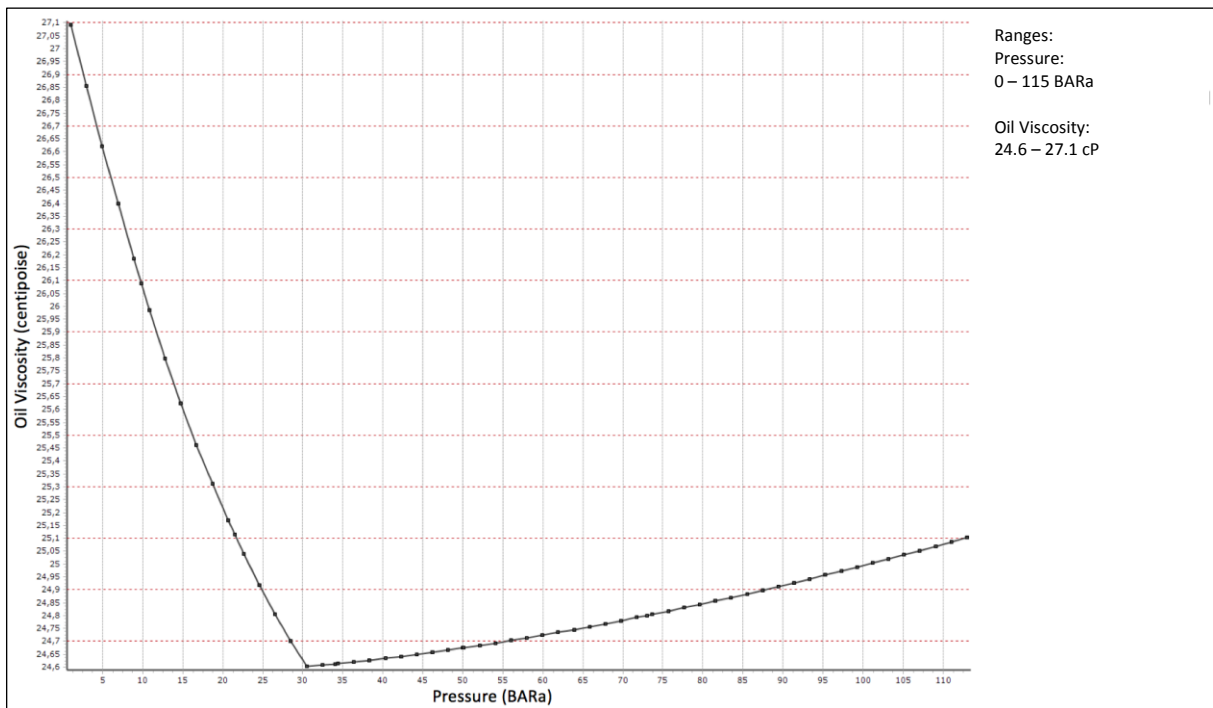


Figure 24 shows the μ_o for the Bockstedt north MBAL model, which was correlated with Beggs et al.

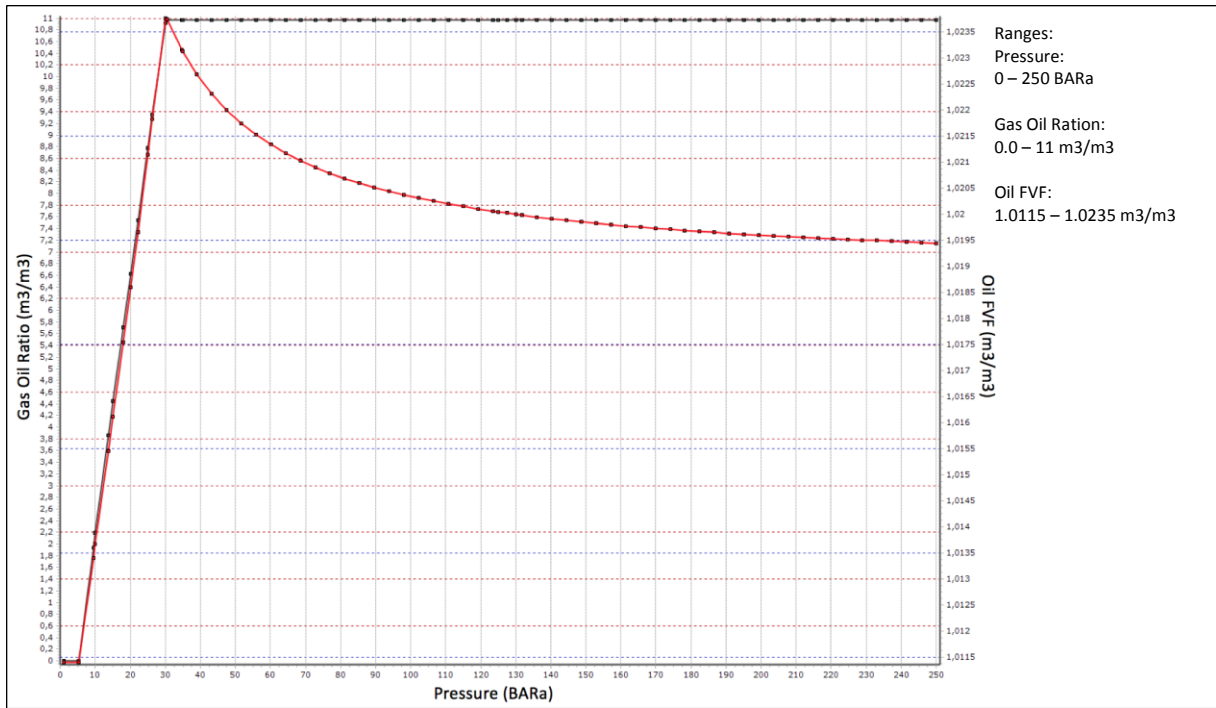


Figure 25 shows the R_s and B_o for the Bockstedt south MBAL model, which were correlated with $Gas\phi$.

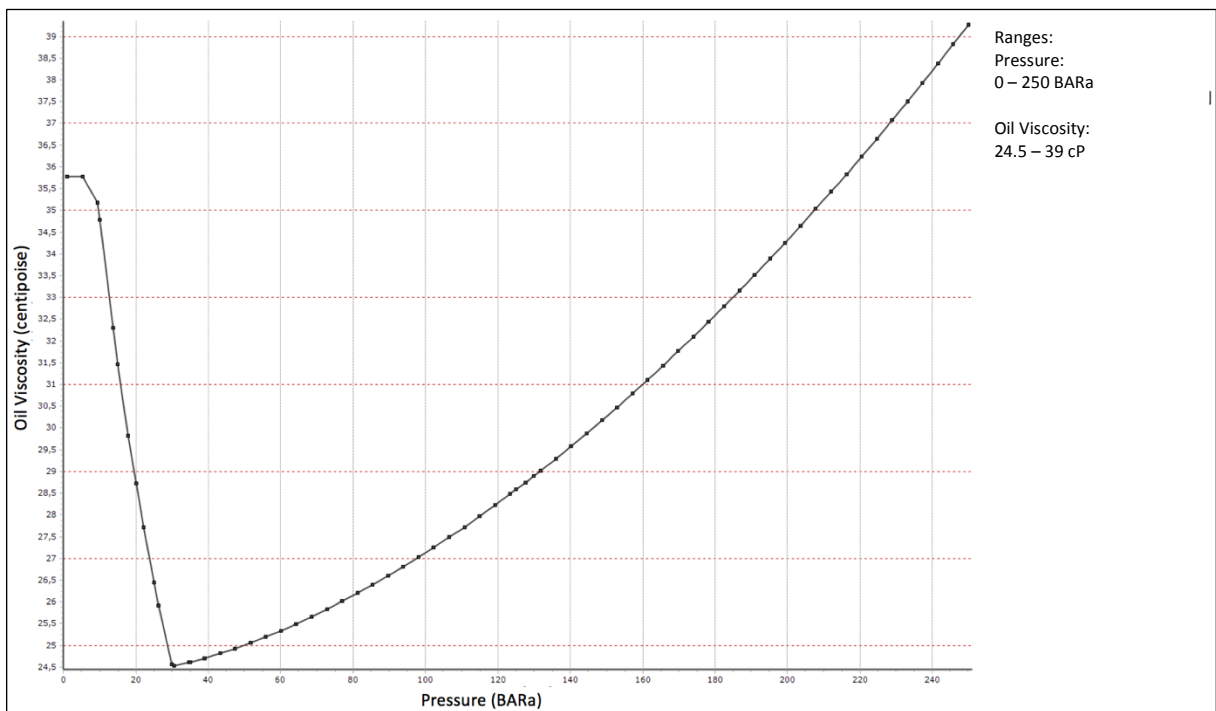


Figure 26 shows the μ_o for the Bockstedt south MBAL model, which was correlated with Beggs et al.

15 Dueste Eclipse Model

Compared to the Bockstedt Eclipse model, the Dueste Eclipse model is more developed and history matched. Therefore, it was able to use it in the full field model. The implementation process in RE-SOLVE is described in the chapter 'Eclipse Reservoir Simulator for Dueste'. A representation of the model can be seen in Figure 27.

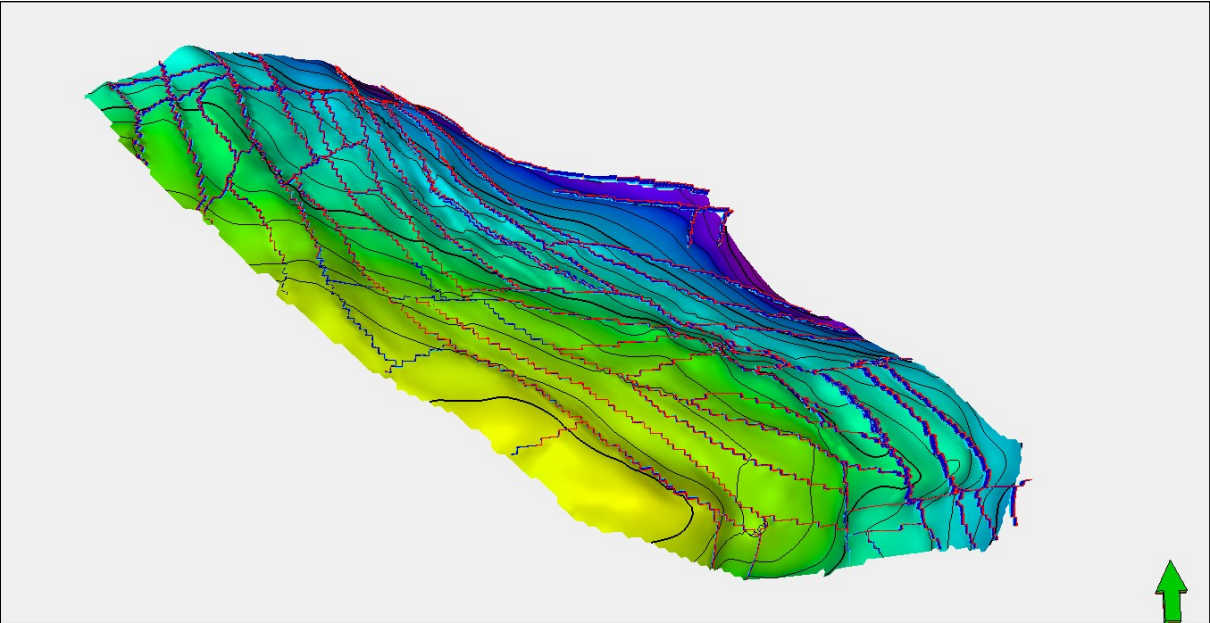


Figure 27 illustrates the Dueste Eclipse model, whereas the saturation property is plotted (blue = water; green = oil).

16 Modeling of Surface Facilities

16.1 Multiphase Pump

The multiphase pump in the field Bockstedt is located in the near vicinity of the Bockstedt 056 well-head. Its main purpose is to maintain pressure support for the pipeline transport from Bockstedt to the processing plant in Barnstorf over the distance of almost 4 km. Furthermore, it is a facility for actually saving energy as the backpressure for each well in the Bockstedt field is reduced and less energy per pump is needed. In the model, the multiphase pump was designed as a compressor to be able to insert a fixed pressure drop of 8.0 bar. This value was taken from the basis of the inlet and outlet pressures measured and saved in the ACRON database.

16.2 Injection Pumps

Due to model design purposes, the injection pumps are created as compressors in the GAP model. This allows defining a fixed delta pressure per facility. These delta pressure values were found in the ACRON database, where the inlet and outlet pressures of an injection pump are saved. The entries in ACRON allow on the one hand a cross-checking of the simulated downstream pressures of the injection pipeline segments and on the other hand an easy calculation of the delta pressure acting on the injection pump per injection well.

This approach would allow two different studies on the injection system. The first would be to analyze the prediction with a fixed delta pressure over the whole prediction time and the behavior of the injection rate can be investigated. This study can allow a timely decrease of injection rates, which were caused by various reasons be it directly dependent from the reservoir, because of the natural reservoir pressure decline or indirectly by backpressure effects in the pipeline network. A second approach that can be done is fixing the injection rates and observing the delta pressure at the injection pumps. This allows quickly investigating inflow inefficiencies. However, performing one of the mentioned approaches has its benefits but also weaknesses, so it is important always being aware of the underlying assumption of keeping one parameter constant, which is never realistic, but dependent of what the aim of the current study is.

17 Creation of an Integrated Model with RESOLVE

RESOLVE is used as the main control tool between the different IPM tools such as GAP, PROSPER and MBAL, and further to connect to the Eclipse reservoir simulator or Microsoft Excel files. The integrated modelling allows to fully connect various parts of a field as well as different network system for data exchange. With tools such as the event driven scheduling or the visual workflows it is possible to fully control the system and trigger certain events at various stages in the solving process. Important to note is that using a reservoir simulator within RESOLVE two kinds of timesteps are present (Figure 28). The first timestep is the one used by RESOLVE and is necessary to transfer data from one operating application to another. During this data transfer, it is possible for RESOLVE to save, write or manipulate the data stream. The second timestep is then the internal one used by the simulator for convergence. A synchronization will be performed between the RESOLVE timestep and the internal one from an application to obtain consistency. As it can be imagined, the RESOLVE timestep has always a wider range and the reservoir simulator timestep is allowed to take as many timesteps as needed to reach the RESOLVE timestep.

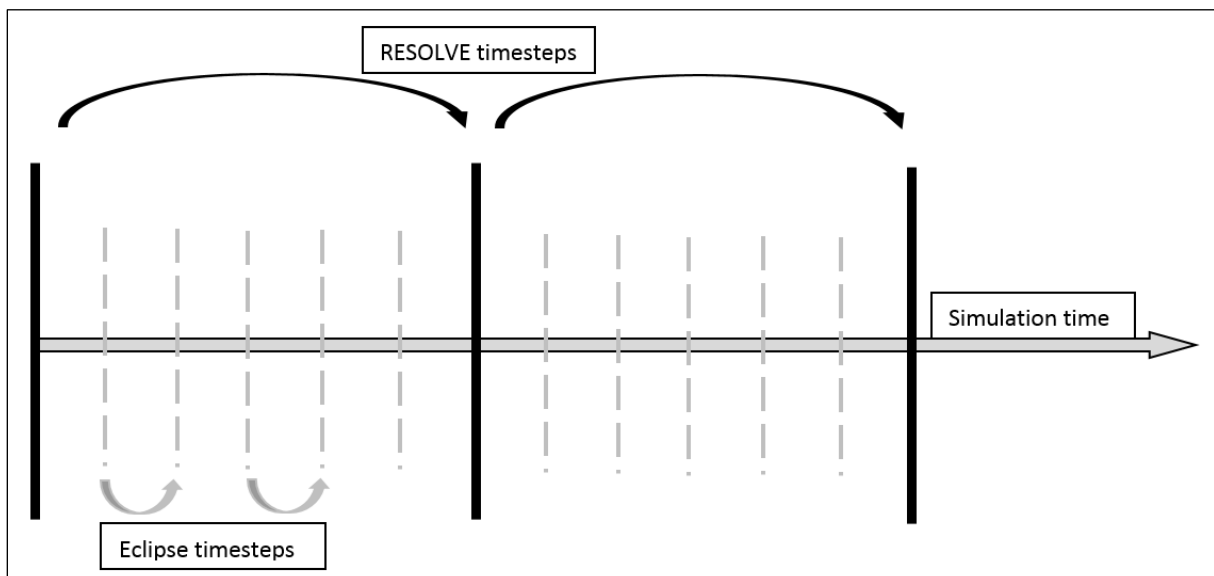


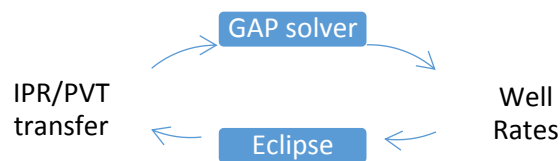
Figure 28 shows the timestep handling between RESOLVE and an external application as for example Eclipse. Between two RESOLVE timesteps Eclipse can use as many steps as needed to converge, whereas a synchronization action will be performed between RESOLVE and Eclipse prior to any further solving action.

Four main important things were investigated when handling the data flow between RESOLVE and the Eclipse reservoir simulator. The first one is that at each timestep from RESOLVE a query is sent to the reservoir simulator to get the inflow performance relationship of each well and further the updated PVT model. The fact that previously in PROSPER one IPR per well was used to match the VLP has now to be aware of, because in the reservoir simulator more than one IPR per well is present, because the inflow is coming from more than one grid block. Therefore, the IPR will be obtained through an in RESOLVE defined scaling method. Secondly, these scaled IPRs are then further passed as lookup tables together with the PVT from the reservoir simulator to GAP. It is very important to define the IPRs in

GAP as lookup tables and not as per default from the underlying PROSPER anymore, otherwise full consistency cannot be guaranteed.

As a next step after the transfer of all data from the simulator to GAP the network in GAP will be solved taking into account the full-integrated response of the system as well as all constraints previously defined in RESOLVE.

The last action is that RESOLVE sends the results such as well rates back to the reservoir simulator, because the reservoir simulator is controlled in rates during a RESOLVE timestep.



It is possible to read or write data in RESOLVE at almost every point in the calculation scheme. Generally, before the GAP systems are solved, which is at the so-called PreSolve state or after solving the networks, which is called the PostSolve. In order to establish all these connections between various tools and to be able to transfer data and to synchronize the timesteps, RESOLVE uses application drivers. Before the setup, it is necessary to configure and establish the needed drivers, where most of them are already pre-installed and have just to be auto registered.

17.1 Implementation of Application Objects

Application Objects in RESOLVE allow the implementation of different software applications such as reservoir simulators like Eclipse or Microsoft Excel. It is able to select the needed object from a predefined list and after inserting, it is necessary to define the path of the underlying project. Moreover, each individual object has some further settings to ensure correct data handling and transfer. The full field model in this thesis requires inserting four application objects. Two GAP software objects, one for the production and one for the injection system, one Eclipse100 reservoir simulator for the underlying Dueste model and one Microsoft Excel file to better comprehend the water rate transfer between the production and injection GAP network. The underlying MBAL models for the Aldorf and Bockstedt fields do not have to be implemented as application objects in RESOLVE as they are directly implemented as tanks in GAP. In RESOLVE, it is also possible to extract application variables even from the underlying MBAL tanks, although they are not directly implemented as application objects in the workspace itself.

17.1.1 GAP Production and Injection Network

The first application object inserted was the GAP production system. After defining the path to the already created surface network, the enabled wellheads were extracted to the workspace in RESOLVE. Whereby RESOLVE distinguishes immediately between data providers (sources) and data receivers (sinks). A data provider is therefore from the view of the surface network all injection wells as they

provide the water rate data. The production wells are then data receiver, as they need the liquid rate data from an underlying reservoir model, be it a simulator, a material balance tank or just a decline curve. It was further defined in the GAP application object settings to save the forecast snapshots, because this will make debugging and the study of individual wellbore behavior possible. Another additional decision that was made is to split up the individual separation streams for oil, water and gas of the GAP production network. These output streams of the phases allow a further connection to a Microsoft Excel file. Furthermore, it was defined not to perform a regression on the IPR data passed from the reservoir simulator to the GAP and to pass the table IPR data from the simulator directly to the GAP network solver. This decision was made to have a direct data transfer and no manipulation in between, as the regression would add further uncertainty to the data.

17.1.2 Eclipse Reservoir Simulator for Dueste

The field Dueste is the only field where currently a valid history matched Eclipse model is provided. This matched case of the Dueste field is called the BASE case and was run until 01.10.2014. Therefore, the prediction simulations start from a restart case based on this matched base case. On the one hand, this allows fast initialization and results, but on the other hand starting from an earlier date than 01.10.2014 will result in errors as the schedule file for the restart case was adjusted for RESOLVE implementation.

Firstly, it is recommended by Petroleum Experts to remove all underlying lift curves in the Eclipse model. This action should be done if the lift curves from the network (PROSPER) and the ones from Eclipse are not fully consistent. In fact, the possibility not having fully consistent lift curves in every well for each timestep is very high.

Secondly, all time schedule data has to be removed from the schedule file, because RESOLVE will act as the controlling tool and all changes and adjustment at certain times can be made from RESOLVE. Therefore, it is necessary to define mainly the well specifications (WELSPECS) and completion data (COMPDAT) at the time of initialization, so the 01.10.2014.

The WELSPECS section consists mainly of six columns for input data as well name, group name, I direction, J direction, referenced bottom hole pressure and preferred phase. Petroleum Experts recommends not using wellbores under group controls, however, groups can be used for reporting purposes. The group setting was inherited from the initial definition and therefore all active production and injection wells are in 'GROUP 1'.

The COMPDAT section consists of 14 parameters, which had to be defined. These parameters are the following, the well name, neighbour grid in I, J, upper and lower K direction, the flag of the well be it open or shut, the saturation table number for the relative permeability, transmissibility factor, wellbore diameter, the effective flow capacity k.h, the skin factor, the D-factor for non-Darcy flow of free gas, the well penetration direction and the pressure equivalent radius according to Peaceman (Peaceman, 1995, November 1). All these completion data were already defined previously in Petrel during the modelling and matching procedure. Therefore, it was merely inherited and sorted. Moreover, for initialization it is necessary to define the characteristics of the wellbore be it an injector or

producer and the rates before the first simulation step. These first liquid rates or injection rates were taken from the well checker measurements or the ACRON database. The input of these data were guaranteed with the WCONPROD and WCONINJE command in the schedule file. The control data for production wells (WCONPROD) requires for initialization the well name, well flag, the control mode, oil, water, gas or liquid rate, the reservoir fluid volume rate target or the bottom hole pressure target. The well flag is set open by default and the control mode will be liquid rate for every production well, therefore the rates have to be inserted, as mentioned, from the well checker measurements. The latter two parameters were previously set to default and inherited with this setting. The control data for injection wells (WCONINJE) requires the following input parameters for input, the well name, fluid type to be injected, the well flag, control mode, the injection rate, reservoir fluid volume rate target and the bottom hole pressure target. The fluid type is for all injection wells defined to be water and the well flag is set by default to open. The injection rate is registered in the ACRON database therefore; it is possible to define it as an initial input, whereas the control mode has to be rate controlled. The reservoir fluid volume target is per default not set and the bottom hole target pressure is inherited. After setting up the redefining schedule file, it was able to start the Eclipse simulator from RESOLVE. The successful start automatically extracted all previously in the schedule file defined production as well as injection files. It was then one simple step through the RESOLVE internal connection wizard to plug the extracted sources and sinks of the reservoir simulator to the corresponding sinks and sources from the production as well as injection system. The whole RESOLVE with the two GAP systems, the Excel and the connected nodes be seen in Figure 29.

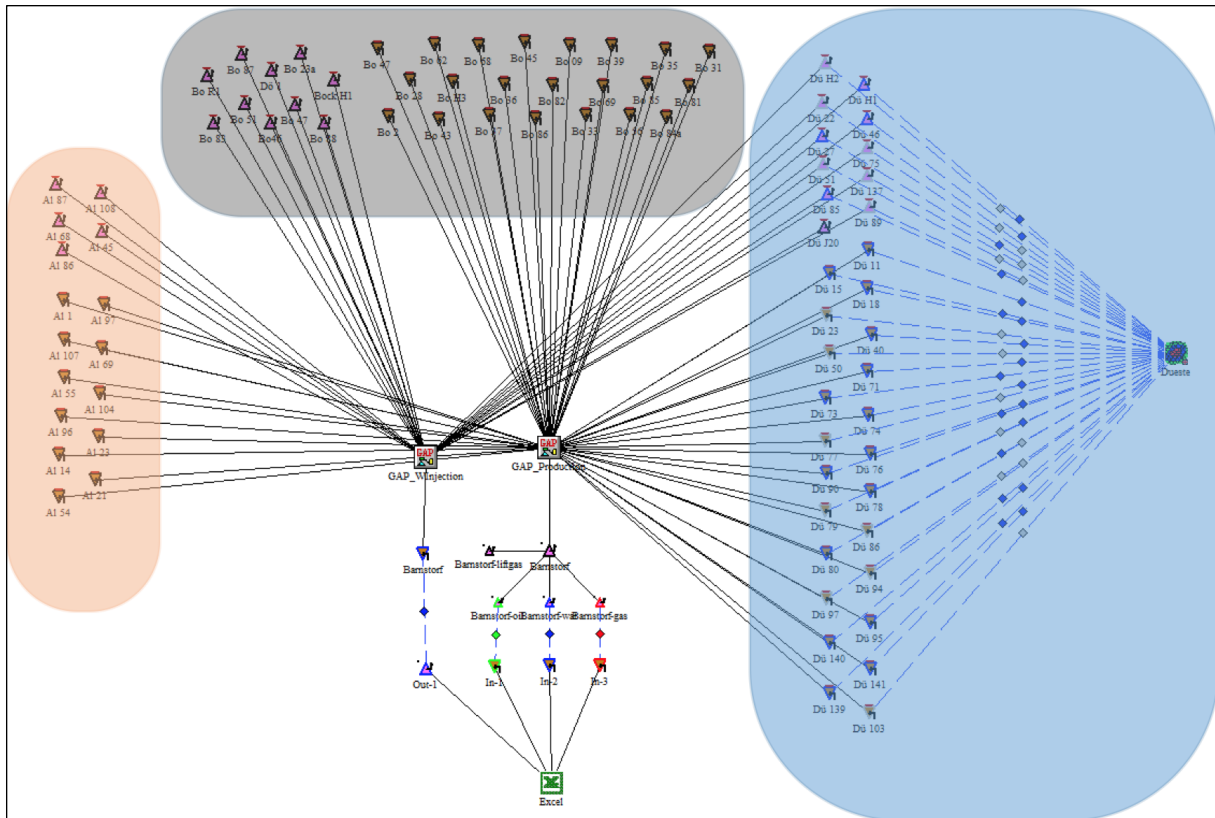


Figure 29 illustrates the connected nodes in RESOLVE between the Eclipse reservoir model for Dueste (blue) and the production as well as injection GAP networks. Furthermore, this overall view shows the Excel transfer file, whereas the three input streams for the oil, gas and water phase and the one output stream for the water target rate to the injection system can be seen. In the north there are the nodes for the Bockstedt wells (black) and in the west, the Aldorf connections (orange) are listed. Because the MBAL models are directly connected within the GAP production system, these nodes are not connected further in RESOLVE.

17.1.3 Microsoft Excel for Data Transfer Control

The connection between the GAP production and injection system is not performed directly through a target link, which would allow a direct connection between two application objects in RESOLVE. The reasons for splitting up the stream in oil, gas and water and performing the transfer of the water phase through an Excel file to the GAP injection system are the following. Firstly, to receive the produced amounts directly in Excel for further analyzation and processing. Secondly, as there is a forecasting and a solver section generated from RESOLVE in the Excel file it would be possible to manipulate the water target rates during the transfer or change the origin of data with for example an underlying macro. Thirdly, it is possible to work with the data in Excel, although the simulation run has not finished yet.

In Figure 30 a closer look of the transfer of the different phases from the GAP production system to the GAP injection system is given.

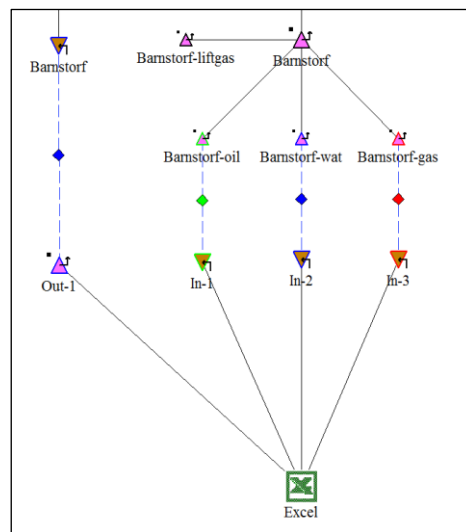


Figure 30 shows a snapshot of the data transfer from the production to the injection system through the Excel file. Four different source streams were provided from the separator in Barnstorf. The 'Barnstorf-oil' (green), 'Barnstorf-wat' (blue), Barnstorf-gas (red) and the 'Barnstorf-liftgas', which is not used as gas lifting is not applied. After importing the phases into different worksheets and sections in the Excel file the water target rate is further given to the Barnstorf injection manifold.

The structure of the Excel file for the transfer is designed as there is for each input stream an Excel worksheet generated and per sheet, as already mentioned a forecasting and a solver section. The former one saves the selected parameters such as rates, pressures, densities and temperature per phase for every timestep previously defined in RESOLVE. Whereas the latter one uses one line in the Excel file and updates it for every new timestep performed. Important to mention is that the calculated pressure from the production network as can be seen in column G in Figure 31 is directly transferred to the injection system. The higher pressure in the injection system can then be reached by introducing a compressor right after the manifold, as can be seen in Figure 6.

	B	C	D	E	F	G	H	I	J	K	L	M	N	O	P	Q	R
Date	Liquid Rate	Oil rate	Water Rate	Gas Rate	Pressure			Date	Oil rate	Water rate	Liquid rate	Gas rate	Pressure	Temperatur	oil s.g.	water s.g.	gas s.g.
01.10.2014	105,004191	105,004191	0	0	2,98676514			28.10.2015	96,6626715	0	96,6626715	0	2,98676514	10,7777585	0,88567377	1,1186176	0,76592648
15.10.2014	104,014164	104,014164	0	0	2,98676514												
29.10.2014	103,024286	103,024286	0	0	2,98676514												
12.11.2014	102,737719	102,737719	0	0	2,98676514												
26.11.2014	102,24902	102,24902	0	0	2,98676514												
10.12.2014	101,66645	101,66645	0	0	2,98676514												

Figure 31 shows a snapshot from the Microsoft Excel for data transfer between the GAP production and injection network in RESOLVE. Column B to G show the forecasting section, whereas column I to R represents the solver section.

18 Data Transfer Overview

Before running the first simulations, a summary of the previous chapters of the development process and the data flow between the individual tools will be provided. The following chapter approaches from the MBAL reservoir models across the individual PROSPER files per well to the surface GAP pipeline system for the network solving. On a second data stream, the underlying Eclipse Dueste model is connected in the RESOLVE software with the GAP system. In the RESOLVE tool, there is further the GAP production system with the injection system connected via an Excel file, which records the rates of the individual phases.

There are two different kind of reservoir representations in the full field system, the Eclipse Dueste model and the MBAL tank models. In Figure 32 the connection between the MBAL tank models and the PROSPER tool can be seen. The matched correlations in the created PROSPER files for each single well are fed with input parameters from the MBAL models for IPR generation. The calculated rates for a specific timestep are then handed back to the MBAL models.

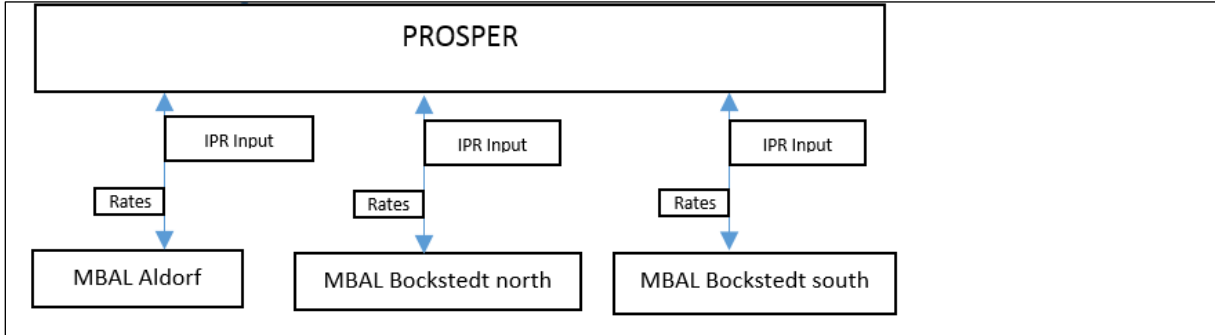


Figure 32 illustrates the data flow scheme between the MBAL tank models and the PROSPER correlations. It can be observed that the Input variables are handed from the MBAL models to PROSPER. Whereas after a new network solving action the rates are given to the MBAL models.

After the IPRs were calculated with the input data from the MBAL models, the next level are the GAP systems (Figure 33). In the GAP systems, the IPRs and the already generated VLPs were used for a network solving action for a specific timestep. The calculated rate data are handed back to the underlying MBAL tanks (Figure 32). An auxiliary tool, as can be seen in Figure 33 as the ‘Excel macro validation’, was built to allow a faster updating of pipeline properties and investigation of network solving actions. Furthermore, it involves a table, which allows the comparison of simulated, well checker and

PDMS data for the end of 2015. This comparison will be explained in the next chapter 'Verification Simulation Runs'.

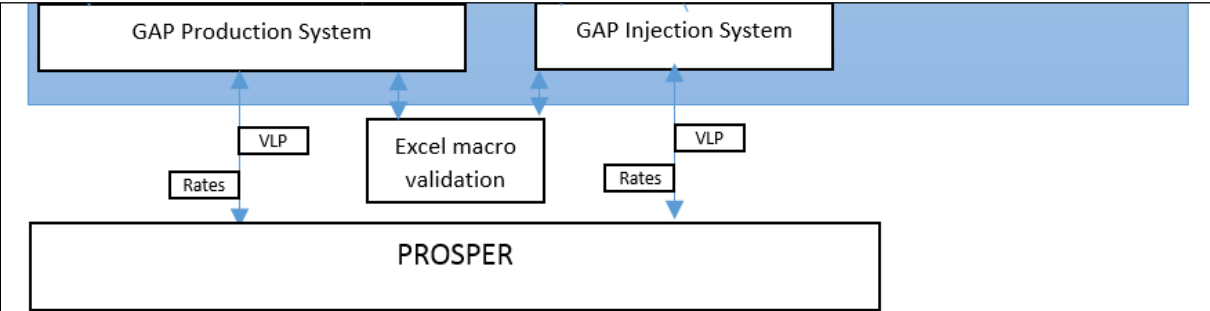


Figure 33 shows the transfer of data across the GAP production as well as injection system and the PROSPER correlations. The correlated IPRs and the corresponding created VLP are used from GAP for performing rate calculations. Furthermore, the Excel macro for updating and revising the pipeline parameters can be seen at this level.

In Figure 34 the whole scheme of the data transfer is shown. The blue area represents the RESOLVE tool within its connection to the application objects such as the Dueste Eclipse model, GAP production and injection system and the Excel for the rate transfer.

The Dueste Eclipse model gives the calculated IPR and PVT data for a certain timestep via the RESOLVE tool to the GAP production system. There, the data will be stored as lookup tables and the corresponding VLPs are taken from PROSPER. The newly calculated liquid rates after a network solve are then on the one hand passed back to the Dueste Eclipse model and on the other hand given to the Excel for rate transfer. In the transfer file, the water rates are further handed to the injection system; there it is used as a target constraint for the network solving action, but not directly back calculated. The calculated injection rates from the solver are then, on the one hand through RESOLVE to the Dueste Eclipse model and on the other hand to the underlying MBAL tanks transferred. As mentioned in previous

chapters the MBAL models are directly linked to the GAP systems, therefore they are not included as an application object in RESOLVE and outside the blue are in Figure 34.

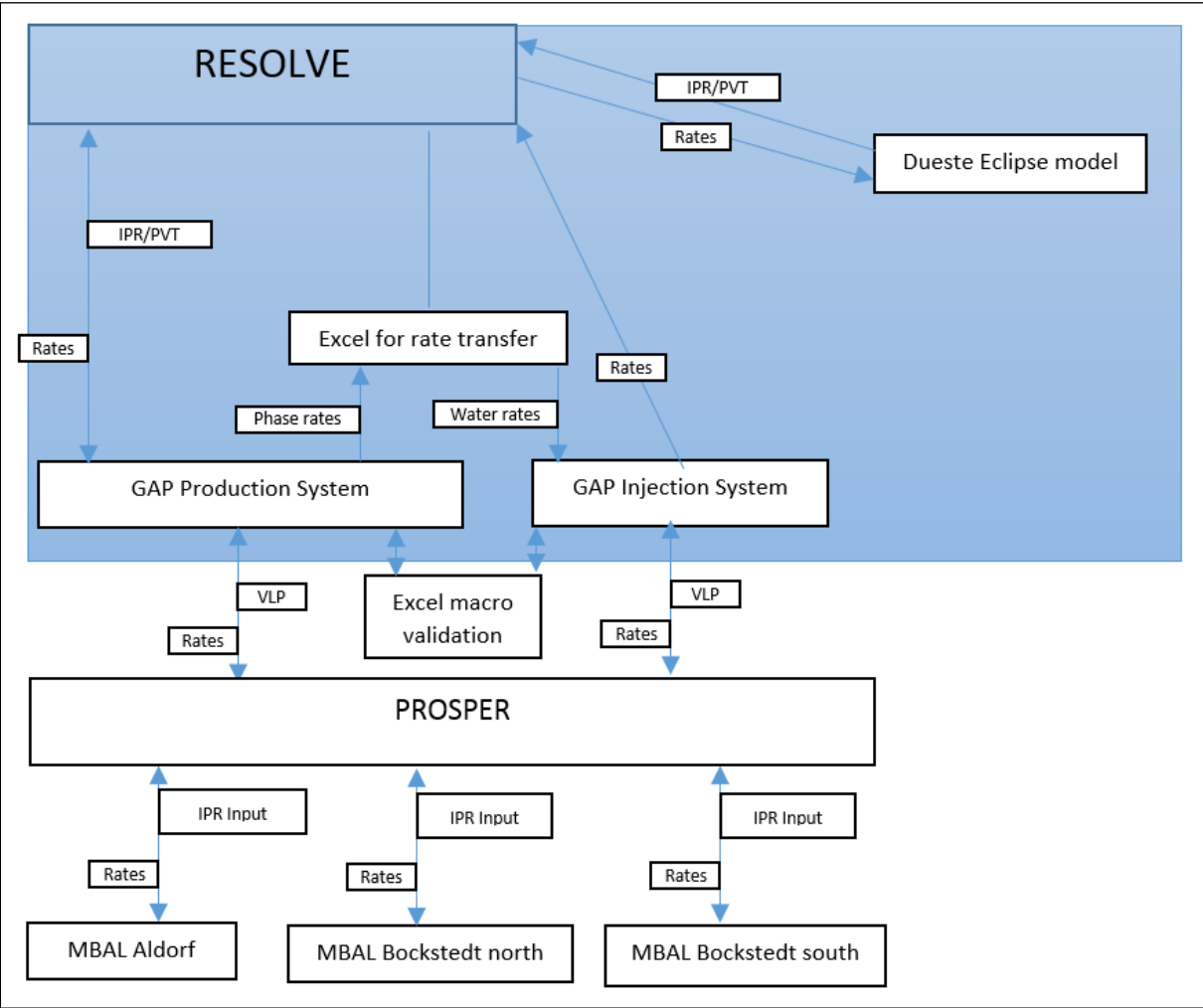


Figure 34 gives an overview of the whole system and how the data is transferred between the different applications. Two separate data streams can be investigated. The one coming from the Dueste Eclipse model and the second one from the MBAL tank models. Whereas both are connected in RESOLVE.

19 Verification Simulation Runs

After setting up the individual surface networks in GAP, be it the production or injection one, configuring all wellbores with their artificial lift system in PROSPER, building of a new MBAL model for Aldorf, revising the MBAL model for Bockstedt, adjusting the Eclipse for Dueste and creating various Microsoft Excel to OpenServer connections with VBA, it was all interconnected with RESOLVE. During the individual stages of setting up the various applications, the validity was tested on a small scale. For example, as described before, the well checker measurements matching with the efficiency or wear factors. However, this microscopic scale compared to the full field model neglects the great influences such as the interferences with other wells, networks and fields. It is of great importance to set up each part of the system as properly as possible with hence less uncertainty, but backpressure effects or bottlenecks over the whole system can just be recognized when performing full field simulation runs. Therefore, the following chapter covers the simulation on a field size to firstly adjust the liquid rates on a macroscopic scale and secondly to not yet be influenced by the backpressure effects of the other fields. The next step will be then to simulate the performance of all three fields Aldorf, Bockstedt and Dueste being connected. This action is necessary to be sure not having yet unknown interactions between the explicit fields.

The simulation runs for the validation has been performed between 01.10.2014 and 31.12.2015 with a timestep size of 2 weeks. The underlying reason is firstly, that the history matched base case of the Eclipse model for the Dueste field ends on the 01.10.2014 and therefore the restart from this case is performed in RESOLVE from this date on. If starting at a later stage in time the Dueste model has run anyway until this later stage. This setup would be on the one hand a loss in simulation time, therefore not efficient, and on the other hand not accurate, because VLPs will be first generated by Eclipse and at a later stage changed to the PROSPER generated ones. Secondly, the period is close to the present to have the latest production data as well as reports quickly present for comparison and validation. The timestep size of two weeks was then chosen to be on the one hand small enough to capture occurring effects and on the other hand, to be big enough to have fast simulation runs. The initial pipeline pressure in the productions system was taken from the IFIX system with 4 bar and the pressure for the injection system directly after the processing plant was inserted with 13 bar. These initial values were chosen for all field validation runs and furthermore no internal GAP optimizer was used for the runs to receive results faster.

19.1 Dueste

The first verification runs were performed in the field Dueste. It is necessary to disable the particular intersections in the pipeline network to receive production and perform injection into one field. The fact that the Aldorf and Bockstedt fields are both located in the north, and therefore separate already in the near neighborhood of the processing plant in Barnstorf from the pipeline in Dueste, allowed to disable both fields by just turning off one node in the system. After this action in the GAP production as well as injection network, the simulation time was defined in the schedule option in RESOLVE and the simulation was performed. Prior to the validation run in RESOLVE a network solving action was performed in GAP, which show the results as can be seen in Table 15.

Table 15 summarizes the results of the network solver for the field Dueste excluding Aldorf and Bockstedt from the system.

'Barnstorf' pressure	Liquid Rate	Water Rate	Oil Rate	GOR	WC	Temperature
[bar]	[Sm ³ /d]	[Sm ³ /d]	[Sm ³ /d]	[Sm ³ /Sm ³]	[%]	[°C]
4.0	845.9	823.8	22.2	13.6	97.4	9.8

The network solver run shows valid rates as they are in range between the PDMS and overestimating well checker measurements as can be seen in Table 2. After that rough check, the RESOLVE run was performed for the defined interval and the results for the individual wells in the Bockstedt field by 31.12.2015 can be seen in Table 16.

Table 16 gives a comparison of GAP simulation rates and well checker and water cut measurements for the individual wells in Dueste. Wells with blank fields are disabled ones, because they are not in production. The oil rates from the field measurements are calculated from the well checker and water cut measurements.

Wellbore	GAP simulation		Rates from field measurements	
	Liquid rate [Sm ³ /d]	Oil rate [Sm ³ /d]	Liquid rate [Sm ³ /d]	Oil rate [Sm ³ /d]
Dueste 011	134.6	5.5	135.0	4.0
Dueste 015	44.3	0.5	33.0	0.8
Dueste 018	96.1	0.1	130.0	3.0
Dueste 023				
Dueste 040	74.2	1.4	75.0	1.2
Dueste 050				
Dueste 071	35.1	0.1	28.0	2.0
Dueste 073	54.5	0.9	70.0	0.5
Dueste 074	28.4	0.01	5.5	1.2
Dueste 076	17.5	1.1	9.0	1.0
Dueste 077				
Dueste 078	15.7	0.7	18.0	1.0
Dueste 079				
Dueste 080	29.3	1.7	20.0	0.5
Dueste 086				
Dueste 090	55.1	1.7	1.0	0.9
Dueste 094				
Dueste 095	28.8	0.6	15.0	4.5
Dueste 097				
Dueste 139	92.9	4.9	50.0	1.0
Dueste 140	54.5	1.3	77.0	1.6
Dueste 141	34.2	1.0	40.0	1.4
SUM	795.2	21.5	706.5	24.6

Most of the oil production rates in Dueste are in range with the field measurements. Except some wells located in the southern part of the field like Dueste 078, 080 and 090 and Dueste 139 got significantly higher oil rates in the simulation than the measured ones. The well Dueste 090 in the south shows a much higher simulated liquid rate than the reported one. The same can be observed with Dueste 139. As the IPRs and the relative permeability curves are directly transferred from the Eclipse model, it would make no sense to adjust the underlying Darcy IPR models in the PROSPER files. Therefore, the VLP characteristics of the above mentioned wells were slightly adjusted by decreasing the pump efficiency factors.

The produced brine was then reinjected through the GAP injection system to the Eclipse reservoir model. The measured injection pressures and rates are taken from the ACRON system for comparison of the simulated data.

19.2 Aldorf

Performing a field verification run differs from that of the Dueste field, because the underlying reservoir model is now an MBAL model. However, firstly it was necessary to disable the node to the Bockstedt field in the north and the connection to the Dueste field in the east. The runs are then performed directly with the prediction function in GAP, as there is no need for RESOLVE at this stage, because the MBAL model is directly implemented in GAP and there is not any connection to the Dueste model or any workflow or event manipulations needed. Moreover, the simulation is performed more directly and therefore faster, as it is not necessary to pass data from RESOLVE to GAP or the opposite around. At the very beginning, before performing the simulation run for the defined time interval as in the introduction described, a network solve was performed. This action excludes further applications like the underlying MBAL model and is a GAP internal tool to see whether all input data are valid for one certain setting. The result of this network solving action at the processing plant in Barnstorf can be seen in Table 17. Comparing the results of the network solver with the PDMS and field measurements in Table 2, it is visible that the oil rate is with 9.4 Sm³/d significant lower. Nevertheless, this solving action can be seen as 'successful' as there were no extreme deviations or calculation errors accounted.

Table 17 shows the results of the network solver for the field Aldorf excluding Dueste and Bockstedt from the system.

'Barnstorf' pressure	Liquid Rate	Water Rate	Oil Rate	GOR	WC	Temperature
<i>[bar]</i>	<i>[Sm³/d]</i>	<i>[Sm³/d]</i>	<i>[Sm³/d]</i>	<i>[Sm³/Sm³]</i>	<i>[%]</i>	<i>[°C]</i>
4.0	277.5	268.0	9.4	405.8	96.6	9.9

The simulation run for the previously defined time interval with the set timestep allows a better study of the behavior of the system as the MBAL model is now encountered too. Three timesteps of the validation run were picked out in Table 18, the first one from 01.10.2014, 1 intermediate on 13.05.2015 and the latest one in 31.12.2015.

Table 18 illustrates the results of the first simulation run in Aldorf for three selected times.

Date	'Barnstorf' pressure	Liquid Rate	Water Rate	Oil Rate	GOR	WC	Temperature
	[bar]	[Sm ³ /d]	[Sm ³ /d]	[Sm ³ /d]	[Sm ³ /Sm ³]	[%]	[°C]
01.10.2014	4.0	297.6	287.5	10.1	574.9	96.6	9.8
13.05.2015	4.0	294.5	284.7	9.8	299.2	96.7	9.9
31.12.2015	4.0	290.9	281.4	9.5	152.1	96.7	9.8

The oil rate in the simulation run is still lower than expected from the PDMS. The missing amount could be explained with the wells Aldorf 097 and Aldorf 001. These two wells, which production is expected to come from the low-pressure compartment A, show no production during the whole simulation run. Having a look at the latest field measurements, it can be seen that Aldorf 001 has a liquid rate of approximately 10 m³/d with a water cut of 90%. This would result in a daily oil production of 1.0 Sm³/d for Aldorf 001. It is clear that this well is not very weighty compared to the whole field. Differently performs Aldorf 097. The production accounted from the well checker measurements are with about 14.0 m³/d not significantly higher than in Aldorf 001, but the water cut is with 40.0% much lower. This leads to an average oil rate of 8.0 m³/d, and could explain the missing amount in the simulation data compared to the PDMS allocation. A possible explanation of the missing production in Aldorf 097 and Aldorf 001 is that the reservoir pressure in compartment A is already at a very low stage of 11.0 bar, whereas the bubble point pressure of the whole Aldorf field is at 67.0 bar. The gas production is for matching purposes taken from the Finder database and therefore defined as a known, but highly uncertain property. In comparison, the amounts of gas saved in the Finder database are less than it would be with the pressure regime in the MBAL tank. This can be observed when having a look at the gas saturation trend in MBAL in compartment A, which increases enormously (Figure 35). This could indicate a growing gas cap in compartment A. Establishing a simulation run, the rates are assumed unknown and calculated by GAP, therefore all the gas starts to flow, which leads to a massive producing GOR of around 64,000 Sm³/Sm³, which can be investigated when reloading a snapshot of a certain simulation date in GAP. The inability of the well to flow could be explained therefore because of this massive producing GOR from the tank model. Effectively, the sucker rod pumps in Aldorf 097 and Aldorf 001 are attempting to 'pump' gas and not oil. Possible solutions to counteract this high producing GOR as it is a result of the material balance in compartment A, are to increase the tank pressure and therefore lower the gas saturation. However, this intervention would significantly disturb the history match and would have a too severe impact on the other tanks too. A further action, which is of great uncertainty are the underlying relative permeability curves, which were adjusted per wellbore in the GAP system. As the former mentioned approach would intervene and alter the already successfully history matched MBAL model severe, the latter approach will be intended.

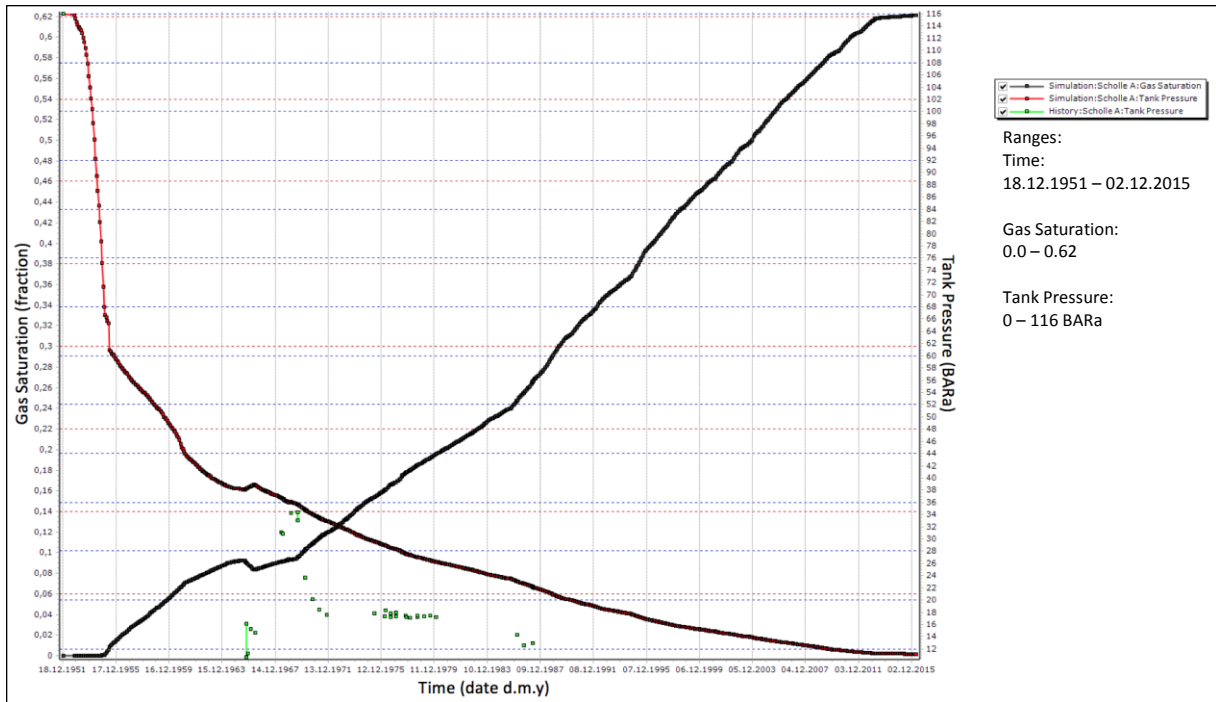


Figure 35 shows the pressure behavior and gas saturation over time in compartment A of Aldorf, which gives an indication of a growing gas cap. The scale on the left y-axis shows the gas saturation fraction, where it can be observed that the amount of gas grows up to 0.62 until the end of 2015. This shows a clear indication of a developing and steadily growing gas cap.

Furthermore, all other liquid and oil rates, which were active in the simulation, are compared in Table 19 for the 31.12.2015.

Table 19 gives a comparison of GAP simulation rates and well checker measurements for the individual wells in Aldorf.

Wellbore	GAP simulation		Rates from field measurements	
	Liquid rate [Sm ³ /d]	Oil rate [Sm ³ /d]	Liquid rate [Sm ³ /d]	Oil rate [Sm ³ /d]
Aldorf 001	0.0	0.0	10.0	1.3
Aldorf 021	61.5	1.1	70.0	7.0
Aldorf 023	23.1	1.6	20.0	2.0
Aldorf 054	76.3	1.3	105.0	2.0
Aldorf 014	29.5	1.2	35.0	4.0
Aldorf 096	29.9	1.2	31.0	1.5
Aldorf 097	0.0	0.0	13.5	10.0
Aldorf 104	30.2	1.2	30.0	0.5
Aldorf 107	40.3	1.6	40.0	1.5

Comparing the rates in Table 19, they show that wells with water cuts exceeding 95% are closer to the field measurements in the model than ones with lower water cuts. Examples for wells with lower water cuts are Aldorf 014 and Aldorf 021. This effect can be explained with the relative permeability curves as they were, as previously described, adjusted with the production data from the Finder database.

Although the daily back-allocation error is already high, this uncertainty increases when averaging the rates on a monthly basis. Furthermore, it is empirically known that the field measurements, which can also be seen in Table 2, overestimate the oil rates. Therefore, a re-adjustment of the relative permeability curves of Aldorf 014, Aldorf 021, Aldorf 054 for primarily reducing the water cut, as well as for Aldorf 001 and Aldorf 097 to reduce the effect of the gas, was performed to get closer oil rates to the field measurements.

Moreover, because of the altering of the relative permeability curves and their resulting higher oil rates, the overall simulated oil production of the Aldorf field increased too. It was also possible to alter the relative permeabilities in such a way that the Aldorf 097 started to get a liquid rate, which is on the 31.12.2015, 0.09 Sm³/d and an oil rate of 0.09 Sm³/d. The same was reached for Aldorf 001, which has a liquid rate of 0.06 Sm³/d and an oil rate of 0.06 Sm³/d after the relative permeability re-adjustment. The rates for the 31.12.2015 for the overall field after the relative permeability revision can be seen in Table 20.

Table 20 gives a comparison of GAP simulation rates with well checker measurements after relative permeability revision in Aldorf

Wellbore	GAP simulation		Rates from field measurements	
	Liquid rate [Sm ³ /d]	Oil rate [Sm ³ /d]	Liquid rate [Sm ³ /d]	Oil rate [Sm ³ /d]
Aldorf 001	0.06	0.06	10.0	1.3
Aldorf 014	29.0	3.2	35.0	4.0
Aldorf 021	58.4	4.1	70.0	7.0
Aldorf 023	20.5	1.4	20.0	2.0
Aldorf 054	45.2	2.4	105.0	2.0
Aldorf 096	29.4	1.2	31.0	1.5
Aldorf 097	0.09	0.09	13.5	10.0
Aldorf 104	29.5	0.6	30.0	0.5
Aldorf 107	39.7	1.6	40.0	1.5
SUM	251.9	14.7	354.5	29.8

As mentioned in the previous chapter with the Dueste field, the produced water was reinjected through the GAP injection system to the individual compartments.

19.3 Bockstedt

The field Bockstedt, located in the most northern part was handled like the Aldorf field, as the underlying reservoir model is an MBAL too. However, it has to be mentioned that this model was provided and not newly generated. The material balance model also allowed running the first field simulation without the use of RESOLVE. Performing network solve actions, which are not accounting the underlying MBAL models, show valid results for the rates when comparing with well checker measurements. The simulation run for the defined time interval shows great errors specifically in the northern part of

the field, which is known has strongly compartmentalized. The fact that some wells produce excessive liquid rates of nearly 1,000 Sm³/d and others were not be able to produce anything. Moreover, water injection wells, which are exceeding their constrained rates, resulted in unacceptable errors in the simulation runs. The small tank sizes of around 200,000 m³ of OIP for the northern compartments react very sensitive to small deviations of the rates. A short example for this high sensitivity could be as following. The current tank for representing the EOR compartment has an OIP of 146,414 Sm³. The three production wells Bockstedt 056, Bockstedt 081 and Bockstedt 085 and one water injection well, the Bockstedt 083 are active in this compartment. If each of the production wells would have a deviation in the simulation of just 3.0 Sm³/d in the oil rate, it would be a monthly increased oil production of:

$$\Delta Oil Production_{EOR} = 3.0 \frac{Sm^3}{d} * 3 Wells * 30 days = 270.0 Sm^3$$

As the rate data for history matching these small tanks are from the Finder database, the resolution is on a monthly basis. This is for a precise and meaningful match not reasonable. If the rates increase slightly on a daily scale as described above the monthly deviation can result in:

$$Deviation_{monthly} = \frac{270.0 Sm^3}{146414.0 Sm^3} \cdot 100 \% = 0.2 \%$$

This is firstly not acceptable for further prediction purposes over several years and secondly, as mentioned above, the deviation of the oil rates is much higher than 3.0 Sm³/d, so the monthly deviation would be much higher too. A further effect, the pressures in the small compartments start to oscillate extremely as in the EOR tank pressure ranges from 30.0 to 280.0 bar could be observed. This is not acceptable at all, therefore, with regard to the above reasons, it leads to the idea to further split up the field Bockstedt into a southern MBAL model and one for the northern compartments for the EOR, 84/86 and D compartment. The split of the field from a reservoir perspective will neglect any flow or backpressure effects between the northern and southern tanks. Nevertheless, it is nor reported nor expected to have a great connectivity between north and south, therefore this separation of the field for modelling is valid. Moreover, the separation made the inspection and therefore the history matching simpler as there were fewer parameters per MBAL model to account for. Like the first MBAL model, also the second one for the northern part was provided from a previous study. It was necessary to adjust the PVT between the two MBAL models before implementing the northern part. After the implementation of the second model the three tanks, EOR, 84/86 and D, which represent the northern part in the original MBAL model, were disabled. Therefore, the corresponding wellbores were connected to the newly implemented tanks of the second MBAL. The disabling of the above mentioned tanks lead to a missing pressure support of for the other tanks. This pressure drop could be fixed by increasing the aquifer support quite well. These performed actions for the Bockstedt field results in a daily oil rate of 62.82 Sm³/d on 31.12.2015 in the validation run, with an average water cut of 95%. In the following Table 21 a comparison between the validation run and the well checker measurements of the rates of each individual well can be seen.

Table 21 gives a comparison of GAP simulation rates and well checker measurements for the individual wells in Bockstedt

Wellbore	GAP simulation run		Rates from field measurements	
	Liquid rate [Sm ³ /d]	Oil rate [Sm ³ /d]	Liquid rate [Sm ³ /d]	Oil rate [Sm ³ /d]
Bockstedt 009	131.5	3.4	150.0	6.0
Bockstedt 028	55.3	1.8	28.0	13.0
Bockstedt 031	15.7	0.8	1.5	1.4
Bockstedt 033	0.0	0.0	0.0	0.0
Bockstedt 035	270.5	13.6	115.0	4.5
Bockstedt 036	195.7	14.9	216.0	20.0
Bockstedt 037	24.5	1.2	25.0	2.5
Bockstedt 039	144.9	7.3	170.0	7.0
Bockstedt 043	0.0	0.0	0.0	0.0
Bockstedt 045	122.9	6.2	130.0	7.0
Bockstedt 047	0.0	0.0	0.0	0.0
Bockstedt 056	27.3	1.9	98.0	3.6
Bockstedt 062	0.0	0.0	0.0	0.0
Bockstedt 068	30.2	0.8	43.0	2.7
Bockstedt 069	24.3	0.6	21.0	2.5
Bockstedt 081	0.0	0.0	14.0	2.5
Bockstedt 082	0.0	0.0	1.7	0.7
Bockstedt 084a	23.8	1.6	13.0	6.0
Bockstedt 085	74.0	5.1	80.0	0.08
Bockstedt 086	24.1	4.0	9.0	4.5
SUM	1,164.7	63.2	1,115.2	83.98

The brine was then reinjected through the GAP injection system to the individual compartments like mentioned in the previous two validation runs.

19.4 Full Field

After the adjustment of the relative permeability curves in the previous sections, minor IPR shifting actions in GAP to fit the performance even better and a re-creation of all IPR and VLP curves to make sure getting rid of inconsistencies, because of the re-adjustment actions, a full field validation run was performed. The results per well for the liquid rate (q_{liq}), the oil rate (q_o) and the water cut (WC) can be seen in Table 22. The table was created with a macro to quickly update the simulation data over the whole field. The PDMS and well checker rates were manually inserted for the comparison. The code for the macro can be seen in Appendix F.

Table 22 gives an overview of the full field validation run. A comparison between the simulation run (left columns), the well checker measurements (middle column) and the PDMS (right column) can be seen for the end of 2015.

Well	Simulation			Well Checker			PDMS		
	q_{liq} [Sm ³ /d]	q_o [Sm ³ /d]	WC [%]	q_{liq} [Sm ³ /d]	q_o [Sm ³ /d]	WC [%]	q_{liq} [Sm ³ /d]	q_o [Sm ³ /d]	WC [%]
Al 1	0.3	0.3	0.0	10.0	1.3	87.0	9.7	0.5	94.4
Al 14	29.3	3.2	89.0	35.0	4	88.6	30.3	2.1	92.9
Al 21	78.0	5.5	93.0	70.0	7	90.0	20.3	1.1	94.6
Al 23	22.5	1.6	92.7	20.0	2	90.0	20.5	1.0	94.9
Al 54	75.6	3.4	95.5	105.0	2	98.1	94.3	2.2	97.6
Al 55									
Al 69									
Al 96	29.8	1.2	95.9	31.0	1.5	95.2	32.5	1.2	96.3
Al 97	0.2	0.2	0.0	13.5	10	25.9	11.8	7.9	33.2
Al 104	29.3	0.6	98.0	30.0	0.5	98.3	38.3	0.3	99.2
Al 107	40.2	1.7	95.9	40.0	1.5	96.3	38.3	1.1	97.0
SUM	305.1	17.8		354.5	29.8		295.9	17.5	
Bo 02									
Bo 09	134.2	3.8	97.2	150.0	6.0	96.0	144.2	4.3	97.0
Bo 28	33.8	4.4	86.9	28.0	13.0	50.0	24.0	1.4	94.2
Bo 31	15.7	0.9	94.5	1.5	1.4	0.6	0.8	0.4	50.0
Bo 33									
Bo 35	108.8	6.0	94.5	115.0	4.5	95.0	108.7	5.3	95.4
Bo 36	240.0	15.3	93.6	216.0	20.0	90.0	200.4	3.0	98.6
Bo 37	23.4	1.3	94.5	25.0	2.5	83.0	13.5	6.3	53.3
Bo 39	142.8	7.9	94.5	170.0	7.0	96.0	137.2	7.8	94.3
Bo 43									
Bo 45	118.6	6.5	94.5	130.0	7.0	95.0	125.5	3.5	99.1
Bo 47									
Bo 56	55.6	4.8	91.3	98.0	3.6	98.0	89.0	0.8	95.4
Bo 62									

Bo 68	27.7	1.7	93.9	43.0	2.7	93.0	41.0	1.9	95.4
Bo 69	26.5	1.6	93.9	21.0	2.5	84.0	15.3	3.3	78.4
Bo 81	16.4	1.4	0.0	14.0	2.5	82.0	23.6	3.6	84.7
Bo 82	0.0	0.0	0.0	1.7	0.7	58.0	1.3	0.5	61.5
Bo 84a	21.8	4.7	78.5	13.0	6.0	48.0	18.3	9.1	50.3
Bo 85	37.4	0.8	97.7	80.0	0.08	99.0	38.0	2.0	94.7
Bo 86	17.6	3.2	81.6	9.0	4.5	40.0	12.1	7.7	36.4
<i>SUM</i>	<i>1,020.2</i>	<i>64.4</i>		<i>1,115.2</i>	<i>84.0</i>		<i>992.8</i>	<i>60.9</i>	
Dü 11	134.4	5.5	95.9	135.0	4.0	99.0	131.4	1.9	98.6
Dü 15	29.8	0.4	98.7	33.0	0.8	97.0	25.9	0.5	98.1
Dü 18	104.3	0.1	99.9	130.0	3.0	98.0	123.6	1.3	98.9
Dü 23									
Dü 40	74.2	1.6	97.8	75.0	1.2	98.0	70	0.5	99.3
Dü 50									
Dü 71	27.5	0.1	99.5	28.0	2.0	90.0	21.8	1.9	91.3
Dü 73	54.3	0.9	98.4	70.0	0.5	99.0	68.9	1.2	98.3
Dü 74	15.3	0.0	99.9	5.5	1.2	78.0	5	0.9	82.0
Dü 76	20.3	1.6	92.2	9.0	1.0	90.0	8.8	0.4	95.5
Dü 77									
Dü 78	23.0	1.2	94.7	18.0	1.0	95.0	11.2	2.6	76.8
Dü 79									
Dü 80	22.2	1.4	93.6	20.0	0.5	98.0	15.9	0.8	95.0
Dü 86									
Dü 90	9.2	0.5	95.0	1.0	0.9	10.0	1	0.6	40.0
Dü 94									
Dü 95	27.3	0.6	97.7	15.0	4.5	95.0	13.2	2.7	79.5
Dü 97									
Dü 139	47.7	2.3	95.2	50.0	1.0	98.0	47	0.6	98.7
Dü 140	46.0	1.2	97.3	77.0	1.6	98.0	68.8	0.7	99.0
Dü 141	27.8	0.8	96.9	40.0	1.4	93.0	35.1	1.3	96.3
<i>SUM</i>	<i>663.2</i>	<i>18.2</i>		<i>706.5</i>	<i>24.6</i>		<i>647.6</i>	<i>17.9</i>	

In Table 22, the difference between the three individual calculation schemes over the whole field. Once again, it is shown that the well checker is highly overestimating the liquid rate with 2,176.2 Sm³/d and the oil rate from the field measurements with 138.4 Sm³/d. The sum of the liquid rates of the PDMS concludes to 1,936.3 Sm³/d and the oil rates to 96.3 Sm³/d. Summing up the rates, be it liquid or oil, in the full field simulation result in 1,988.5 Sm³/d and 100.4 Sm³/d for the oil.

Table 23 gives a summary of the liquid and oil rates per field compared to the different systems. The data are from the end of 2015 and therefore differ from the comparison in the introduction (Table 2).

	Model		PDMS		Well Checker	
	q_{liq}	q_o	q_{liq}	q_o	q_{liq}	q_o
	[Sm ³ /d]		[Sm ³ /d]		[Sm ³ /d]	
Aldorf	305.1	17.8	295.9	17.5	354.5	29.8
Bockstedt	1,020.2	64.4	992.8	60.9	1,115.2	84.0
Dueste	663.2	18.2	647.6	17.9	706.5	24.6
SUM	1,988.5	100.4	1,936.3	96.3	2,176.2	138.4

It can be observed that the liquid rates simulated by the full field model are for each field between the well checker and the PDMS results, when comparing the different rates of the full field model, the well checker and the PDMS per field. For each field it can be seen that the simulated rates are much closer to the PDMS as to the rates measured by the well testing units. Furthermore, it can be seen that the calculated oil rates of the model are also between the PDMS and the well checker and water cut measurements. Even the oil rates are slightly higher are very close to the back-allocation per field from the PDMS.

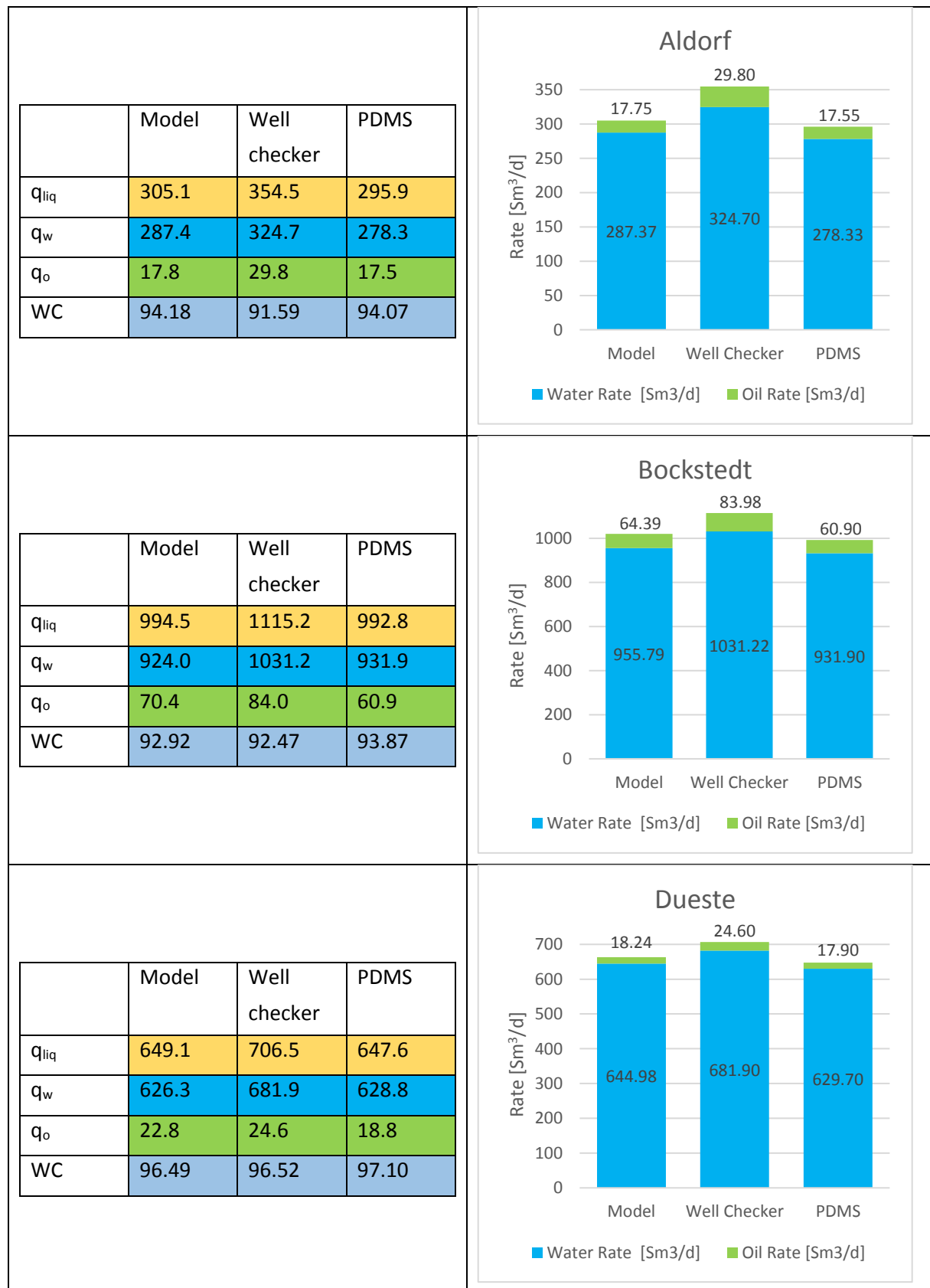
The individual deviations per field and system for the end of the verification run can be seen in Table 24. It can be clearly observed that the well testing unit highly overestimates the liquid rates, especially in the Aldorf field.

Table 24 summarizes the individual deviations per field and system for the end of 2015.

	Model	<i>PDMS</i>	<i>Well Checker</i>	PDMS	<i>Model</i>	<i>Well Checker</i>	Well Checker	<i>Model</i>	<i>PDMS</i>
	[Sm ³ /d]	[%]	[%]	[Sm ³ /d]	[%]	[%]	[Sm ³ /d]	[%]	[%]
Aldorf	305.1	3.0	-16.2	295.9	-3.1	-19.8	354.5	13.9	16.5
Bockstedt	1,020.2	2.7	-9.3	992.8	-2.8	-12.3	1,115.2	8.5	11.0
Dueste	663.2	2.4	-6.5	647.6	-2.4	-9.1	706.5	6.1	8.3

Table 25 shows the comparison between the PDMS, well checker and the full field model results for the end of 2015. The left column shows the rates per phase and water cut per calculation system. The charts on the right illustrate the rates as stacked column per field and calculation system. It can be observed that the liquid rate and are between the PDMS and the well

checker. The oil rates are close to the allocated rates from the PDMS and except of the Dueste field between the PDMS and well checker and water cut measurements. The rates are given in Sm³/d and the water cut in %.



The close fit of the oil rates between the PDMS and the simulation model shows that the model has a good match on a macroscopic point of view concerning the back-allocation. Furthermore, the full field validation run and the results of late 2015 show that the back-allocation of the PDMS on a field scale is satisfying, but it shows the overestimation of the rates of the well checker and water cut measurements.

Having a look at the simulation trend during the whole year in 2015 at the separator in Barnstorf, it can be observed that the liquid rate increases until July 2015 and then the growth steadily starts to attenuate and in October 2015 the liquid rate further increases (Figure 36). Contrary to this short attenuation of the growth the water cut is still rising, which also results in a small kink in the oil rate in October 2015 as can be seen in Figure 37. The minor changes in the slopes of the rates in October could be explained as a calculation issue from the model. A possible example could be given from Bockstedt, where various smaller tanks (EOR or 84/86) react sensitive to small pressure changes. In the whole system backpressure effects from another field could trigger a process that accelerates (or attenuates) the liquid and therefore, oil production if the slope of the water cut stays the same.

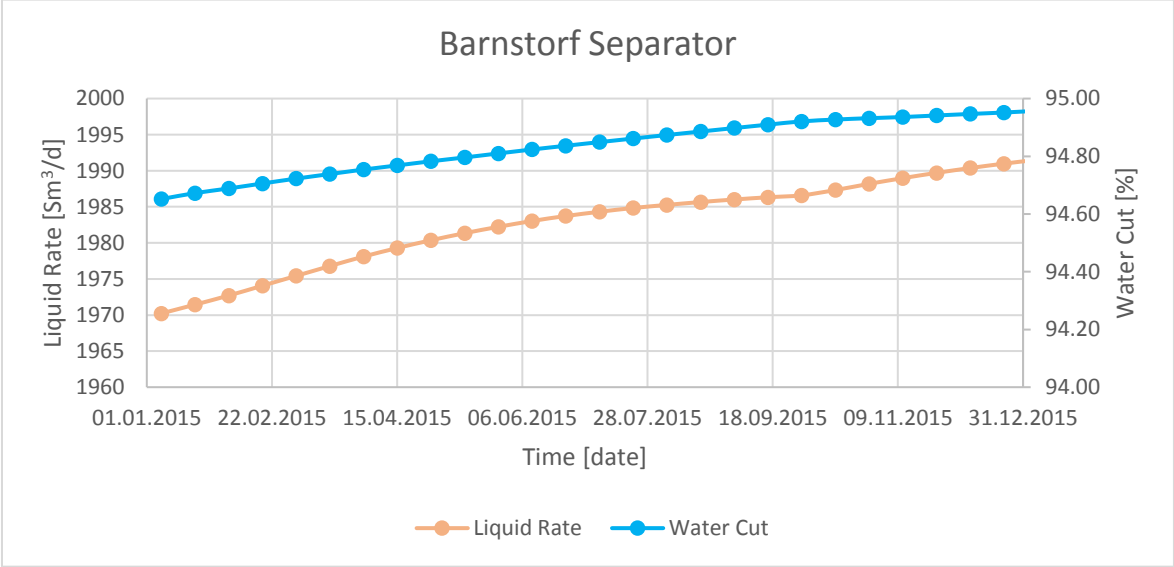


Figure 36 illustrates the liquid production and water cut of the full field model validation run in 2015.

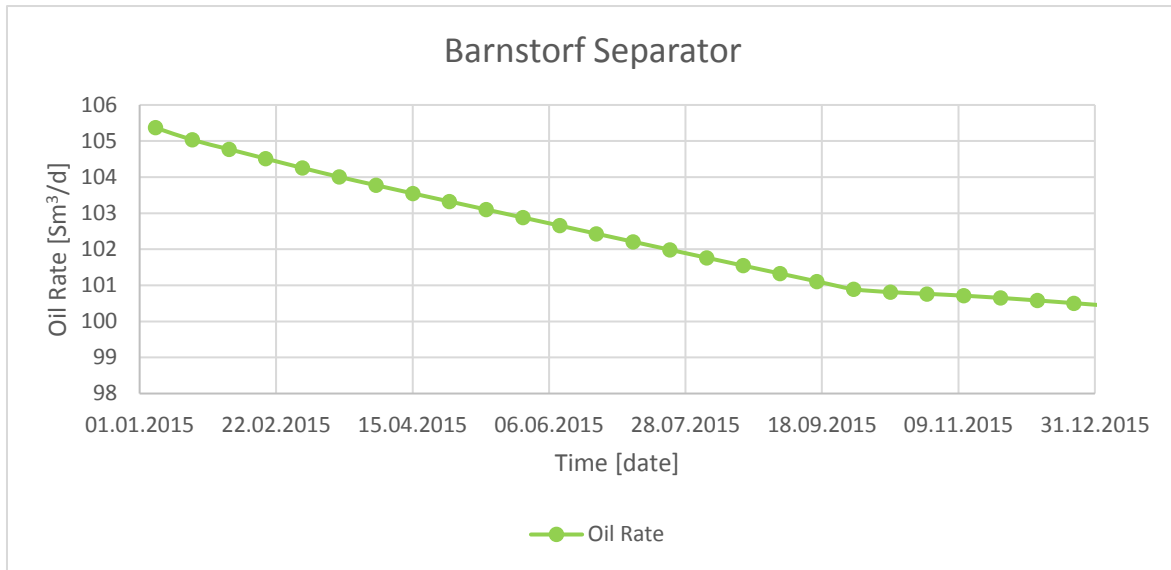


Figure 37 shows the oil rate in 2015 of the full field run. A steady decline can be observed.

Interestingly to see is that the company internal target rate for 2016 of 78.6 tones/d matches good with the full field model result by the end of 2015. The simulated oil rate and oil gravity for 31.12.2015 is 100.4 Sm³/d and 885.70 kg/m³. This results in 88.9 tones/d. The overestimation of 10.3 tones/d of the model, which concludes in a deviation of 13.1% based on the reported target rate. Keeping in mind the empirical uncertainty of around 30% of the back allocated production data, the deviation is from a macroscopic point of view in an acceptable range.

The liquid rate, oil rate and water cut of the full field validation run are further split up to the individual fields to better understand the allocation action of the model of the total rates, which were plotted in Figure 36 and Figure 37. The main pipelines were taken into account for this analysis, whereas for the Dueste and Bockstedt field pipeline connect the whole field, which are in the model Dü NÖ 2.0.1 and Bo NÖ 3.2. In Aldorf, it is different because there are three connections to the main pipeline, which further runs to Bockstedt. These three pipelines are in the model AI NÖ 1.1.1, AI NÖ 1.4 and AI NÖ 2.5.2. A snapshot of the pipeline connections can be seen in Figure 38. The individual pipeline rates were exported to Microsoft Excel for easier reporting preparation such as summation of the individual pipelines in Aldorf.

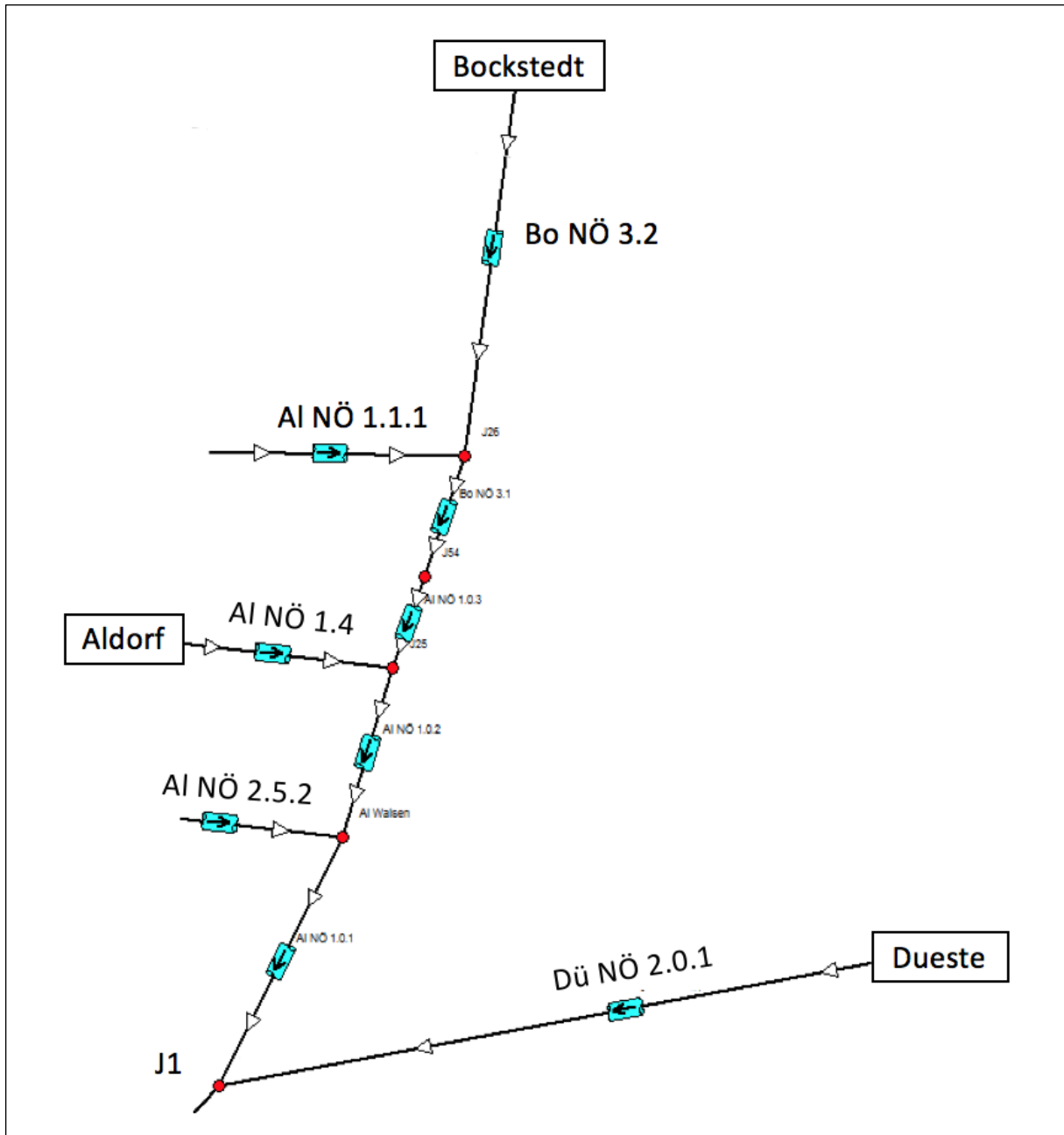


Figure 38 illustrates a snapshot of the GAP production system, where the main connection pipelines for the individual fields. The node J1 in the bottom left corner gives the direct connection to the processing plant in Barnstorf.

It can be observed that in Aldorf the water cut is slightly rising, but can be seen as constant with 94.25% during 2015. The liquid rate experiences also a minor decline, steadily from 306.8 to 304.8 Sm³/d (Figure 39). The oil rate shows the same declining trend as the liquid rate as can be seen in Figure 40 with a slightly shallower slope, because of the rising water cut.

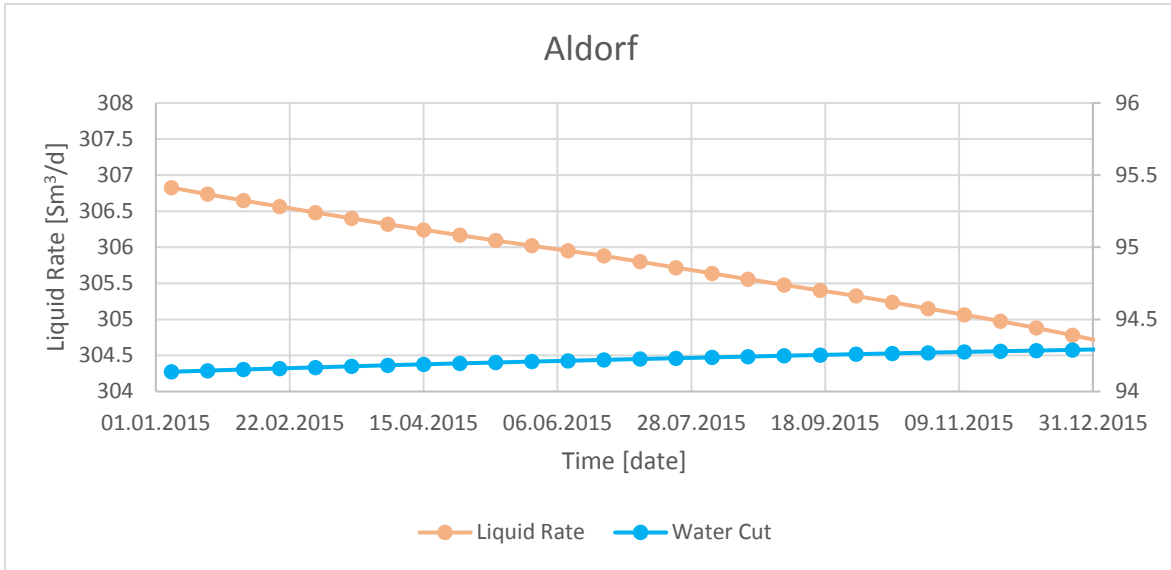


Figure 39 shows the liquid rate and water cut in Aldorf for 2015.

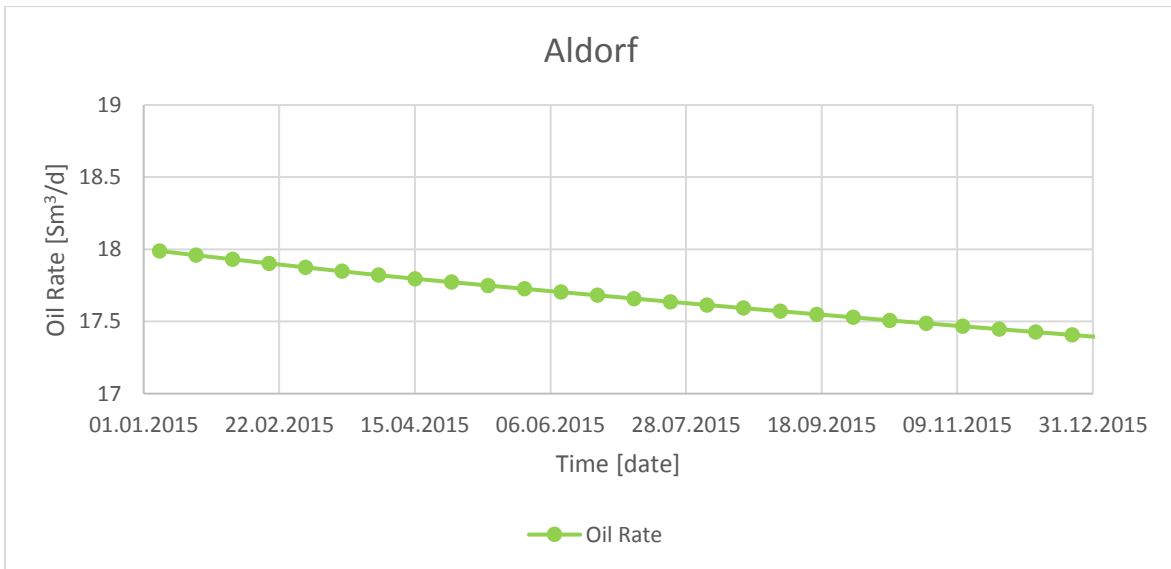


Figure 40 shows the oil rate in Aldorf for 2015.

The Bockstedt field shows the same effect with the kink in the liquid rate (Figure 41) as the separator in Barnstorf as can be seen in Figure 36. The increasing behavior of the water cut and decline of the oil rate (Figure 42) is also the same as before in the separator.

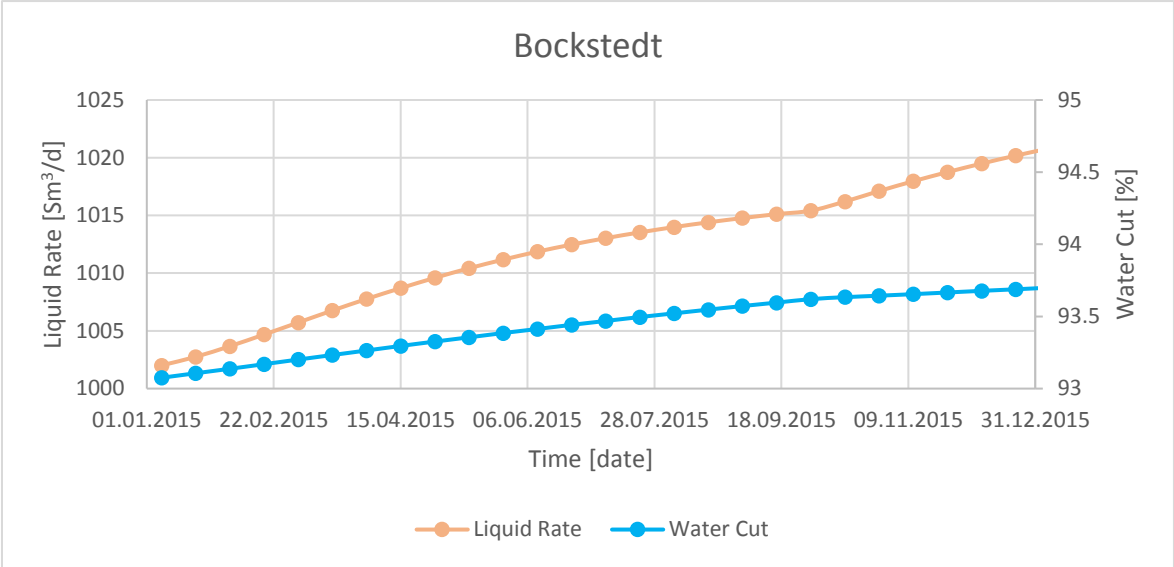


Figure 41 shows the liquid rate and water cut in Bockstedt for 2015.

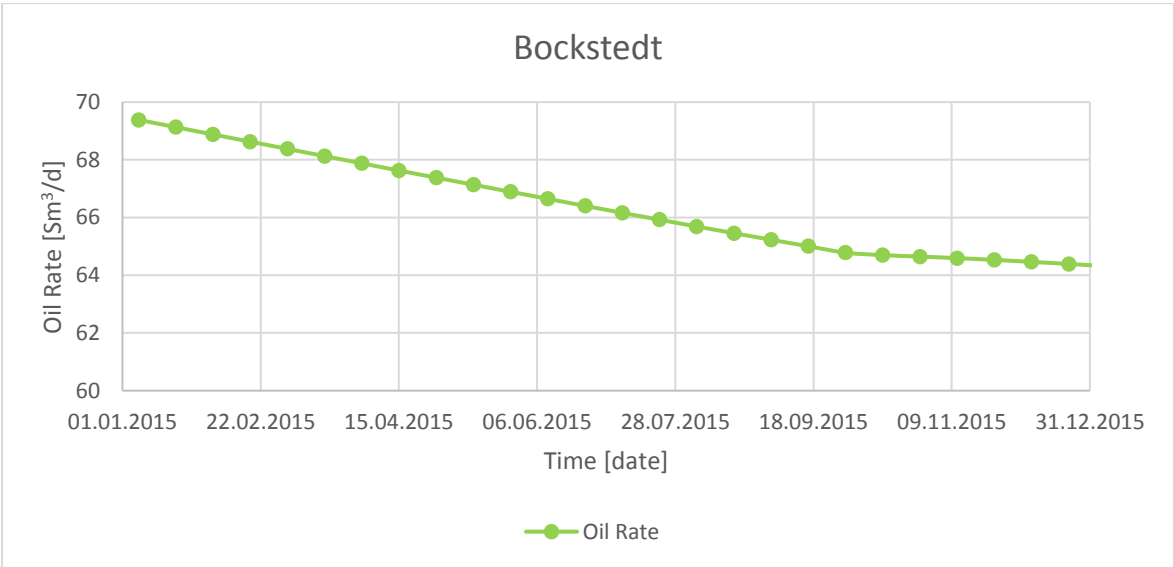


Figure 42 shows the oil rate in Bockstedt for 2015.

A trend, which is not expected at first, can be seen in the field Dueste in Figure 43. The liquid rate increases as in Bockstedt, or Aldorf before, but the water cut slightly decreases. Nevertheless, this decline in the water cut is minor when having a look at the scale and therefore not alarming as it can

be seen as a constant value of 97.25% during 2015. As an effect of this declining water cut the oil rate, as can be observed in Figure 44, is continuously increasing.

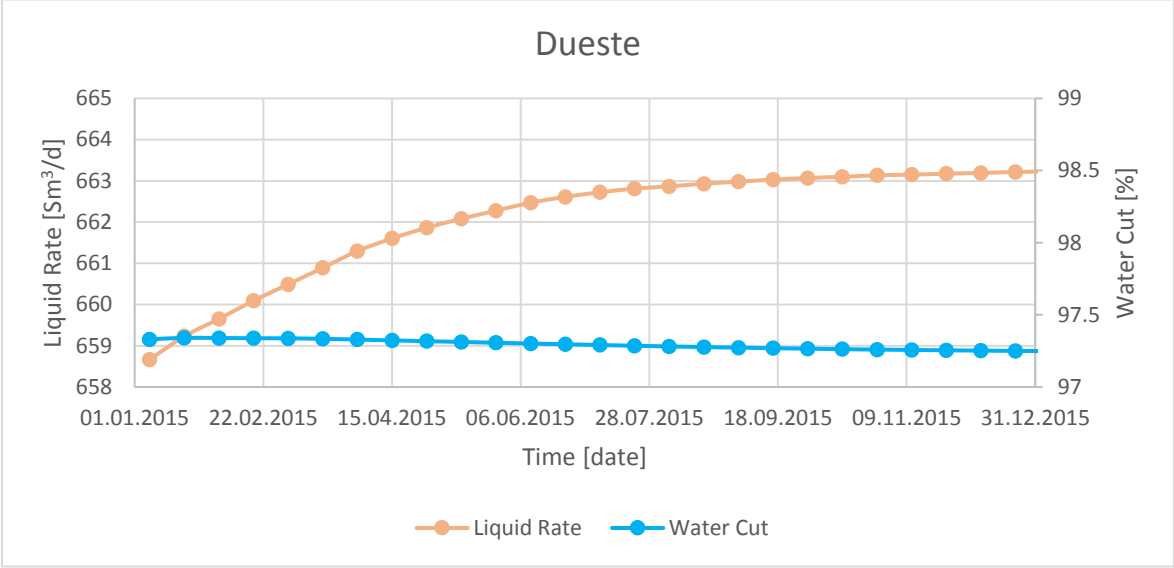


Figure 43 shows the liquid rate and water cut in Dueste for 2015.

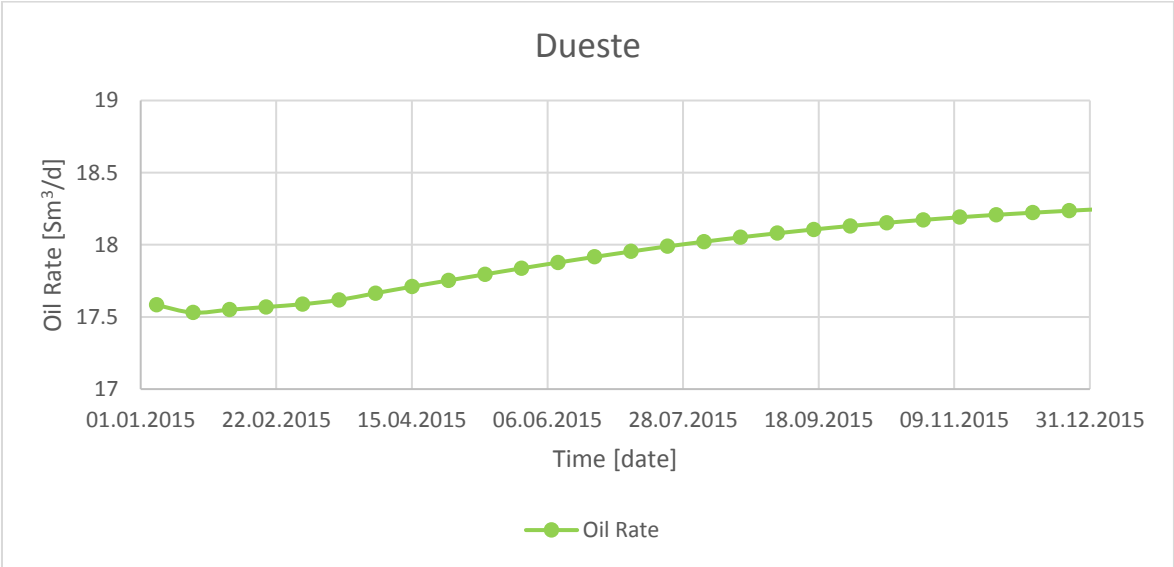


Figure 44 shows the oil rate in Dueste for 2015.

Moreover, the injection rates per well for the end of 2015 were verified and compared with the rates from the ACRON database. An important issue that was focused on was the injected amounts of water rate on a field scale, to keep the volume balance per field as accurate as possible. The next level of investigation was to make sure the balance per tank is in an acceptable range. Furthermore, it has to be reminded as mentioned in the chapter 'Data Transfer Overview' that the full field water rates are passed from the production system as target rates to the injection system. Therefore, deviations from the total produced water, which is transferred to the injection system and the amounts of the network solver at the injection system can occur. This deviation is expected to be higher at early simulation times when the model is still converging to the target rate.

The three different full field water amounts per 31.12.2015 can be seen in Table 26.

Table 26 shows the produced amount of water, which is passed from the production to the injection system as the target rate on the left. In the middle the amount of water, which was calculated by the network solver from the injection system can be seen. The right column illustrates the amount of water saved in the ACRON system.

	Produced Water	Injected Water	ACRON
	<i>[Sm³/d]</i>	<i>[Sm³/d]</i>	<i>[Sm³/d]</i>
Full Field	1,890	1,927	1,930

The target rate of 1,890 Sm³/d deviates on the 31.12.2015 37 Sm³/d from the amount calculated from the network solver of the injection system of 1,927 Sm³/d. The rate from the injection system compared to the approximate rate of the ACRON database differs 3 Sm³/d. The maximal deviation is given between the ACRON and target rate of 40 Sm³/d. The difference, be it 3 Sm³/d or 40 Sm³/d, is a very good fit. This can be stated, of two main reasons. The first one is when having a look at Table 24 the lowest deviation between the model and the PDMS in the Dueste field is with 2.4% higher than the one between the ACRON water and the target rate with 2.1%. Secondly, the individual water rates in the ACRON system are not constantly the same as they underlie variations and measurement errors. The following Table 27 shows the comparison between the calculated injection rates between the GAP system and the ACRON.

Table 27 illustrates the injection rates per well in Aldorf, Bockstedt and Dueste from the ACRON and the GAP injection network solver for 31.12.2015.

Injection Well	GAP Injection System	ACRON
	<i>[Sm³/d]</i>	<i>[Sm³/d]</i>
Aldorf 068	113	100
Aldorf 086	94	100
Aldorf 108	122	170
SUM	329	370
Bockstedt 046	246	250
Bockstedt 051	98	80
Bockstedt 083	110	100
Bockstedt 087	137	100
Bockstedt 088	105	120
SUM	696	650
Dueste H1	310	350
Dueste H2	0	100
Dueste 022	177	170
Dueste 027	152	90
Dueste 046	183	100
Dueste 085	80	100
SUM	902	910

The rates per field have a maximum deviation in Bockstedt of 46 Sm³/d (7%), which is acceptable. Furthermore, Bockstedt 087 and Bockstedt 088 are both injecting into the same tank, which allows summing up the rates for comparison. This leads to 242 Sm³/d compared to 220 Sm³/d, which slightly reduces the uncertainty for this part of the field.

The highest deviation is in Dueste H2, where there is no calculated rate with the given input parameters, but the ACRON system shows an injection rate of 100 Sm³/d.

Moreover, interesting to see is, when comparing the injection rates in Table 27 with the produced water rates per field of Table 25 that the volume balances per field are not given. Especially in Bockstedt, where approximately 200 Sm³/d are less injected and Dueste, where the injected amount is almost 300 Sm³/d higher than the produced water. The Aldorf field is not experiencing such alarming differences in the injection – production volume balance.

This effect could be explained with an injection into an aquifer, which would account for higher injection rates like in Dueste H1 or Dueste 22, which injection pressures are accounted in ACRON with 16 bar and 40 bar. Contrary, Dueste 027 or Dueste H2 show much lower injection rates or were not able to design an injection rate at all with the given input. The injection pressure is for Dueste 027 50 bar and Dueste H1 12 bar. An explanation for this could be that they are not injecting into an aquifer with a combination of a highly damaged near wellbore area, which would fit with designed PROSPER of Aldorf and Bockstedt too.

20 Full Field Forecasts

After the systematic adjustment of the whole model – the production as well as the injection part – as described in the previous chapter ‘Verification Simulation Runs’ short term prediction runs from 01.01.2016 to 31.12.2020 were performed with a time interval of 2 weeks.

Three different scenarios were created, whereas in the first scenario, all production and injection wells were active and no alteration of the input data was performed. In the second forecast scenario, it was assumed that the strongest production wells in Bockstedt were disabled. Starting on January 2017 and shutting down one producer by the beginning of every month. The third scenario represents the case when the wells in the injection system continuously stop to work. The shutdown of the injection system is performed per field. Firstly, the injection wells in Aldorf will be turned off by the beginning of 2017 followed by Bockstedt after 6 months and Dueste by the end of 2017.

These scenarios with their different settings were created in RESOLVE with the scenario manager and the event driven scheduling tool. At first the ‘masking’ property per well was imported from GAP to RESOLVE, which allows to enable and disable certain facilities, such as wells and pipeline segments. As a next step, the schedule for the individual scenario was created in the PreSolve section.

20.1 Scenario 1

In scenario 1 no alteration or shutdown of individual facilities was performed. The simulation results for the individual fields from 01.01.2016 to 31.12.2020 can be seen from Figure 45 to Figure 50.

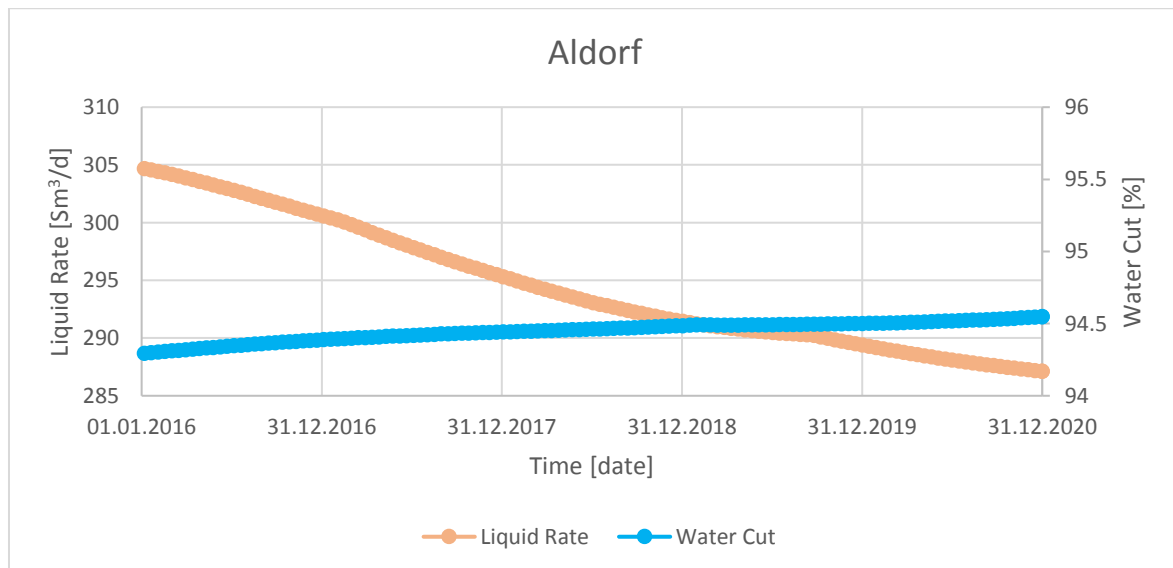


Figure 45 illustrates the liquid rate and water cut forecast in field Aldorf from 01.01.2016 to 31.12.2020.

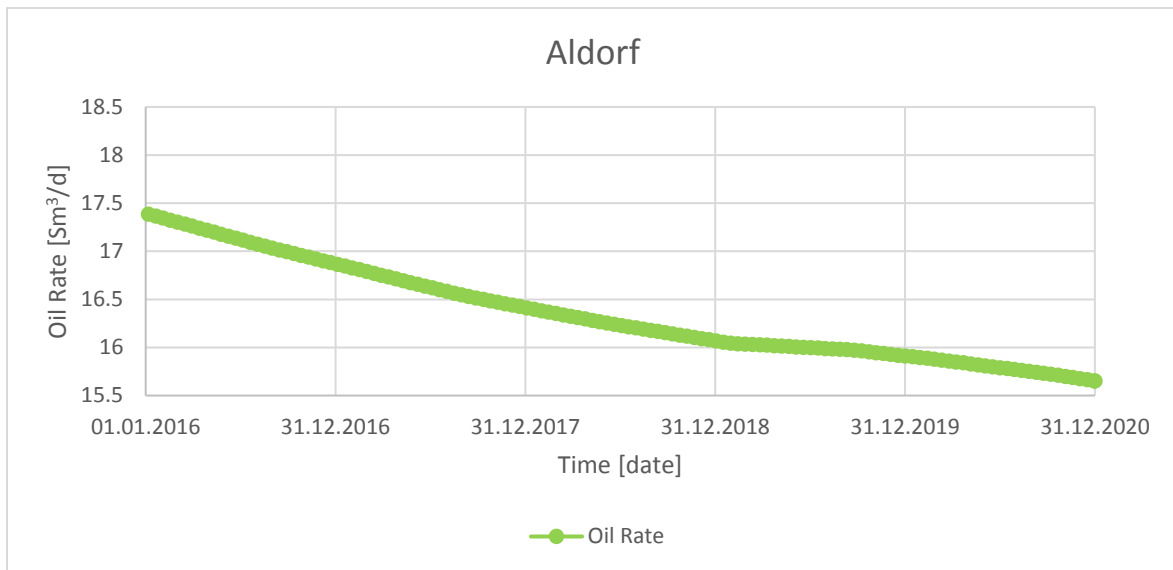


Figure 46 shows the oil rate decline in field Aldorf from 01.01.2016 to 31.12.2020.

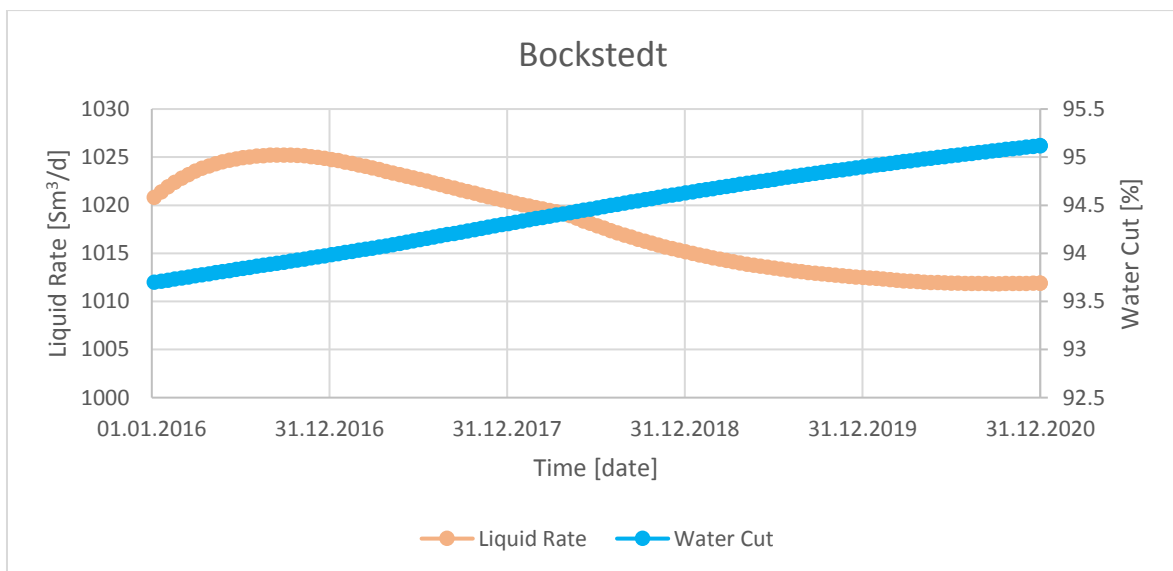


Figure 47 illustrates the liquid rate and water cut forecast in field Bockstedt from 01.01.2016 to 31.12.2020.

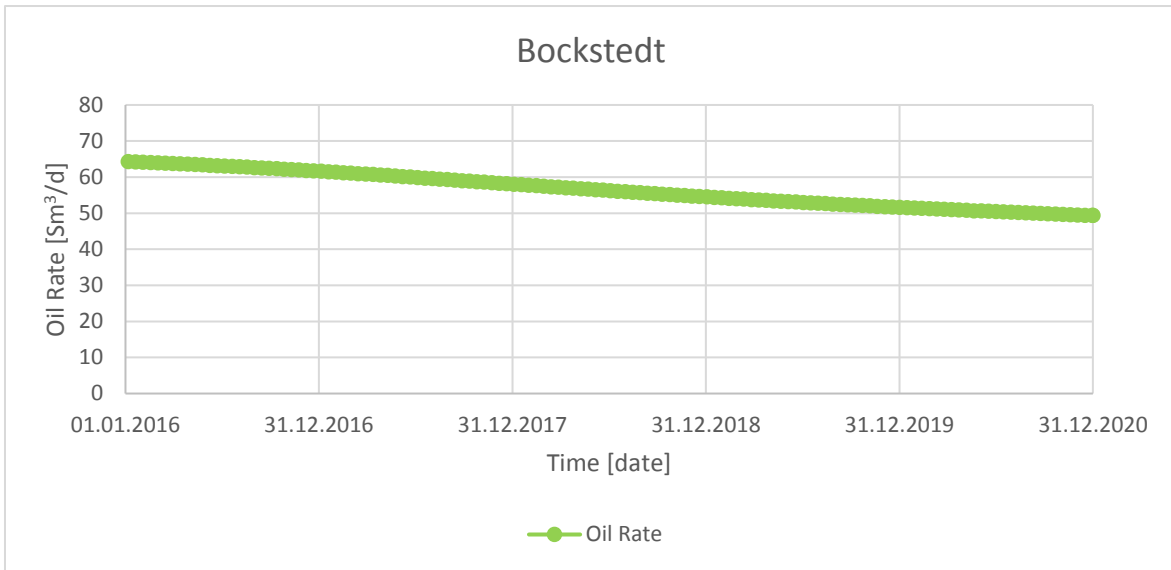


Figure 48 shows the oil rate decline in field Bockstedt from 01.01.2016 to 31.12.2020.

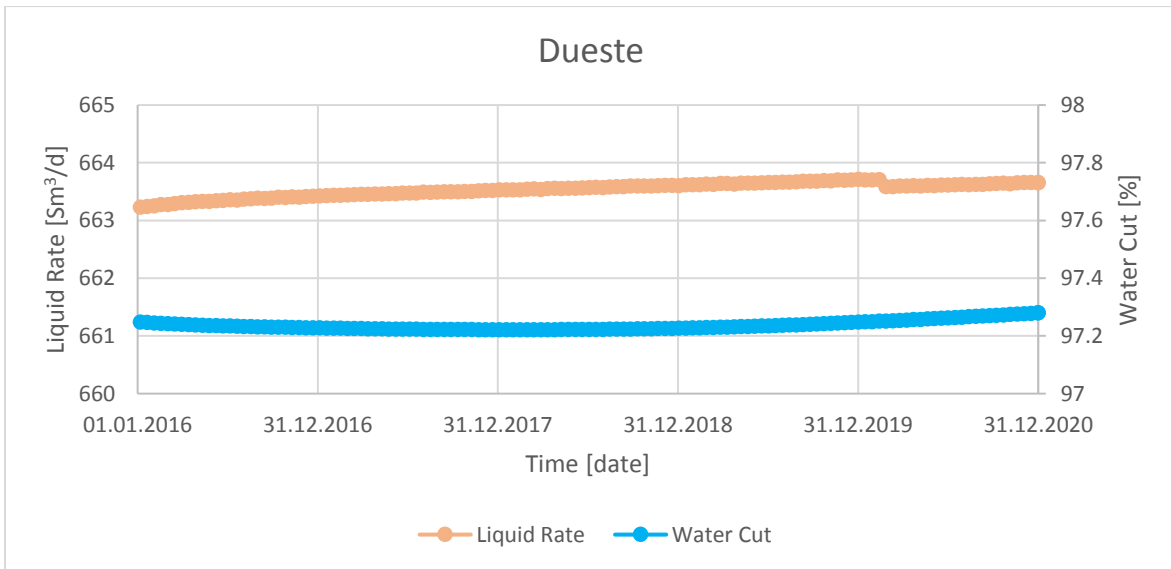


Figure 49 illustrates the liquid rate and water cut forecast in field Dueste from 01.01.2016 to 31.12.2020.

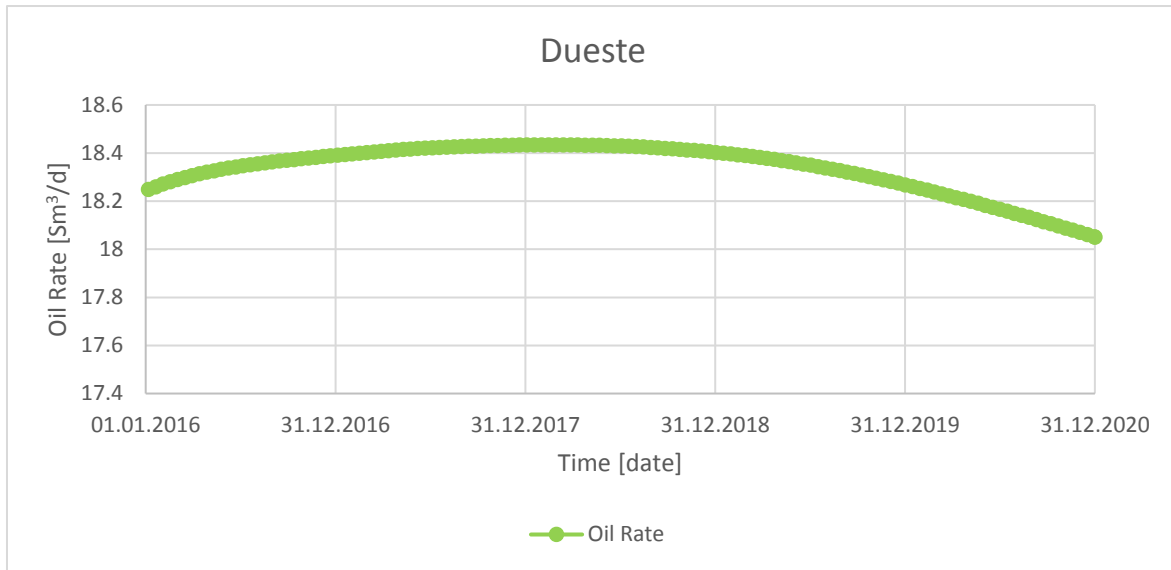


Figure 50 shows the oil rate decline in field Dueste from 01.01.2016 to 31.12.2020.

The cumulative oil rates per field as well as for the separator in Barnstorf for the simulation period can be seen in Table 28.

Table 28 summarizes the cumulative oil produced per field after the simulation period.

Field	Cumulative oil produced (31.12.2020) [Sm³]
Aldorf	2,158
Bockstedt	7,457
Dueste	2,420
Barnstorf	12,200

20.2 Scenario 2

In forecast scenario 2 it was assumed that the best production wells were disabled. For this action, six wells were chosen and the start of the shut in of the first production well was defined to 01.01.2017. The following wells were disabled from the system monthly. The shut in of the six wells was ranked according to their simulated oil production from the 31.12.2015 as can be seen in Table 22. The chosen wells and their underlying ranking can be seen in Table 29.

Table 29 shows the chosen production wells, their simulated oil rates from 31.12.2015 and shut in date.

Well	Oil rate by 31.12.2015 [Sm³/d]	Shut In [dd/mm/yyyy]
Bockstedt 039	8.3	01/01/2017
Bockstedt 035	5.8	01/02/2017
Bockstedt 009	4.1	01/03/2017
Bockstedt 084	4.1	01/04/2017

Bockstedt 086	3.3	01/05/2017
Bockstedt 037	1.4	01/06/2017

After running the simulation the continuously shut in of the defined wells can be seen in Figure 51.

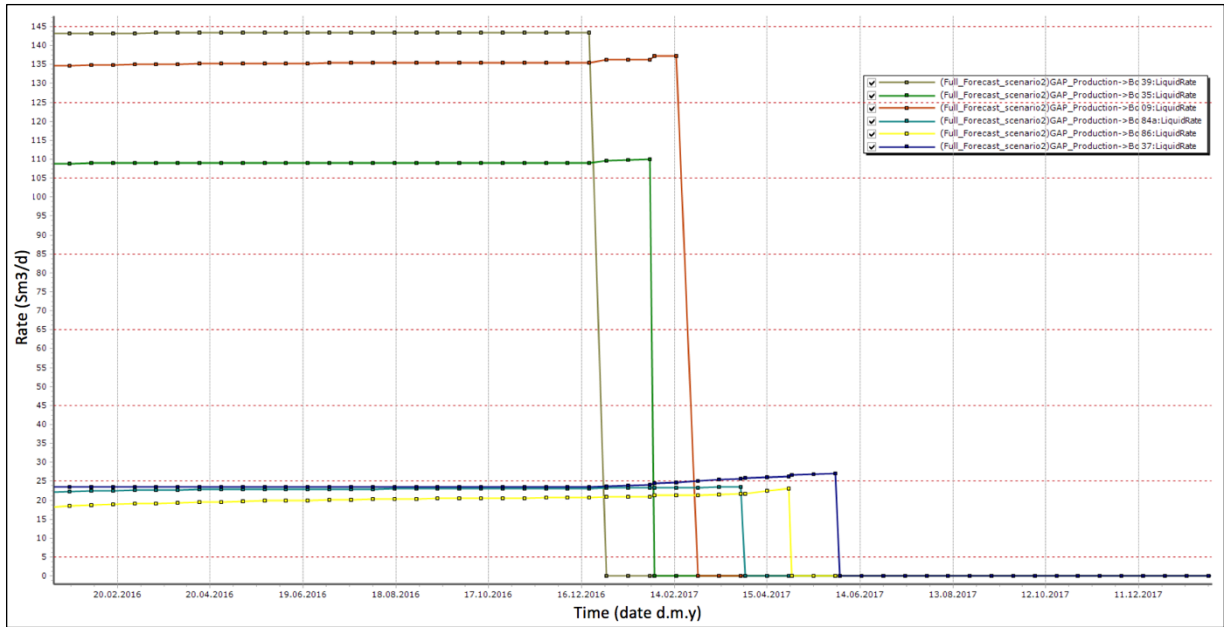


Figure 51 shows the liquid rates and shut in of the defined wells in Bockstedt.

Furthermore, the liquid rate, the water cut and the oil rate for the field Bockstedt and the separator in Barnstorf can be seen from Figure 52 to Figure 55.

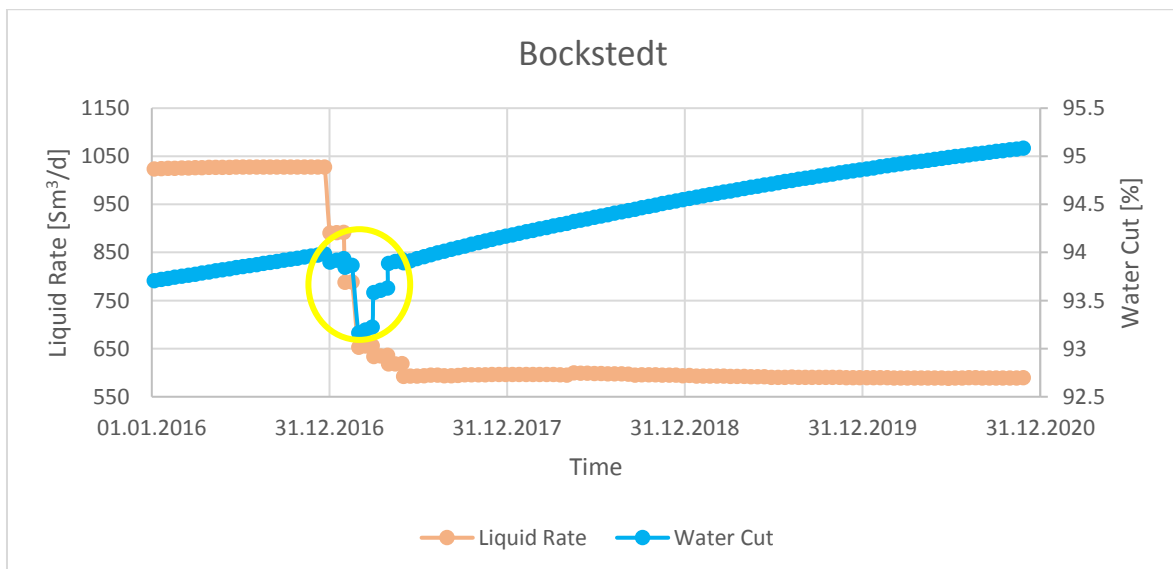


Figure 52 illustrates the liquid rate and water cut forecast in field Bockstedt for scenario 2 from 01.01.2016 to 31.12.2020. The sudden drop of the water cut (yellow) could be described as numerical errors, because of the quick and massive changes of the rates in the system in the first half of 2017.

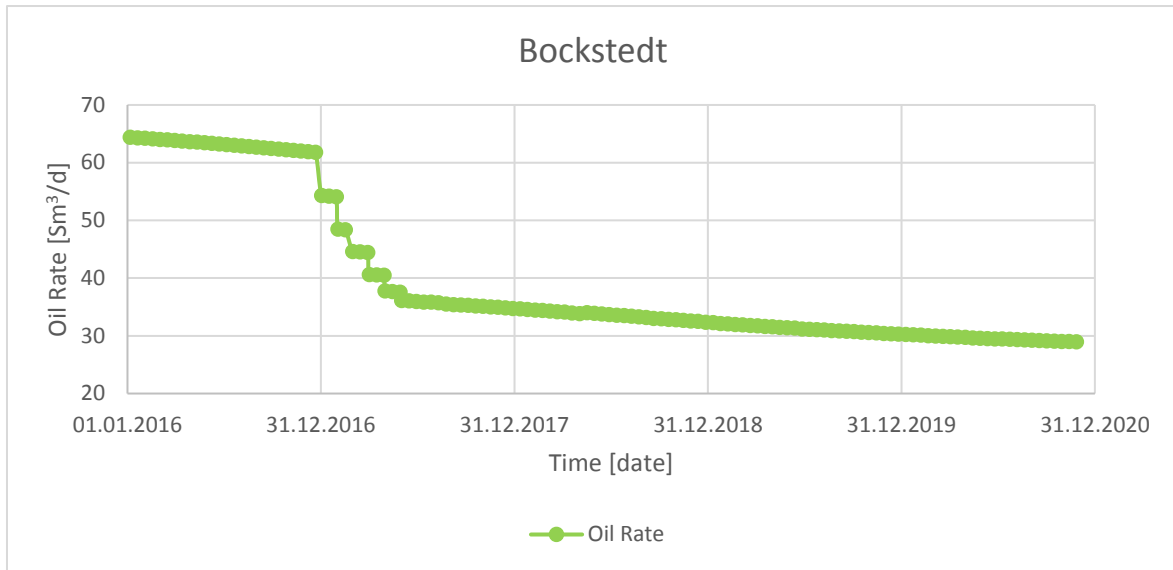


Figure 53 shows the oil rate decline in field Bockstedt for scenario 2 from 01.01.2016 to 31.12.2020. The shut in of each well can be clearly observed in the oil rate behavior of the whole field.

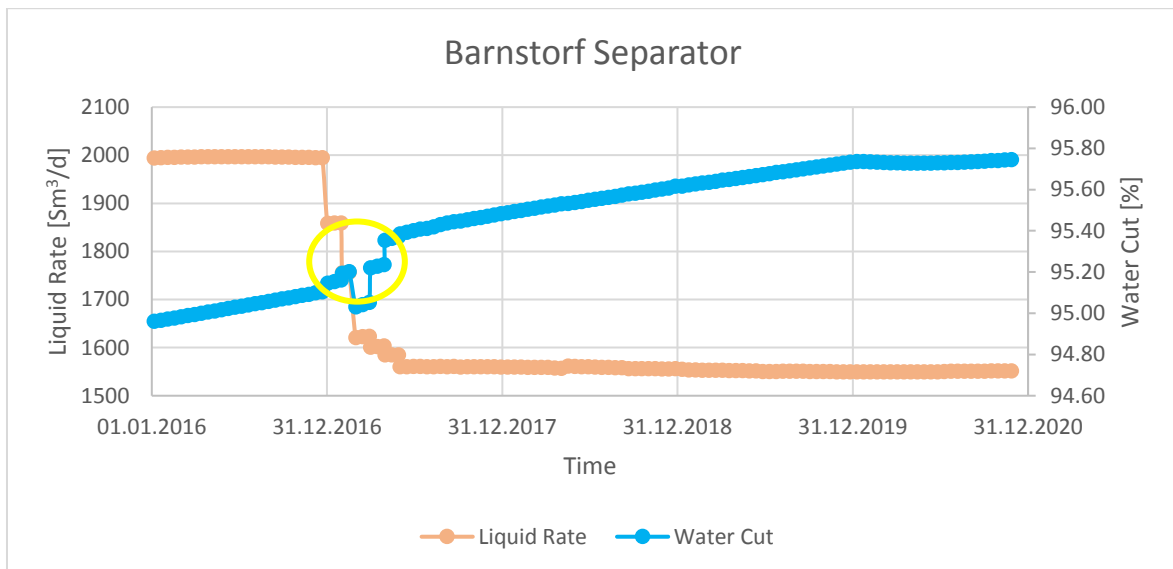


Figure 54 illustrates the liquid rate and water cut forecast in the separator in Barnstorf for scenario 2 from 01.01.2016 to 31.12.2020. The trend is equal to the one of the field Bockstedt as can be seen in Figure 52. The yellow marked area illustrates the possible numerical error in the water calculation.

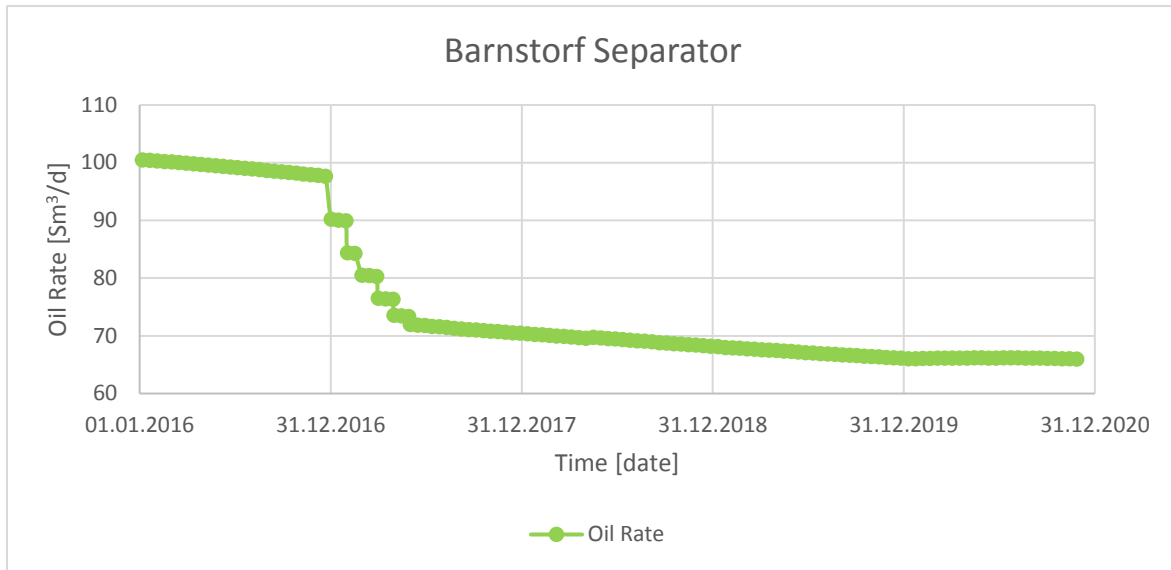


Figure 55 shows the oil rate decline in field Bockstedt for scenario 2 from 01.01.2016 to 31.12.2020. The trend is equal to the one in field Bockstedt as can be seen in Figure 53.

The charts of the rates for the field Aldorf and Dueste were spared, as there were no alterations from scenario 1 visible.

Moreover, because of the decreased liquid production in Bockstedt the injection rate is lowered too as can be seen in Figure 56. The total produced water rate dropped from 1,897 Sm³/d (12.12.2016) as can be seen in Figure 54 to 1,486 Sm³/d, which results in a liquid loss of 411 Sm³/d. Having a look at the injection rate the loss between the same dates concludes to 321 Sm³/d. This deviation between the target water rate and the produced water was already observed in the 'Full Field' section in the 'Verification Simulation Runs' chapter. It seems to be that the lower the produced target water rate is, the higher the difference to the injected water will be.

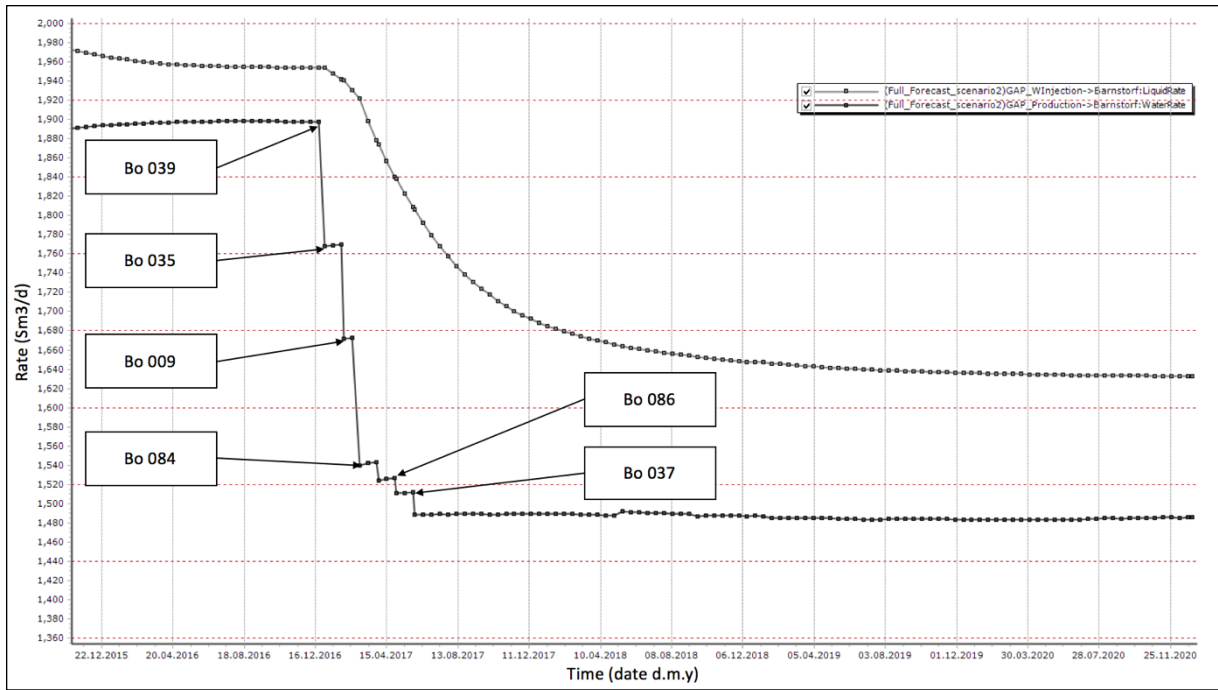


Figure 56 illustrates the total produced water rate (target rate for the injection system) and the injected water rate. Furthermore, the shut in actions of the defined production wells are marked.

20.3 Scenario 3

This scenario shows the impact of a continuously shutoff of the injection system and therefore no pressure support anymore. The shutdown of the injection wells start in Aldorf on the 01.01.2017, followed by the wells in Bockstedt on the 01.06.2017. Finally, on the 01.12.2017 all still residual injectors in Dueste were closed. This continuously shut in of the injection per field can be seen in Figure 57.

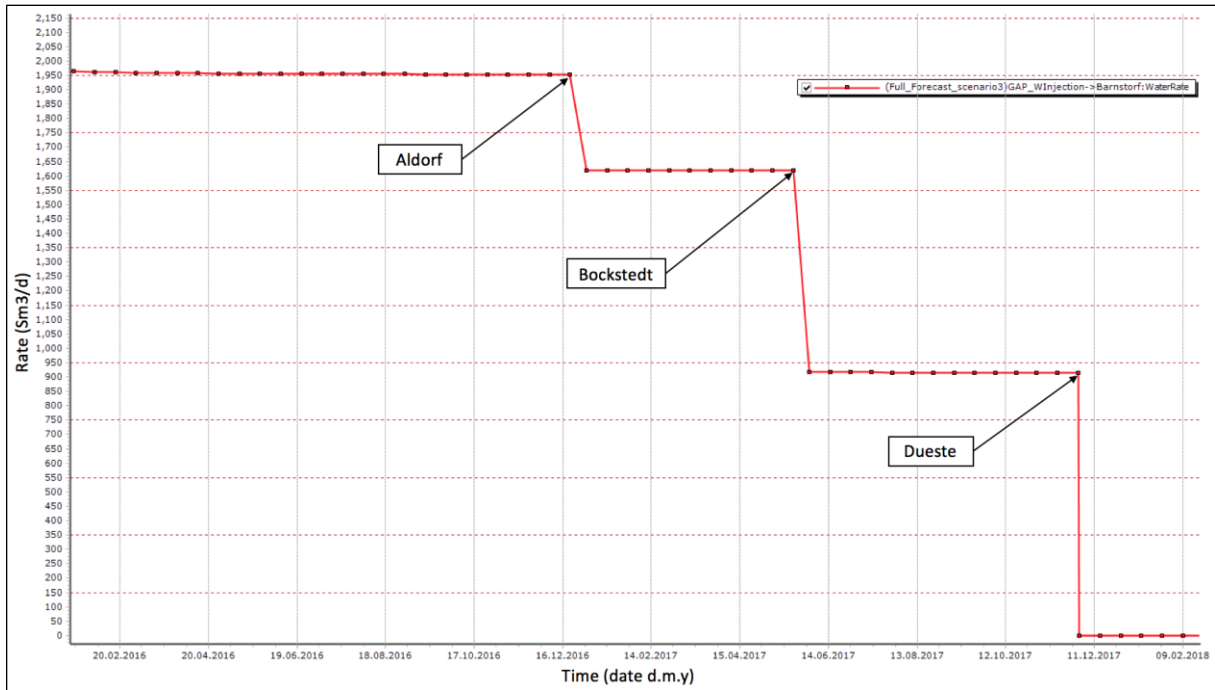


Figure 57 shows the water rate in the injection system during the continuously shut in per field as marked in the chart.

The following charts show that influence of the continuously shutdown of the injection system to the individual field performance.

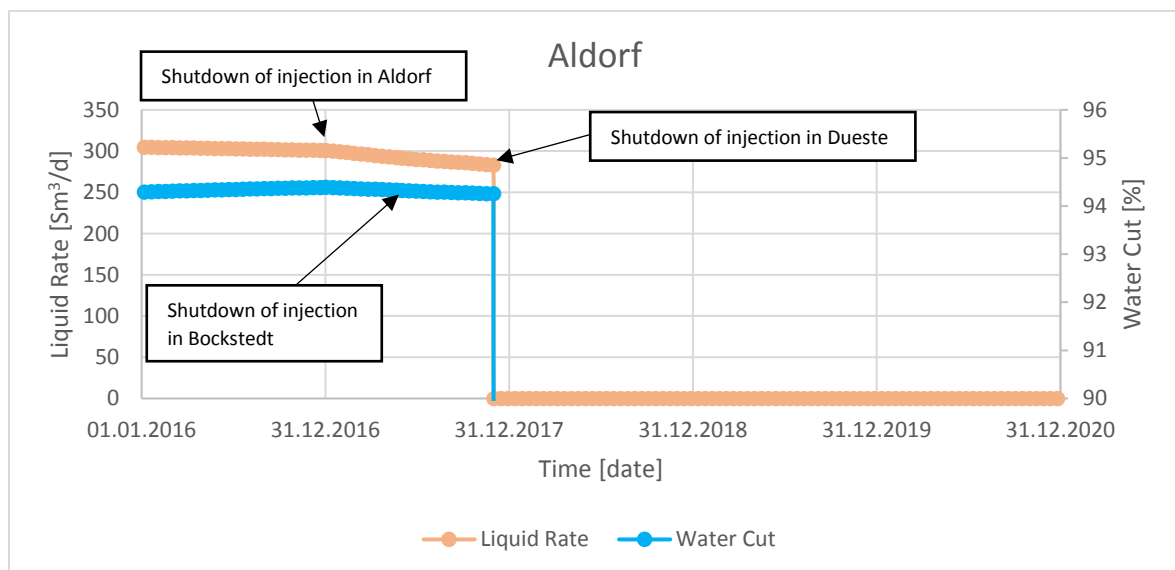


Figure 58 shows the liquid rate and water cut in Aldorf for scenario 3.

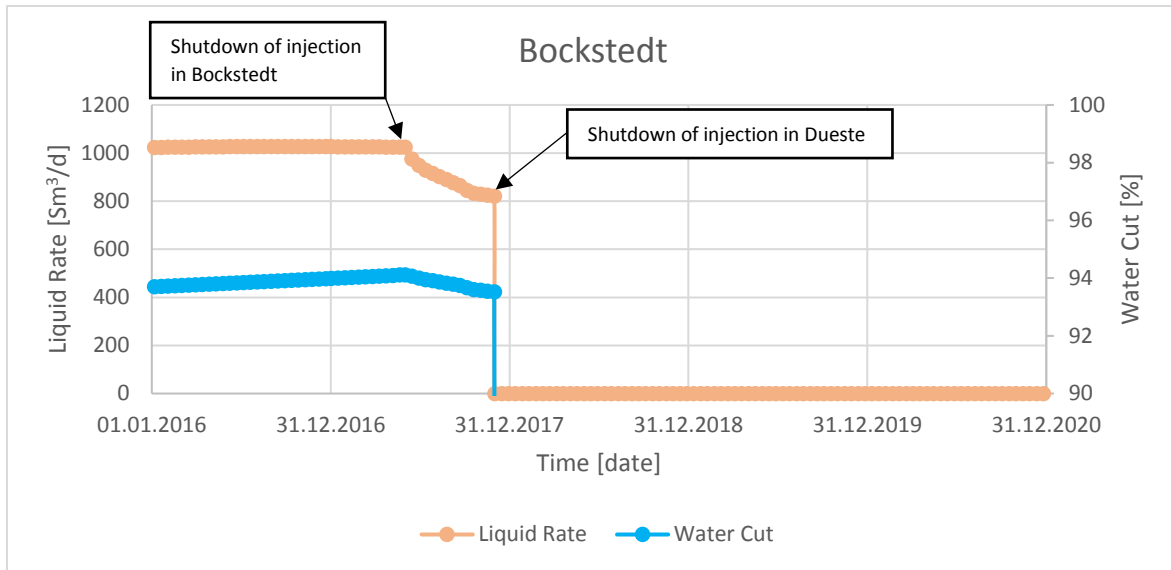


Figure 59 shows the liquid rate and water cut in Bockstedt for scenario 3.

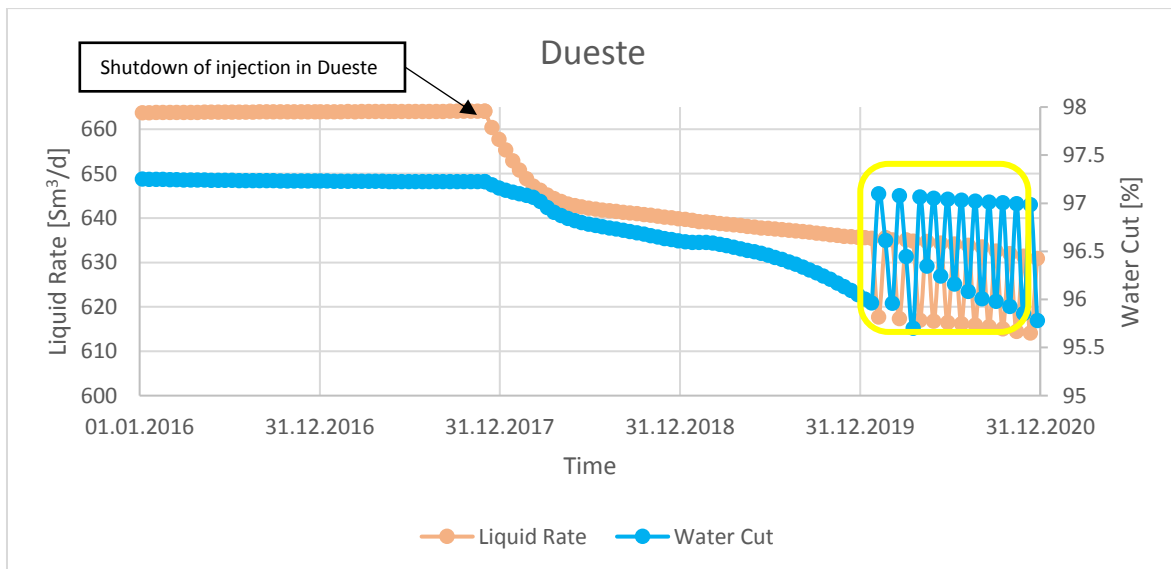


Figure 60 shows the liquid rate and water cut in Dueste for scenario 3. Moreover, in the last simulation year severe oscillation of the simulated liquid rate as well as the water cut were observed (yellow).

Figure 58 illustrates that the impact of a shutdown of the injection system in Aldorf is associated with minor losses of the liquid rate and no visible changes when shutting off the Bockstedt injection wells. Disabling the whole injection system in Bockstedt has a much greater influence on liquid rate than in Aldorf. Comparing the liquid rate losses of Aldorf from the beginning of the shutdown (01.01.2017) until the total shutdown in Dueste (01.12.2017) with Bockstedt in the same time interval. It can be observed that the rate decreased in Aldorf from 300 to 282 Sm³/d and in Bockstedt from 1,027 to 821 Sm³/d. This leads to a loss of 6 % in Aldorf and 20 % in Bockstedt. This can be explained with the higher overall permeability in the field Bockstedt compared to Aldorf. Interestingly to see is, the moment the injection system in Dueste is disabled, and therefore no injection is present anymore, the liquid rate in Aldorf and Dueste dropped to zero. The liquid rate in the Dueste field also starts to decline, but did not

drop to zero like in the other two fields. Furthermore, the water cut in Dueste started declining, which led to an increased oil rate as can be seen in Figure 61.

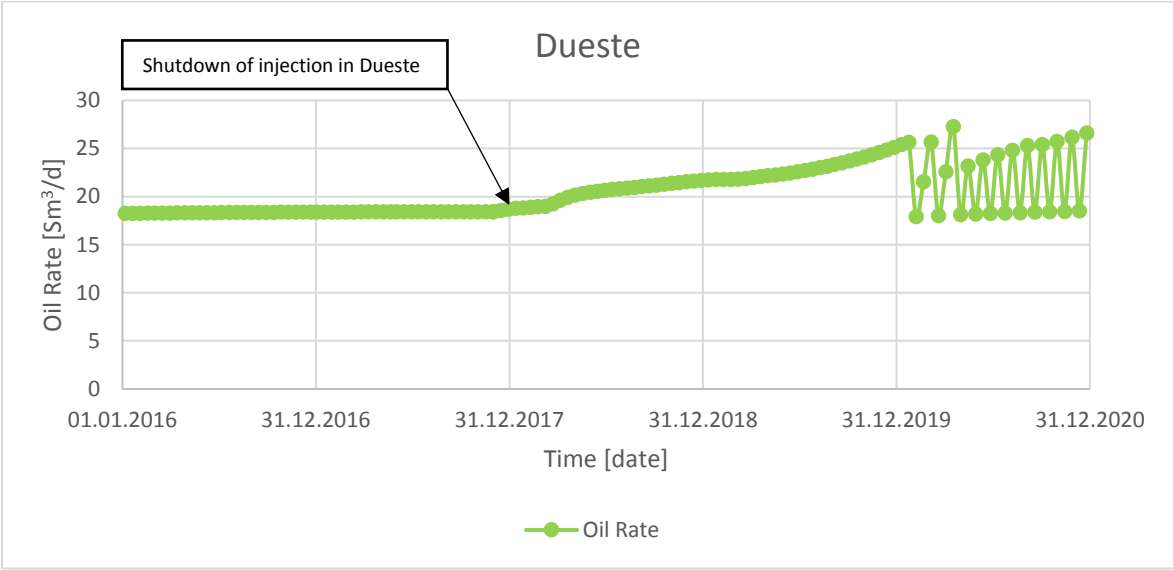


Figure 61 shows the oil rate in the Dueste field for scenario 3.

Moreover, the Eclipse Dueste model experiences in the last simulation year in 2020 a massive oscillation of the rate and water cut (Figure 60). The effect of the increased oil rate in the simulation can be explained that without injection, the amount of water in the system is much lower and therefore the water cut will decrease. Due to no pressure support the reservoir pressure decreases, which results in the decreased liquid rate. Comparing now the impact of the injection wells in Dueste between the pressure support and the increased amount of water in the reservoir. It can be concluded that the water cut is more sensitive on the oil production than the pressure support according to the Dueste Eclipse model.

Another explanation for this effect could be, because of the already long injection time that the injection created channels to the production wells and therefore the sweep efficiency is very low. Turning off the injection system would then decrease the overall water cut at the production wells, as the water from the injectors is not disturbing the inflow from the reservoir anymore assuming a highly fingered environment.

20.4 Comparison of Forecast Scenarios

The following chart shows the cumulative oil production at the separator in Barnstorf for the three different scenarios.

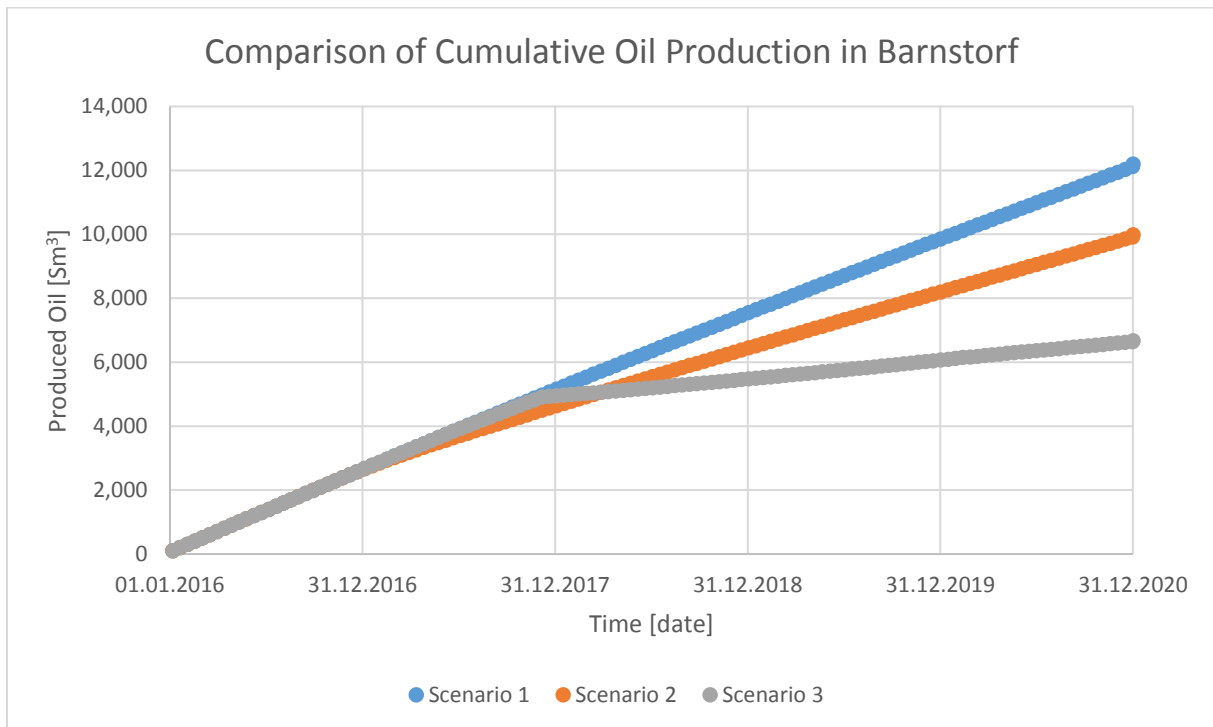


Figure 62 illustrates the cumulative oil production of the three different prediction scenarios from 01.01.2016 to 31.12.2020.

Assuming that the system will run without any shutdowns, which is represented by scenario 1, a cumulative oil production from 01.01.2016 until 31.12.2020 of 12,200 Sm³ can be expected according to the simulation.

Scenario 2, where a shutdown of six strong production wells in Bockstedt was assumed led to a cumulative oil production of 9,982 Sm³ by the end of 2020. This would be a loss of 2,218 Sm³ of oil based on scenario 1.

In scenario 3 it was assumed that the injection system continuously shut down. In this case also greater calculation errors, especially in the last year of simulation in Dueste occurred, which has to be kept in mind. Furthermore, a total stop of liquid production in Aldorf and Bockstedt was simulated by the model. This effect can be explained as the representation of the reservoirs of Aldorf and Bockstedt are based on material balance tanks. The fact that the water saturation in these fields is already at a very high stage and the pressure support, because of the long field production, is very weak, immediately led to a total loss of the liquid production, as there is no balance given anymore. Therefore, scenario 3 has the lowest cumulative oil production by the end of 2020 with 6,669 Sm³, which results in a loss of 5,531 Sm³ of oil compared to scenario 1.

Table 30 summarizes the results of the cumulative oil production from the different scenarios by the end of 2020.

	Cumulative oil produced	Deviation from scenario 1	
	<i>[Sm³]</i>	<i>[Sm³]</i>	<i>[%]</i>
Scenario 1	12,200	-	-
Scenario 2	9,982	2,218	18
Scenario 3	6,669	5,531	45

21 Areas of Improvement

Although the fully integrated model for Aldorf, Bockstedt and Dueste was created with the current best knowledge and conscience, there were encountered some weaknesses and problems. The following points will require persistent observation and continuous revising to guarantee steady improvement.

The producing GOR during the history matching process dropped in 1970 to zero in compartment D in Aldorf. It was tried to intervene this by increasing the pressure support to lower the solubility, but this approach was not successful as it influences the whole system to severe.

In the used RESOLVE software version were some issues and bugs encountered, which were further reported to Petroleum Experts. One smaller illustrative problem was that all source nodes in RESOLVE, which were extracted from the GAP production system, were automatically labelled as naturally flowing. The system does not differ between artificial lifting systems and naturally flowing. Furthermore, there was a problem encountered with the transfer of the salinity from the GAP production system through the Excel transfer file to the GAP injection system. After a full field simulation run it can be observed that the salinity of the water phase in the separator is with approximately 150,000 ppm much higher than the 0.8 ppm in the injection manifold. It was experienced that in the current used version of RESOLVE it was not possible to start two Eclipse models simultaneously.

As described previously, especially in the 'Verification Simulation Runs' chapter it can be investigated that production in individual wells such as Aldorf 001, Aldorf 097 and wells in the EOR compartment is not able to simulate adequately. In most cases, this is because of a combination of the underlying tanks, which are small compared to the OIP and therefore very sensitive and already very low production rates.

A further area with high uncertainty that should be kept in mind is the matching procedure of injection wells, which can be read in the chapter 'Injection Wells' as there were no well tests available and all rates for matching were taken from the ACRON database.

Moreover, because there were two different MBAL models implemented, which were created independently from each other there exist three slightly different PVTs in Bockstedt. The first one as can be seen in Appendix C, which was used for generating the PROSPER files. The second one in the initial MBAL model that now represents the southern part of the Bockstedt field and the third PVT model, which is used in the northern MBAL model of Bockstedt. The PVTs are slightly different and the matched correlations are for every PVT model the same (Glasø for R_s , B_o and Beggs et al for μ_o) as can be seen in Appendix C and the chapter 'Bockstedt MBAL Model Implementation'.

22 Conclusion and Recommendation

The ultimate goal of this thesis was the development of a fully integrated network for the Aldorf, Bockstedt and Dueste field. This model should enable cross-checking of the data from the PDMS to give a better understanding of the field behavior and reduce the massive uncertainty between the PDMS and well testing units in 2014 of 30% as can be read in the chapter 'The Back – Allocation Scheme'. It was empirically known that the well testing unit overestimates the rates, but provides the basis for the allocation scheme. Furthermore, the PDMS has more precise daily full field measurements, but is for the back-allocation based on the measurements of the well testing unit. This led to my first assumption that the full field liquid rate in the verification process has to be between the PDMS measurement and the sum of all well testing unit measurements, but closer to the PDMS as it provides a daily measurement of the tank level behind the separator. In Table 24 and plotted in Table 25 it can be seen that the adjusted full field model fits this assumption. Moreover, it can be seen that the back-allocation per field fit the simulated rates per field very well, where the highest deviation between the PDMS and the model is in Aldorf with 3%. Greater attention has to be paid when studying the impact of individual wells to the whole system as some wells like Aldorf 001, Aldorf 097 and the injection well Dueste H2 could not be matched accurately enough. Furthermore, the injection system was analyzed, which can be read at the end of the chapter 'Verification Simulation Runs'. It was observed that the smaller the target water rate provided by the production system, the bigger is the deviation to the calculated injected amount of water.

To demonstrate the predictive functionality of the model three full field forecasts with different settings were created, which can be seen in the chapter 'Full Field Forecasts'. The short-term simulations from 01.01.2016 to 31.12.2020 provide a case where no changes were made (Scenario 1). Another study was created, where an intervention to the production system was made by continuously disabling strong production wells in Bockstedt (Scenario 2). The third case shows the impact of a continuously shutdown of the injection system (Scenario 3). It was expected and verified that the cumulative rates by the end of 2020 are going to decrease from scenario to scenario.

Important to mention are the huge skin factors and highly reduced permeabilities of the near wellbore area, which were applied in the PROSPER files. Skin factors up to 80 or permeability reductions up to 99 % are not common and have just been performed to match the injection rates. I would highly recommend reviewing the injectivity and integrity of the injection wells in Aldorf, Bockstedt and Dueste.

Moreover, the Bockstedt EOR compartment was found to be too small for one proper MBAL for the whole field. This is mainly because of calculation errors and production data input from Finder, where the resolution is with a monthly basis inaccurate. The simulated pressures in the tanks started to oscillate. Therefore, another solution for representing the field Bockstedt has to be found. This led to the idea to implement the second MBAL model, which represents the northern part more accurate. The northern part consists of the EOR, 84/86 and D compartments and could be investigated more precisely, because of the up splitting the influencing uncertainty factors were reduced. Moreover, it has to be mentioned that the strict separation into two different models will not account for backpressure effects and flow communication between the north and south of the Bockstedt field.

The implementation of the various reservoir models be it Aldorf, Bockstedt or Dueste showed that all well rates and water cuts react very sensitive to the relative permeability models. This can be explained by the already long lifetime of the field and therefore high water cuts and high recovery factors, which already act on the top end of the residual oil saturation. Therefore, it was important to revise after connecting the wellbores in GAP with the underlying tanks all relative permeability models, especially the Brooks-Corey exponents and the maximal endpoints of the water relative permeability.

One PVT model per field was used, although it is known that the individual fields are very complex as they are highly compartmentalized, multi-layered and more than one fluid type per field is expected. This assumption is valid, because on the one hand it is not expected that the individual fluid types differ greatly and on the other hand the main uncertainty is the back-allocated production data. Although various PVTs per field could be expected, because of the very long production time and therefore possible continuously cross flow between the layers a far advanced mixing would already be present.

During the history matching process of the Aldorf field the producing GOR in compartment D could not be simulated according to the gas production input. In 1970, it was reported from MBAL that the producing GOR dropped to zero. It was tried to match this issue with an increase in pressure support, which would reduce the solubility R_s , but this intervention disturbed the overall MBAL model and especially the adjacent tanks G and C too severe. When increasing the pressure support further numerical errors could be observed as the simulated pressure started to oscillate. As this effect occurs quite early in the field life, there could not be any pressure disturbances reported as can be seen in Figure 19, and the pressure trend matches, especially for advanced times quite well. The solubility as can also be seen in Appendix A is small, which was also a reason why I decided to not further bother with this problem. However, I would recommend attempting new approaches for this region as the southern area in the field Aldorf, especially compartment D required the launch of an auxiliary tank, as it was very hard to match.

Moreover as described in the previous chapter 'Bockstedt MBAL Model Implementation' the Eclipse model was not used, because it is not yet history matched. Therefore, as soon as it is matched I would highly recommend implementing it in RESOLVE and connect it to the full field model. This change in the reservoir model will increase the simulation time significantly, but the geological accuracy will be much higher than with the currently used MBAL tanks, because it is based on the newly shot seismic, which was performed in 2013.

Concluding the usability of the system, I experienced that RESOLVE is a powerful, but also very complex tool with some underlying bugs and difficulties as discussed in the previous chapter 'Areas of Improvement'.

The main benefit of RESOLVE is the interaction and communication with many other applications and simulators on the market, but this great versatility has its downside as the simulation times are becoming longer with each implemented tool. Firstly, they have to be initialized individually by RESOLVE and secondly there are application drivers acting for each object for data transfer. Therefore, I would recommend for integrated modelling using GAP assuming that no connection to an external reservoir

simulator is needed. It is much faster in simulation time, easier to handle, has a more user-friendly interface and the engineers in the company are more used to it.

Although the full field model is matched as properly as possible, it is very important to continuously update the production data and pressure tests if performed. After the updating procedure of the latest data the history matching of the implemented MBAL models should be re-run and if necessary, because newly occurring trends, re-matched. This action is very important, as the validity of the model is highly dependent on these continuously updating actions.

The PDMS allocation is the bottleneck in the system. It is of great importance to revise the back-allocation scheme as well as to adjust the measurement tools after the separator properly and on a continuous basis. The reason for this is, the back allocated data is the starting point for every further analysis, study and forecasting operation and as the uncertainty of this input data is as explained in the chapter 'The Back – Allocation Scheme' more than 30% referenced to the well testing units in 2014. The accuracy of the output, be it a simple decline curve analysis or a more sophisticated study like the created full field model will always be as good as the uncertainty of the underlying input data, but never better. Therefore, it follows that the full field model will have in the best case the same accuracy as the PDMS, because the model is based on these data. Although the full field model will have at least the same uncertainty, it will be more reasonable for future production allocation than then PDMS. This is because in the full field model are much more parameters like back pressures from other wells, pump settings and communication between compartments encountered. This leads compared to the PDMS allocation, which encounters the well checker and water cut measurements as well as the down-times of the wells, to a more valuable allocation.

Finally, I want to mention that when running the full field model one has to be aware of the underlying models and their uncertainties. The reservoir representations of Aldorf and Bockstedt are based on a material balance. Although the IPM MBAL software provides a great tool for adjusting the tanks, such as various aquifer models with different complexity, the tank models cannot reach the level of a reservoir simulation, such as the Eclipse Dueste model. Moreover, the Eclipse model is, of course, just as good as its history match and underlying assumptions.

23 Nomenclature

R_s	Solubility	m^3/m^3	Scf/stb
GOR	Gas oil ratio	m^3/m^3	Scf/stb
μ_o	Viscosity of oil	cP	Pa s
μ_w	Viscosity of water	cP	Pa s
B_o	Formation volume factor of oil	m^3/m^3	bbl/stb
B_{ob}	Formation volume factor of oil @ p_b	m^3/m^3	bbl/stb
p_b	Bubble point pressure	bara	psia
T	Temperature	°C	°F
t	time	s	s
γ_o	Specific gravity of oil	-	-
γ_g	Specific gravity of gas	-	-
WC	Water cut	%	%
q	Liquid rate	m^3/d	bbl/d
q_o	Oil rate	m^3/d	bbl/d
q_w	Water rate	m^3/d	bbl/d
q_g	Gas rate	m^3/d	Scf/d
AOF	Absolute open flow	m^3/d	bbl/d
Q_o	Cumulative oil production	m^3	bbl
k_{ro}	Relative permeability of oil	-	-
k_{rw}	Relative permeability of water	-	-
$k_{ro,max}$	Endpoint relative permeability of oil	-	-
$k_{rw,max}$	Endpoint relative permeability of water	-	-
n_o	Brooks-Corey exponent for oil	-	-
n_w	Brooks-Corey exponent for water	-	-
S_{wc}	Connate water saturation	-	-
S_{or}	Residual oil saturation	-	-
S_w	Water saturation	-	-
S_o	Oil saturation	-	-
f_w	Fractional flow of water	-	-
STOIIP	Stock tank oil initial in place	Sm^3	stb
OIP	Oil in place	m^3	bbl
σ	Standard deviation	bara	
ALDF	Aldorf		
BOCK	Bockstedt		
DSTE	Dueste		
PDMS	Production Data Management System		
ACRON	Data Management System		

Finder	Backup Database
IPM	Integrated Production Modelling
GAP	General Allocation Package
MBAL	Material Balance Program
PROSPER	Well Performance Program
RESOLVE	Master Controller Program
OpenServer	IPM Tools API Protocol
API	Application Programming Interface
IPR	Inflow Performance Relationship
VLP	Vertical Lift Performance
SRP	Sucker Rod Pump
PCP	Progressive Cavity Pump
ESP	Electrical Submersible Pump

24 References

- Barrufet, M. A. (2012). http://engineering.tamu.edu/barrufet/public_html/PETE310/. Von http://www.pe.tamu.edu/barrufet/public_html/PETE310/pdf/L30-31-Oilfield_Waters.pdf abgerufen
- Brooks, R. H., & Corey, A. T. (1964). *Hydraulic Properties of Porous Media*. Colorado State U.
- Buckley, S. E., & Leverett, M. C. (1942). *Mechanism of Fluid Displacement in Sands*. AIME.
- Dake, L. P. (1978). *Fundamentals of Reservoir Engineering*. Amsterdam, The Netherlands: Elsevier Science B.V.
- Fetkovich, M. J. (1971, July 1). *A Simplified Approach to Water Influx Calculations-Finite Aquifer Systems*. Society of Petroleum Engineers. doi:10.2118/2603-PA
- GAP Technical User Manual. (2015, March). (10). Edinburgh, Scotland: Petroleum Experts Ltd. Retrieved from www.petex.com
- Hofstätter, H. (2014). *Artificial Lift Systems Lecture Slides*. Montanuniversität Leoben.
- Kord, S. (2014). *PVTX Course Slides*. Montanuniversität Leoben.
- Kord, S. (2014). *Reservoir Engineering Lecture Notes and PDF Slideshow*. Montanuniversität Leoben.
- Langbauer, C. (2015). *Nodal Analysis Lecture*. Montanuniversität Leoben.
- Lübben, H., & Nolte, H.-O. (Dezember 1978). *Valendis-Pool Scholen - Lagerstätten, Produktion, Aquifer*. Erdoel-Erdgas-Zeitschrift.
- MBAL Technical User Manual. (2014, December). (11). Edinburgh, Scotland: Petroleum Experts Ltd. Retrieved from www.petex.com
- Microsoft Excel VBA Library*. (2016). Von Microsoft Development Center: <https://msdn.microsoft.com/en-us/library/office/fp179694.aspx> abgerufen
- OpenServer Technical User Manual. (January 2015). Edinburgh, Scotland: Petroleum Experts Ltd. Von www.petex.com abgerufen
- Peaceman, D. W. (1995, November 1). *A New Method for Representing Multiple Wells With Arbitrary Rates In Numerical Reservoir Simulation*. Society of Petroleum Engineers. doi:10.2118/29120-PA
- PROSPER Technical User Manual. (2015, March). Edinburgh, Scotland: Petroleum Experts Ltd. Retrieved from www.petex.com
- RESOLVE Technical User Manual. (2015, March). (6). Edinburgh, Scotland: Petroleum Experts Ltd. Retrieved from www.petex.com
- Schlumberger. (2015). Eclipse Technical Description.

Sutton, R. P., & Farshad, F. (1990, February 1). *Evaluation of Empirically Derived PVT Properties for Gulf of Mexico Crude Oils*. Society of Petroleum Engineers. doi:10.2118/13172-PA

Van Everdingen, A. F., & Hurst, W. (1949, December 1). *The Application of the Laplace Transformation to Flow Problems in Reservoirs*. Society of Petroleum Engineers. doi:10.2118/949305-G

Welge, H. J. (1952). *A Simplified Method for Computing Oil Recovery by Gas or Water Drive*. AIME.

25 List of Figures

1. *Figure 1 Basic scheme of the back-allocation in Barnstorf. The liquid levels in the tanks are measured every day at 6 am to get the production from the previous day. These daily-calculated quantities are then back allocated to each individual well in the field based on the well checker measurements. The brine will be pumped back to the fields through the injection wells and the separated oil is transported away with the railway. As can be further seen the gas is not measured directly behind the separator- 14 -*
2. *Figure 2 Data processing and database systems. There are three main databases the ACRON, PDMS and Finder and one operating system the IFIX. The IFIX is for operators and broadcasts real time values from the gauges at the well side and further alerts if limits are reached. This high frequency data is then saved in the ACRON database. Furthermore, the back allocated production data is saved on a daily basis in the PDMS. As a back-up tool the Finder database stores various information, be it production data or of other relevant origin, on a monthly basis. - 15 -*
3. *Figure 3 shows pie charts, which compare the well checker rates (left column) with the PDMS rates (right column) per field and the distribution of the rates for each production well. It can be observed that the error per well for the oil rate between the PDMS and the well checker measurements is not high for any individual well (maximum of 3%)..... - 18 -*
4. *Figure 4 shows a map of the production (red pipelines) and injection (blue pipelines) system connecting Aldorf (orange), Dueste (blue) and Bockstedt (black) fields with the processing plant in Barnstorf (red circle)..... - 22 -*
5. *Figure 5 illustrates the surface network of the production system in GAP. The northern part represents Bockstedt, with the multiphase pump installed as a compressor. All green triangles represent production wellheads, whereas the various symbols in the triangles represent the pump type. Arrows in the pipelines indicate flow direction. Green segment symbols represent tanks from the underlying MBAL models. All grey symbols are currently disabled elements. The most southern facility (indicated in red) represents the processing plant in Barnstorf..... - 23 -*
6. *Figure 6 shows the surface network of the injection system in GAP. Blue-mirrored triangles represent injection wellheads and the green segments show the MBAL tanks. The most southern facility represents the injection manifold at the processing plant in Barnstorf. Green circle segment symbols represent underlying MBAL tanks. All grey facilities are currently disabled elements..... - 24 -*
7. *Figure 7 shows on the left the input screen for defining a PCP in the PROSPER internal database. After defining the pump specifications, it was able to generate the performance chart for the pump (right). . - 28 -*
8. *Figure 8 shows the recommended sensitivity variables and ranges for a naturally flowing oil well. . - 29 -*
9. *Figure 9 shows the recommended sensitivity parameters and ranges for various artificial lifting systems. - 30 -*
10. *Figure 10 Example of a matched IPR for a water injection well of Dueste 085. It was necessary to zoom in to the low rate region as it is on the edge of the relationship. - 32 -*
11. *Figure 11 shows the possible sensitivity variables and their ranges for water injection wells as recommended by Petroleum Experts. - 33 -*
12. *Figure 12 illustrates the different depth definitions. The reference depth in Aldorf of 1090 m can be seen at the bottom. This depth is further used to calculate all historical pressure points to a common depth. - 35 -*

13. *Figure 13 illustrates the pressure history of field Aldorf (referenced to 1090 m). The different colors represent the different compartments as can be seen in Figure 11. - 36 -*
14. *Figure 14 Re-defined compartments based on the digitalized shut-in pressure history in the field Aldorf. The pressure difference between compartment A and B was with almost 60 bar quite significant, whereas the other ones were not that clear and therefore mainly separated between already interpreted faults. Compartment E include pressure tests near the oil water contact and is therefore not locally defined as the others are..... - 37 -*
15. *Figure 15 illustrates an example (compartment A): Fractional flow matching based on cumulative oil production (left); Relative permeability curves of oil and water based on the Brooks-Corey model (right) - 40 -*
16. *Figure 16 illustrates the underlying MBAL model of the Aldorf field with the six active tanks and seven active transmissivities. It can be seen that all tanks, except ‘Tank01’ are divided into green and blue color code. This represents an oil tank with an underlying aquifer. Tank01 has two different intensities of blue, which represents a water tank with an underlying aquifer too. The rhombus symbols connecting the individual tanks represent the transmissibilities in the MBAL model. Grey tanks and transmissibilities are disabled in the model..... - 42 -*
17. *Figure 17 represents the location of injection well Aldorf 031 in the near vicinity of an interpreted fault, which separates the injector from the main field. - 43 -*
18. *Figure 18 History matched pressure result for compartment A, B and G. In compartment A a steep pressure decline at the early life can be observed, which is quickly attenuated and stabilizes at around 10 to 15 bar. Compartment B and G show in the 1960s an increase in pressure, which can be explained with establishing the waterflooding operations. A further significant pressure increase in 1980 can be explained with an overall reduction in liquid production. Furthermore, yellow marked are the pressure measurements performed in Aldorf H001 as they are not in the normal range of compartment A. . - 46 -*
19. *Figure 19 History matched pressure result for compartment C and D. It can be seen that the pressure in compartment C slowly starts to increase, which is a result of the reduced overall production. The pressure increase is not yet alarming as there are no active wells in that compartment. A further result is the stop of decline in compartment D in 1987..... - 46 -*
20. *Figure 20 Simulated pressure decline and oil production compartment D. It can be observed that the oil production decreased in the 1987s, which further resulted in a stop of the pressure decline in the corresponding tank D..... - 47 -*
21. *Figure 21 represents the northern part of the Bockstedt field in MBAL. The green squares show the three compartments, which were created for this study. Furthermore, one auxiliary tank ‘Hilfe-86’ was implemented. The circles represent wells, whereas green ones are production wells and blue ones for representing injectors. It can be seen that no aquifer model was activated in this representation, as there is no influence encountered. - 48 -*
22. *Figure 22 illustrates the southern part of the Bockstedt field in MBAL, whereas the grey tanks and transmissibilities represent disabled items, which were replaced by an extra MBAL model as can be seen in Figure 21. The southern part of the Bockstedt field experiences influence from an aquifer (Lübben & Nolte, Dezember 1978), therefore chosen aquifer models were inserted at specific locations in the MBAL model. The red shaded parts represent gas caps in specific tanks. - 49 -*
23. *Figure 23 shows the R_s and B_o for the Bockstedt north MBAL model, which were correlated with Glasø. - 50 -*

24. Figure 24 shows the μ_o for the Bockstedt north MBAL model, which was correlated with Beggs et al. - 50 -
25. Figure 25 shows the R_s and B_o for the Bockstedt south MBAL model, which were correlated with Glasø. - 51 -
26. Figure 26 shows the μ_o for the Bockstedt south MBAL model, which was correlated with Beggs et al. - 51 -
27. Figure 27 illustrates the Dueste Eclipse model, whereas the saturation property is plotted (blue = water; green = oil). - 52 -
28. Figure 28 shows the timestep handling between RESOLVE and an external application as for example Eclipse. Between two RESOLVE timesteps Eclipse can use as many steps as needed to converge, whereas a synchronization action will be performed between RESOLVE and Eclipse prior to any further solving action. - 54 -
29. Figure 29 illustrates the connected nodes in RESOLVE between the Eclipse reservoir model for Dueste (blue) and the production as well as injection GAP networks. Furthermore, this overall view shows the Excel transfer file, whereas the three input streams for the oil, gas and water phase and the one output stream for the water target rate to the injection system can be seen. In the north there are the nodes for the Bockstedt wells (black) and in the west, the Aldorf connections (orange) are listed. Because the MBAL models are directly connected within the GAP production system, these nodes are not connected further in RESOLVE. - 58 -
30. Figure 30 shows a snapshot of the data transfer from the production to the injection system through the Excel file. Four different source streams were provided from the separator in Barnstorf. The 'Barnstorf-oil' (green), 'Barnstorf-wat' (blue), Barnstorf-gas (red) and the 'Barnstorf-liftgas', which is not used as gas lifting is not applied. After importing the phases into different worksheets and sections in the Excel file the water target rate is further given to the Barnstorf injection manifold. - 59 -
31. Figure 31 shows a snapshot from the Microsoft Excel for data transfer between the GAP production and injection network in RESOLVE. Column B to G show the forecasting section, whereas column I to R represents the solver section. - 60 -
32. Figure 32 illustrates the data flow scheme between the MBAL tank models and the PROSPER correlations. It can be observed that the Input variables are handed from the MBAL models to PROSPER. Whereas after a new network solving action the rates are given to the MBAL models. - 60 -
33. Figure 33 shows the transfer of data across the GAP production as well as injection system and the PROSPER correlations. The correlated IPRs and the corresponding created VLP are used from GAP for performing rate calculations. Furthermore, the Excel macro for updating and revising the pipeline parameters can be seen at this level..... - 61 -
34. Figure 34 gives an overview of the whole system and how the data is transferred between the different applications. Two separate data streams can be investigated. The one coming from the Dueste Eclipse model and the second one from the MBAL tank models. Whereas both are connected in RESOLVE. - 62 -
35. Figure 35 shows the pressure behavior and gas saturation over time in compartment A of Aldorf, which gives an indication of a growing gas cap. The scale on the left y-axis shows the gas saturation fraction, where it can be observed that the amount of gas grows up to 0.62 until the end of 2015. This shows a clear indication of a developing and steadily growing gas cap. - 67 -
36. Figure 36 illustrates the liquid production and water cut of the full field model validation run in 2015... - 75 -
37. Figure 37 shows the oil rate in 2015 of the full field run. A steady decline can be observed..... - 76 -

38. Figure 38 illustrates a snapshot of the GAP production system, where the main connection pipelines for the individual fields. The node J1 in the bottom left corner gives the direct connection to the processing plant in Barnstorf.	- 77 -
39. Figure 39 shows the liquid rate and water cut in Aldorf for 2015.	- 78 -
40. Figure 40 shows the oil rate in Aldorf for 2015.	- 78 -
41. Figure 41 shows the liquid rate and water cut in Bockstedt for 2015.	- 79 -
42. Figure 42 shows the oil rate in Bockstedt for 2015.	- 79 -
43. Figure 43 shows the liquid rate and water cut in Dueste for 2015.	- 80 -
44. Figure 44 shows the oil rate in Dueste for 2015.	- 80 -
45. Figure 45 illustrates the liquid rate and water cut forecast in field Aldorf from 01.01.2016 to 31.12.2020.	- 83 -
46. Figure 46 shows the oil rate decline in field Aldorf from 01.01.2016 to 31.12.2020.	- 84 -
47. Figure 47 illustrates the liquid rate and water cut forecast in field Bockstedt from 01.01.2016 to 31.12.2020.	- 84 -
48. Figure 48 shows the oil rate decline in field Bockstedt from 01.01.2016 to 31.12.2020.	- 85 -
49. Figure 49 illustrates the liquid rate and water cut forecast in field Dueste from 01.01.2016 to 31.12.2020.	- 85 -
50. Figure 50 shows the oil rate decline in field Dueste from 01.01.2016 to 31.12.2020.	- 86 -
51. Figure 51 shows the liquid rates and shut in of the defined wells in Bockstedt.	- 87 -
52. Figure 52 illustrates the liquid rate and water cut forecast in field Bockstedt for scenario 2 from 01.01.2016 to 31.12.2020. The sudden drop of the water cut (yellow) could be described as numerical errors, because of the quick and massive changes of the rates in the system in the first half of 2017. -	87
53. Figure 53 shows the oil rate decline in field Bockstedt for scenario 2 from 01.01.2016 to 31.12.2020. The shut in of each well can be clearly observed in the oil rate behavior of the whole field.	- 88 -
54. Figure 54 illustrates the liquid rate and water cut forecast in the separator in Barnstorf for scenario 2 from 01.01.2016 to 31.12.2020. The trend is equal to the one of the field Bockstedt as can be seen in Figure 51. The yellow marked area illustrates the possible numerical error in the water calculation. -	88 -
55. Figure 55 shows the oil rate decline in field Bockstedt for scenario 2 from 01.01.2016 to 31.12.2020. The trend is equal to the one in field Bockstedt as can be seen in Figure 52.	- 89 -
56. Figure 56 illustrates the total produced water rate (target rate for the injection system) and the injected water rate. Furthermore, the shut in actions of the defined production wells are marked.	- 90 -
57. Figure 57 shows the water rate in the injection system during the continuously shut in per field as marked in the chart.	- 91 -
58. Figure 58 shows the liquid rate and water cut in Aldorf for scenario 3.	- 91 -
59. Figure 59 shows the liquid rate and water cut in Bockstedt for scenario 3.	- 92 -
60. Figure 60 shows the liquid rate and water cut in Dueste for scenario 3. Moreover, in the last simulation year severe oscillation of the simulated liquid rate as well as the water cut were observed (yellow). -	92 -
61. Figure 61 shows the oil rate in the Dueste field for scenario 3.	- 93 -
62. Figure 62 illustrates the cumulative oil production of the three different prediction scenarios from 01.01.2016 to 31.12.2020.	- 94 -

63. Figure 63 shows the correlation chart of water viscosity [cP] versus the reservoir temperature [°F] for various total dissolved solids [%] at atmospheric pressure condition. It can be observed that for a certain isothermal condition the brine viscosity increases with increasing NaCl concentration. - 115 -
64. Figure 64 illustrates the chart of water viscosity ratio versus reservoir pressure. - 115 -
65. Figure 65 shows the R_s and B_o for the Aldorf PROSPER files, which were correlated with Vasquez and Beggs - 117 -
66. Figure 66 shows the μ_o for the Dueste PROSPER files, which was correlated with Beggs et al. - 117 -
67. Figure 67 shows the R_s and B_o for the Dueste PROSPER files, which were correlated with Glasø.... - 124 -
68. Figure 68 shows the μ_o for the Dueste PROSPER files, which was correlated with Beggs et al. - 124 -
69. Figure 69 shows the R_s and B_o for the Bockstedt PROSPER files, which were correlated with Glasø. - 126 -
70. Figure 70 shows the μ_o for the Bockstedt PROSPER files, which was correlated with Beggs et al.... - 126 -

26 List of Tables

1. *Table 1 shows a comparison of the field parameters of Aldorf, Bockstedt and Dueste..... - 13 -*
2. *Table 2 Comparison of oil rates in Sm³/d per field between the PDMS and well checker measurements in 2014. The well checker measurements highly overestimate the rates. - 16 -*
3. *Table 3 shows average water cuts (WC) and liquid rates per field as well as their minimum and maximum values and the standard deviation per property for the year 2014 from the PDMS. Furthermore, the number of encountered production wells for these calculations can be seen at the bottom line. - 17 -*
4. *Table 4 shows the classification matrix for active producers. It was separated between high and low water cuts and liquid rates over all fields. The limit for the water cut as previously defined is set to 90% and for the liquid rate to 80 m³/d. - 19 -*
5. *Table 5 lists the average water cut (WC) and average liquid rate per chosen well..... - 19 -*
6. *Table 6 Initial 'Environment Parameters' as set by Petroleum Experts for temperature calculations in the pipeline segments. - 21 -*
7. *Table 7 Summary of progressive cavity pumps in the field in operation - 27 -*
8. *Table 8 Four main compartments in Aldorf and their active wells. Blue marked ones represent the injection wells; the others are production wells. - 34 -*
9. *Table 9 shows the amounts produced per compartment for oil, gas and water, which was estimated from the wellbores previously defined in the individual compartment. Furthermore, the back-allocated amounts of field Aldorf for MBAL input are noted..... - 38 -*
10. *Table 10 shows the summary table of Brooks-Corey parameters estimated for each compartment in Aldorf - 40 -*
11. *Table 11 Initial settings for every MBAL tank in Aldorf..... - 41 -*
12. *Table 12 shows the resulting transmissibility values for the Aldorf field after history matching. - 43 -*
13. *Table 13 illustrates the parameters of the aquifer model in each compartment after the history matching. - 44 -*
14. *Table 14 Summary of uncorrected pressure data per compartment - 45 -*
15. *Table 15 Results of network solver for the field Dueste excluding Aldorf and Bockstedt from the system. - 64 -*
16. *Table 16 give a comparison of GAP simulation rates and well checker and water cut measurements for the individual wells in Dueste. Wells with blank fields are disabled ones, because they are not in production. The oil rates from the field measurements are calculated from the well checker and water cut measurements. - 64 -*
17. *Table 17 shows the results of the network solver for the field Aldorf excluding Dueste and Bockstedt from the system..... - 65 -*
18. *Table 18 illustrates the results of the first simulation run in Aldorf for three selected times. - 66 -*
19. *Table 19 Comparison of GAP simulation rates and well checker measurements for the individual wells in Aldorf. - 67 -*
20. *Table 20 Comparison of GAP simulation rates with well checker measurements after relative permeability revision in Aldorf..... - 68 -*
21. *Table 21 Comparison of GAP simulation rates and well checker measurements for the individual wells in Bockstedt - 70 -*

22. Table 22 gives an overview of the full field validation run. A comparison between the simulation run (left columns), the well checker measurements (middle column) and the PDMS (right column) can be seen for the end of 2015.	- 71 -
23. Table 23 gives a summary of the liquid and oil rates per field compared to the different systems. The data are from the end of 2015 and therefore differ from the comparison in the introduction (Table 2). . -	73 -
24. Table 24 summarizes the individual deviations per field and system for the end of 2015.	- 73 -
25. Table 25 shows the comparison between the PDMS, well checker and the full field model results for the end of 2015. The left column shows the rates per phase and water cut per calculation system. The charts on the right illustrate the rates as stacked column per field and calculation system. It can be observed that the liquid rate and are between the PDMS and the well checker. The oil rates are close to the allocated rates from the PDMS and except of the Dueste field between the PDMS and well checker and water cut measurements. The rates are given in Sm ³ /d and the water cut in %.....	- 73 -
26. Table 26 shows the produced amount of water, which is passed from the production to the injection system as the target rate on the left. In the middle the amount of water, which was calculated by the network solver from the injection system can be seen. The right column illustrates the amount of water saved in the ACRON system.	- 81 -
27. Table 27 illustrates the injection rates per well in Aldorf, Bockstedt and Dueste from the ACRON and the GAP injection network solver for 31.12.2015.....	- 81 -
28. Table 28 summarizes the cumulative oil produced per field after the simulation period.	- 86 -
29. Table 29 shows the chosen production wells, their simulated oil rates from 31.12.2015 and shut in date.	- 86 -
30. Table 30 summarizes the results of the cumulative oil production from the different scenarios by the end of 2020.	- 95 -
31. Table 31 shows all allocated wells for each newly defined compartment in Aldorf. Green marked wells represent active production wells, blue marked ones represent active injectors. Yellow assigned fields show wells, from which pressure tests were taken and white marked wells were active in the past. -	111 -
32. Table 32 illustrates the permeability, porosity, initial water saturation and irreducible oil saturation values per layer, which were defined and analyzed in 1965 after Lewis.	- 114 -
33. Table 33 shows the initial input values for the net pay and permeability for the IPR models of the Aldorf field in PROSPER.....	- 116 -
34. Table 34 shows the initial input values for the net pay and permeability for the IPR models of the Bockstedt field in PROSPER	- 127 -

27 Appendix A

27.1 Well allocation per re-defined compartment in Aldorf

Table 31 shows all allocated wells for each newly defined compartment in Aldorf. Green marked wells represent active production wells, blue marked ones represent active injectors. Yellow assigned fields show wells, from which pressure tests were taken and white marked wells were active in the past.

A	B	C	D	E	F	G
Aldorf 026	Aldorf 104	Aldorf 008	Aldorf 115	Aldorf 102	Aldorf 011	Aldorf 054
Aldorf 028	Aldorf 014	Aldorf 110	Aldorf 021	Aldorf 103	Aldorf 083	Aldorf 023
Aldorf 030	Aldorf 068	Aldorf 016	Aldorf 027	Aldorf 120	Aldorf 085	Aldorf 045
Aldorf 044	Aldorf 069	Aldorf 035	Aldorf 029	Aldorf 013	Aldorf 093	Aldorf 054
Aldorf 098	Aldorf 089	Aldorf 071	Aldorf 048	Aldorf 060	Aldorf 095	Aldorf 086
Aldorf 099	Aldorf 090	Aldorf 079	Aldorf 050	Aldorf 084	Aldorf 080	Aldorf 118
Aldorf 001	Aldorf H001	Aldorf 105	Aldorf 051	Aldorf 091	Aldorf 081	Aldorf 047
Aldorf 097	Aldorf 005	Aldorf 012	Aldorf 031	Aldorf 018	Aldorf 112	Aldorf 053
Aldorf 040	Aldorf 041	Aldorf 015	Aldorf 010	Aldorf 101	Aldorf 113	Aldorf 043
Aldorf 111	Aldorf 114	Aldorf 002	Aldorf 039	Aldorf 036	Aldorf 007	Aldorf 023
Aldorf 034	Aldorf 066	Aldorf 022	Aldorf 049	Aldorf 020	Aldorf 082	Aldorf 025
Aldorf Z1	Aldorf 087	Aldorf 003	Aldorf 052	Aldorf 056	Aldorf 009	Aldorf 033
Aldorf 042	Aldorf 088	Aldorf 501	Aldorf 057		Aldorf 092	Aldorf 046
Aldorf 019	Aldorf 096	Aldorf 062	Aldorf 058		Aldorf 094	Aldorf 054
Aldorf 107		Aldorf 063	Aldorf 059			Aldorf 055
		Aldorf 064	Aldorf 061			Aldorf H003
		Aldorf 065				
		Aldorf 071				
		Aldorf 072				
		Aldorf 073				
		Aldorf 074				
		Aldorf 077				
		Aldorf 078				
		Aldorf 100				
		Aldorf 104				
		Aldorf 106				
		Aldorf 017				
		Aldorf 024				
		Aldorf 032				
		Aldorf 004				
		Aldorf 006				
		Aldorf 070				
		Aldorf 075				
		Aldorf 076				
		Aldorf 108				

27.2 Aldorf Reservoir and Production Properties

27.2.1 PVT Cell Experiment from Aldorf 002 on the 16.06.1953

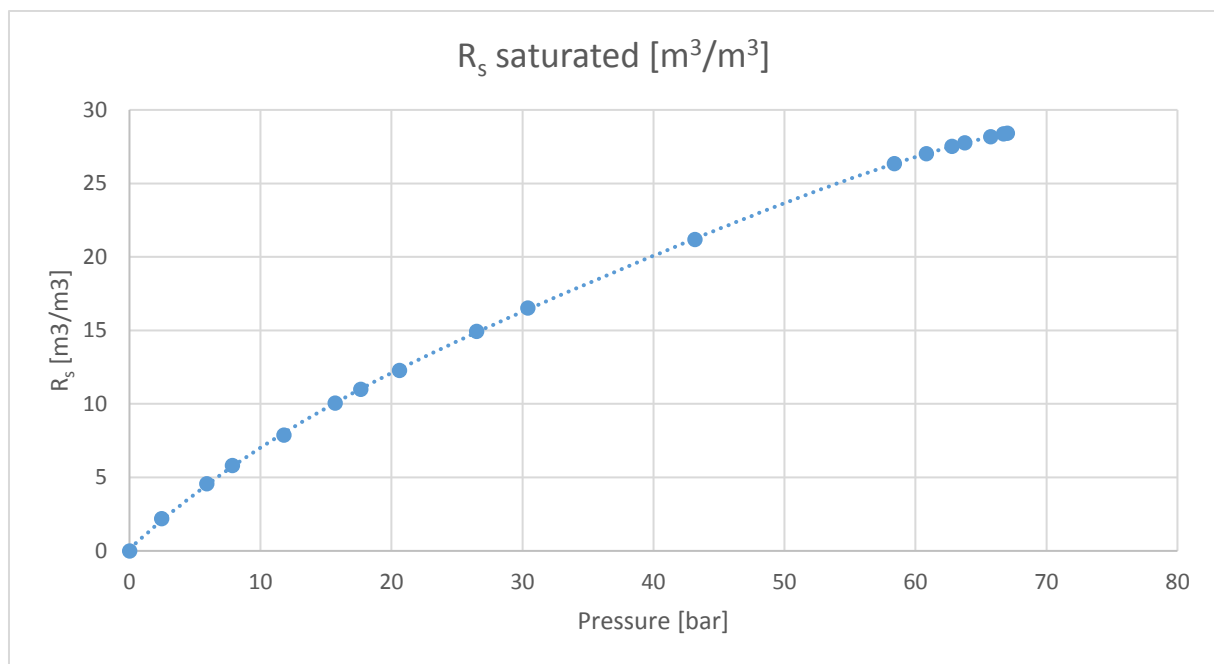
Depth	1040	m		
Volume	407.5	cm ³		
Initial pressure	118	kg/cm ²	116	bar
Temperature	53.4	°C	128.12	°F
Bubble point	68.3	kg/cm ²	67.00	bar
γ_o @53.4 °C	0.85	-	34.97	°API
γ_g	0.78	-		
γ_o (dead oil)	0.87	-		

Pressure	R_s	Viscosity	B_o
<i>[bar]</i>	<i>[m³/m³]</i>	<i>[cP]</i>	<i>[bbl/stb]</i>
240.34	28.42	4.32	1.0570
213.86	28.42	4.15	1.0598
188.35	28.42	3.98	1.0625
155.00	28.42	3.76	1.0660
122.63	28.42	3.55	1.0694
98.10	28.42	3.39	1.0720
67.00	28.42	3.18	1.0753
66.71	28.36	3.18	1.0751
65.73	28.17	3.20	1.0746
63.77	27.75	3.20	1.0735
62.78	27.51	3.21	1.0729
60.82	27.02	3.21	1.0716
58.37	26.33	3.22	1.0698
43.16	21.19	3.42	1.0563
30.41	16.53	3.60	1.0441
26.49	14.92	3.69	1.0399
20.60	12.28	3.83	1.0330
17.66	10.99	3.92	1.0296
15.70	10.06	3.98	1.0272
11.77	7.87	4.10	1.0214
7.85	5.8	4.15	1.0160
5.89	4.56	4.30	1.0128
2.45	2.2	4.40	1.0066
0.00	0	4.61	1.0080

27.2.1.1 Solution Gas Oil Ratio

$$R_s(p)_{saturated} = G_1 \cdot p^4 + G_2 \cdot p^3 + G_3 \cdot p^2 + G_4 \cdot p + G_5$$

G ₁	-0.0000015658379
G ₂	0.00024440643
G ₃	-0.015247696
G ₄	0.81740432
G ₅	0.1419149



27.2.2 Vasquez and Beggs Correlation

27.2.2.1 Oil FVF – Saturated

$$B_o = 1 + A_1 \cdot R_s + A_2 \cdot (T - 60) \cdot \left(\frac{\gamma_{API}}{\gamma_g} \right) + A_3 \cdot R_s \cdot (T - 60) \cdot \left(\frac{\gamma_{API}}{\gamma_g} \right)$$

C ₁	0.000467
C ₂	0.000011
C ₃	0.000000001377

27.2.2.2 Oil FVF - Undersaturated

$$B_o = B_{ob} \cdot e^{(c_o(p_b - p))}$$

B_{ob}	1.0753 rbbl/stb
c_o	0.00000672 psi ⁻¹
P_b	984.66 psi

27.2.3 Layers Petro Physical Parameters

The values in Table 32 were estimated in 1965 after the analysis of cores from the Aldorf field from the contractor Lewis. Amongst other input properties based on these values as a reference, the Aldorf MBAL tanks were set up.

Table 32 illustrates the permeability, porosity, initial water saturation and irreducible oil saturation values per layer, which were defined and analyzed in 1965 after Lewis.

	Permeability	Porosity	S_{wi}	S_{oi}
	[mD]	[-]	[-]	[-]
Serpelkalk	35.1	0.125	0.526	0.474
Gigas-Schichten	45	0.146	0.451	0.549
Kimmeridge	74.5	0.165	0.312	0.688
Ob. Doggerepsilon	23.6	0.13	0.57	0.43
Unt. Doggerepsilon	7.6	0.13	0.76	0.24

27.2.4 Brine Viscosity Correlation

The brine viscosity at reservoir conditions is a necessary input parameter for the proper estimation of the fractional flow of water. Therefore, the following correlation charts were applied (Barrufet, 2012). First, the brine viscosity at reservoir temperature and atmospheric pressure condition was estimated in Figure 63, where the viscosity of the water at 1 atm results in 0.8 cP. Figure 64 shows the brine viscosity ratio versus the reservoir pressure, whereas the initial reservoir pressure of 1705 psi was applied. This results in a water viscosity ratio of 1.05 and with the above estimated brine viscosity at reservoir temperature to a final brine viscosity at reservoir conditions of 0.84 cP.

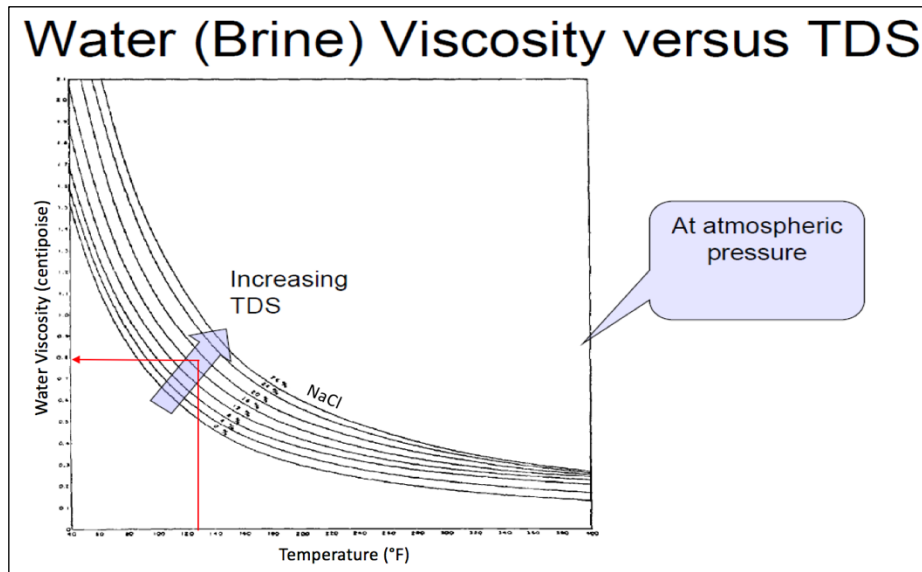


Figure 63 shows the correlation chart of water viscosity [cP] versus the reservoir temperature [°F] for various total dissolved solids [%] at atmospheric pressure condition. It can be observed that for a certain isothermal condition the brine viscosity increases with increasing NaCl concentration.

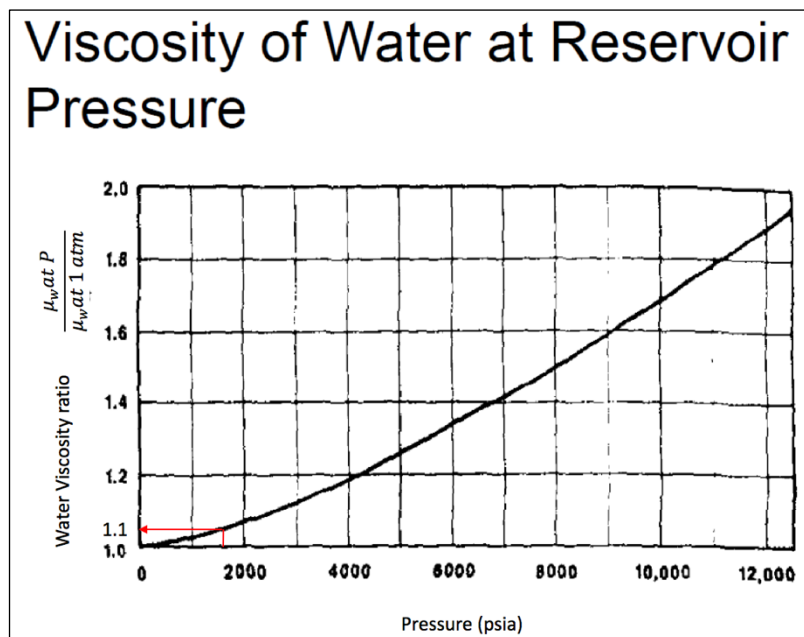


Figure 64 illustrates the chart of water viscosity ratio versus reservoir pressure.

27.2.5 Parameters for IPR generation in Aldorf

The permeability values were for initial purposes taken from the top three layers of Table 32, which were the Serpelkalk, Gigas-Schichten and Kimmeridge, which accounts for one average value of 50 mD over the whole field. The net pay estimated from downhole drawings, but it was further tried to follow trend of increase thickness from northeast to southwest. The values were continuously adjusted during the IPR generation in PROSPER and development of the model.

Table 33 shows the initial input values for the net pay and permeability for the IPR models of the Aldorf field in PROSPER

Well	Net pay	Permeability
	<i>[m]</i>	<i>[mD]</i>
Aldorf 001	15	50
Aldorf 097	15	50
Aldorf 107	15	50
Aldorf 104	45	50
Aldorf 096	80	50
Aldorf 054	50	50
Aldorf 023	45	50
Aldorf 014	50	50
Aldorf 021	50	50
Aldorf 108	50	50
Aldorf 068	50	50
Aldorf 087	50	50
Aldorf 045	50	50

27.2.6 PVT Matching in PROSPER field Aldorf

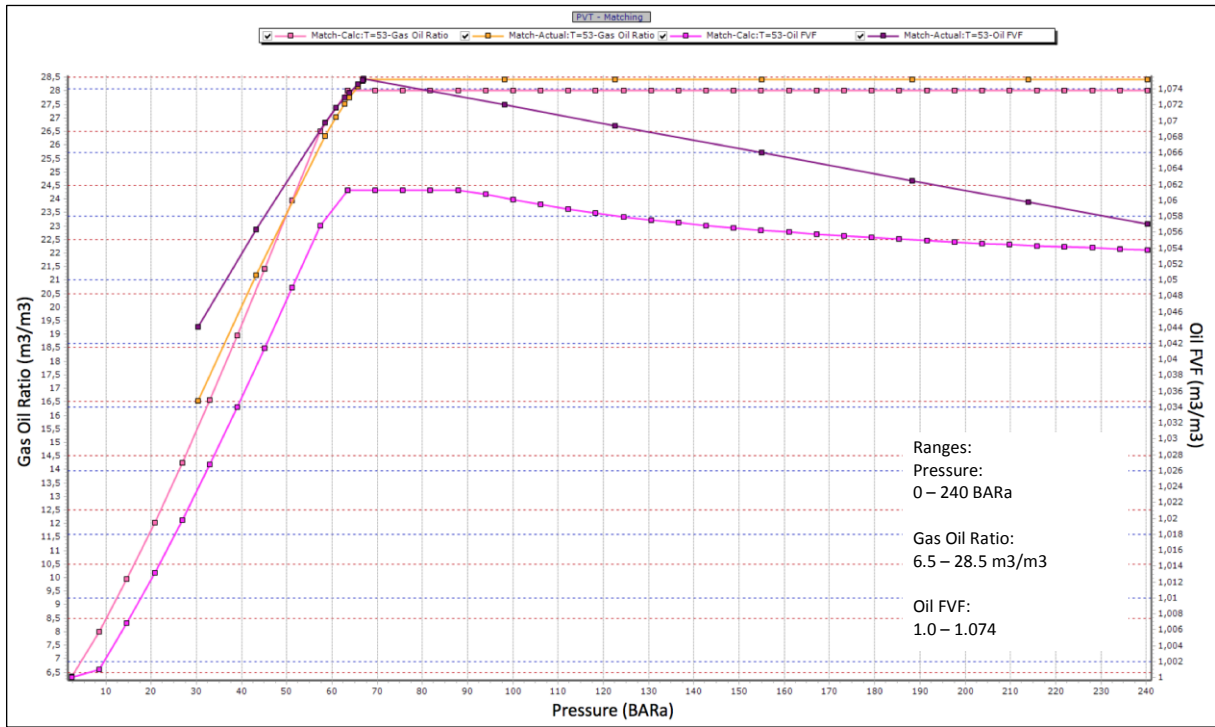


Figure 65 shows the R_s and B_o for the Aldorf PROSPER files, which were correlated with Vasquez and Beggs

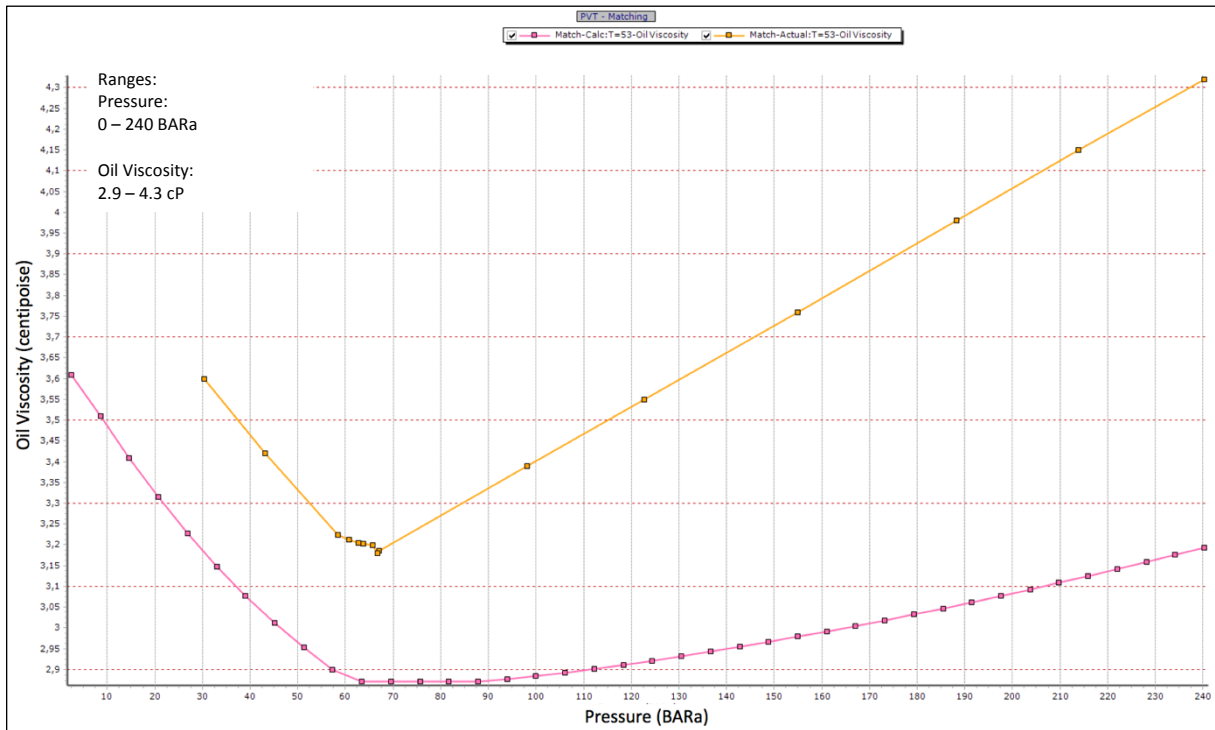


Figure 66 shows the μ_o for the Dueste PROSPER files, which was correlated with Beggs et al.

28 Appendix B

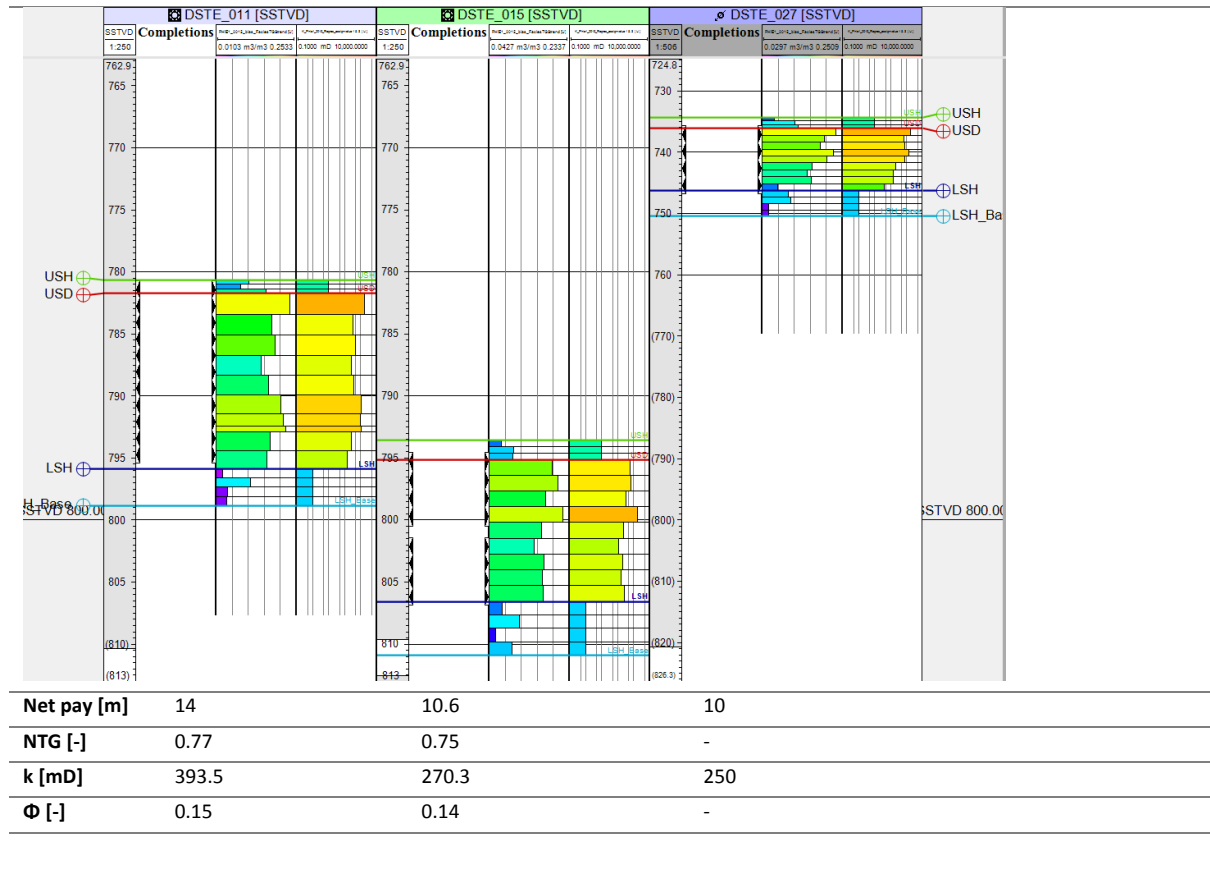
28.1.1 PVT Cell Experiment from Dueste 008 on the 17.02.1955

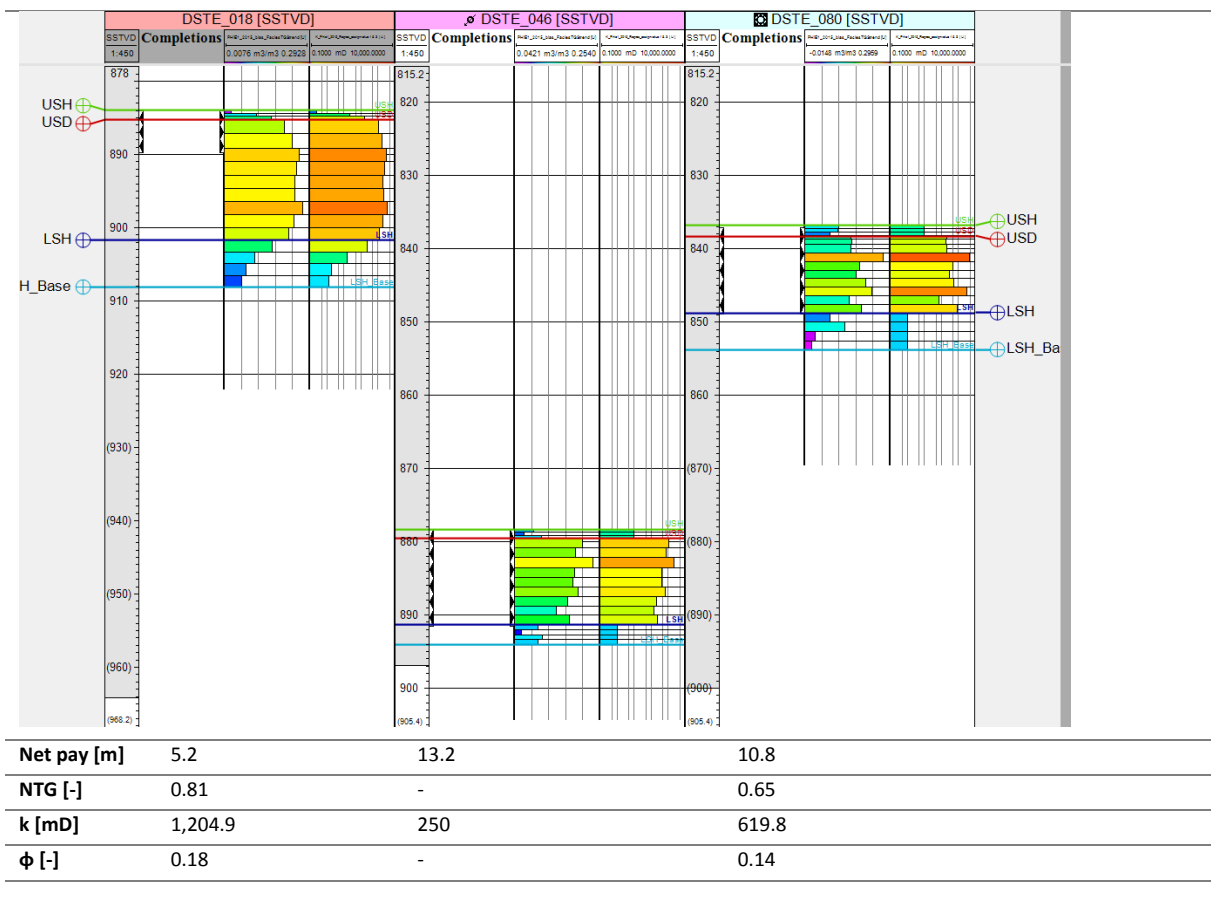
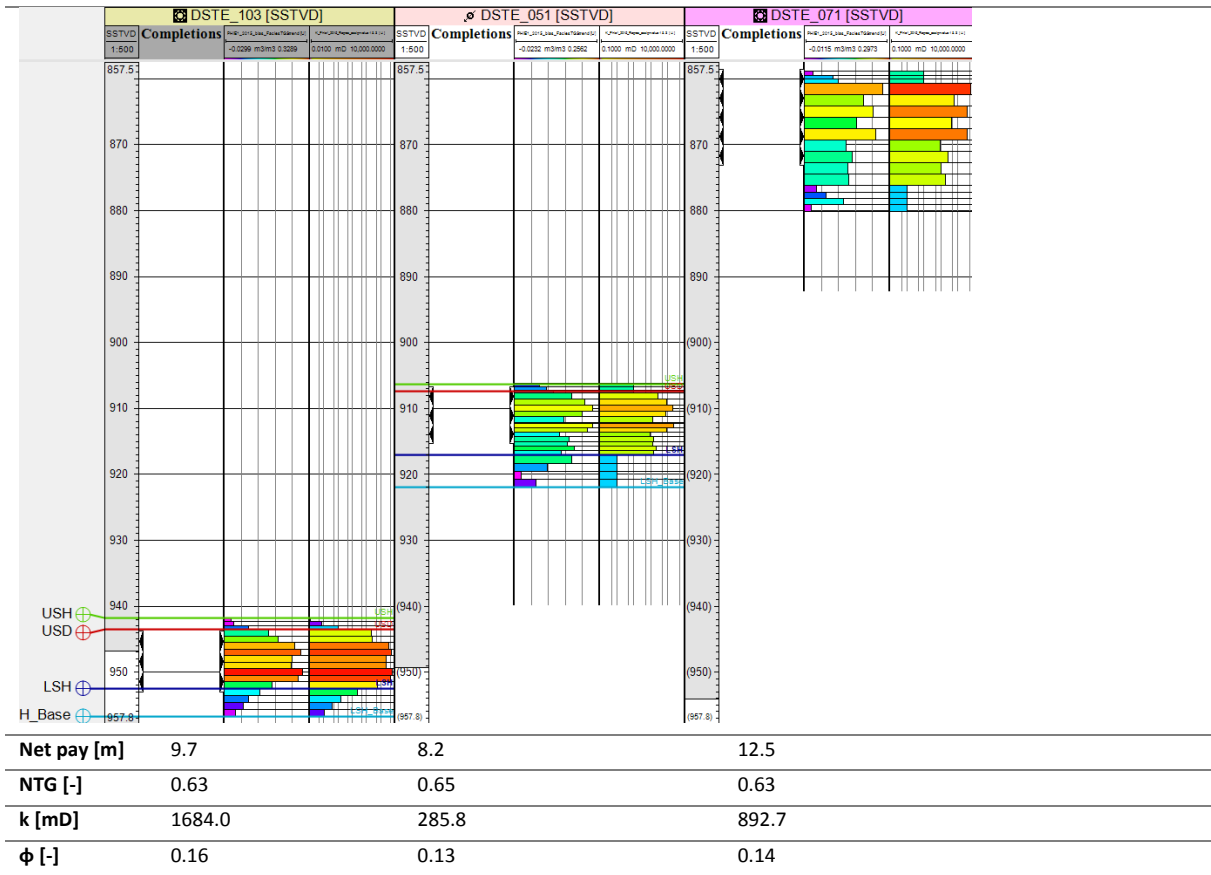
Depth	818	m		
Volume	388.4	cm ³		
Initial pressure	250	kg/cm ²	245.25	bar
Temperature	37.7	°C	99.86	°F
Bubble point	38.3	kg/cm ²	37.57	bar
γ_o @37.7 °C	0.87	-	31.33	°API
γ_g	0.62	-		

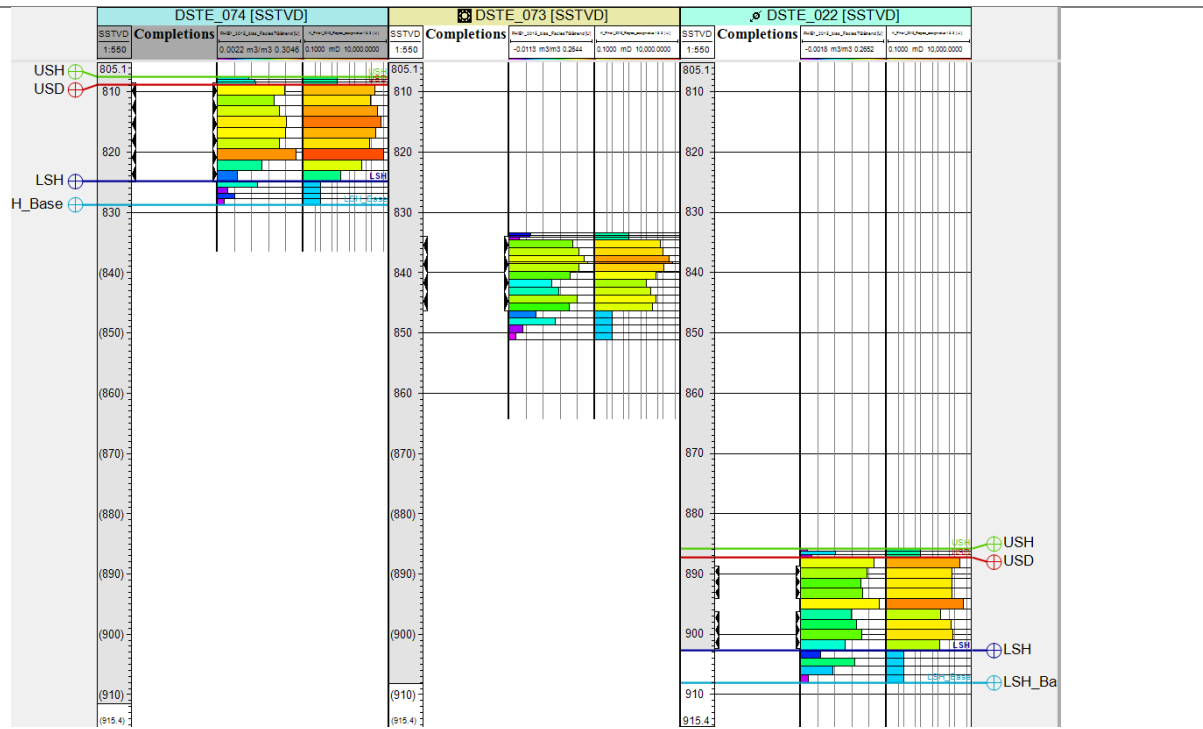
Pressure	R_s	Viscosity	Bo
<i>[bar]</i>	<i>[m³/m³]</i>	<i>[cP]</i>	<i>[bbl/stb]</i>
249.14	13.49	31.4	1.0178
203.07	13.49	29.3	1.0218
152.06	13.49	26.5	1.0261
103.00	13.49	24.9	1.0303
57.88	13.49	22.7	1.0342
39.24	13.49	21.8	1.0358
37.57	13.49	21.7	1.0360
36.79	13.21	21.69	1.0352
35.61	12.85	21.62	1.0343
34.83	12.61	21.58	1.0337
33.84	12.32	21.54	1.0329
33.06	12.01	21.51	1.0321
30.41	11.28	21.46	1.0302
26.00	10.07	21.53	1.0270
22.56	8.93	21.73	1.0240
21.09	8.41	21.84	1.0227
19.13	7.98	22.3	1.0215
15.70	6.58	22.45	1.0179
13.73	5.82	22.74	1.0159
10.79	4.76	23.1	1.0131
4.91	2.49	24.2	1.0071
3.92	1.99	24.77	1.0058
2.94	1.38	25.02	1.0042
2.06	0.99	25.26	1.0032
0.98	0.37	25.56	1.0016
0.00	0.00	26.1	1.0006

28.1.2 Logs Dueste field

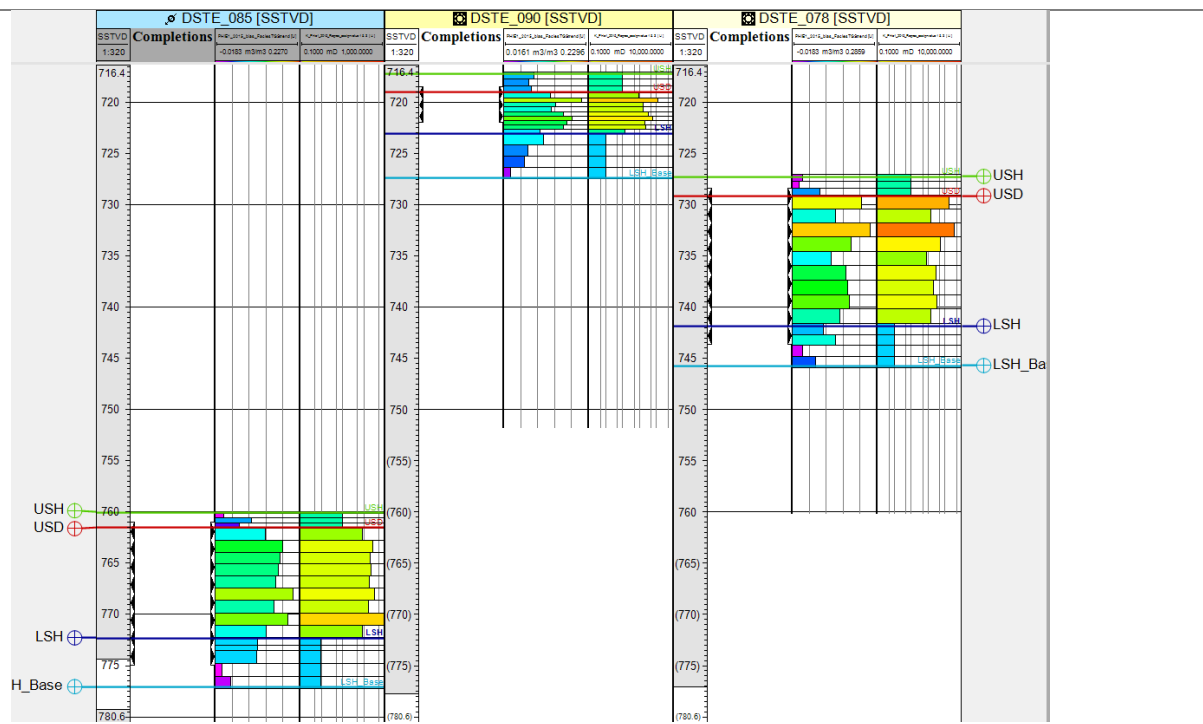
The following facies and permeability logs of the wells in the Dueste field were extracted from the Petrel Dueste model for creating the IPR curves in PROSPER. The left column further shows the perforated interval per well. The middle column the facies log and the right the permeability. The perforated interval was used as the net pay for PROSPER input. If it was not possible for some reason to extract the parameters, an educated guess for the permeability was chosen as can be seen in the table. This guess is based on surrounding wells. The values listed below are initial values, therefore adjustments for some PROSPER files were made.



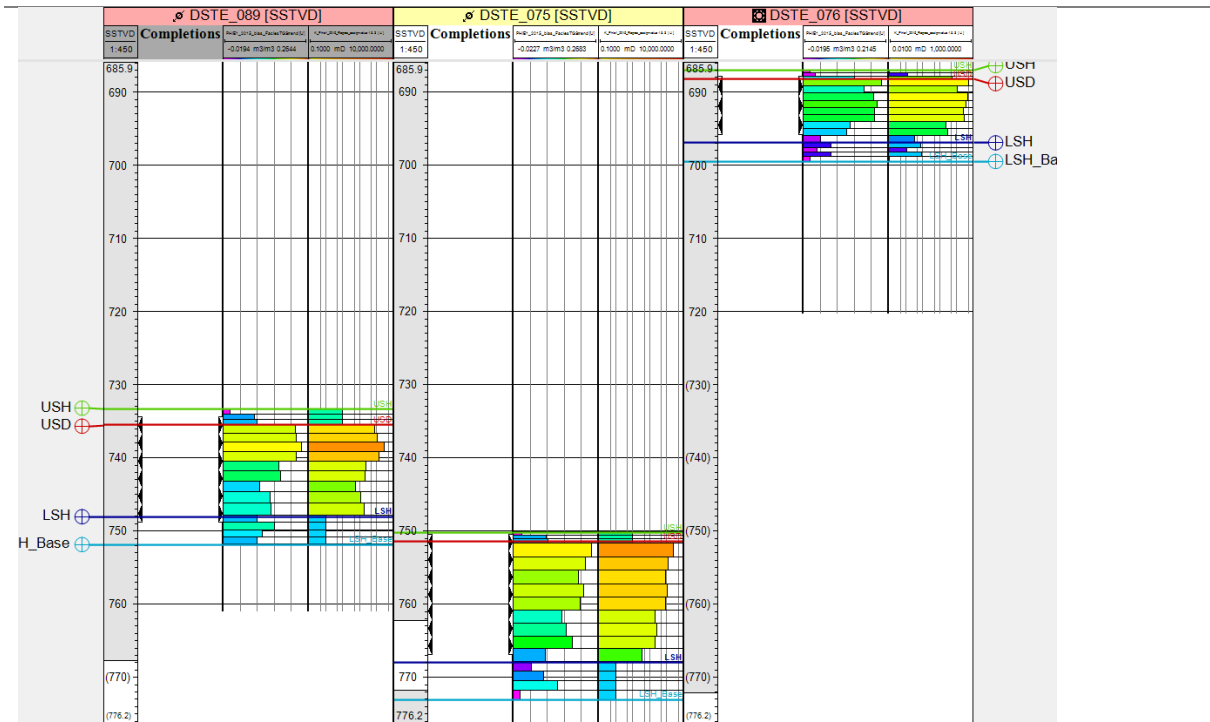




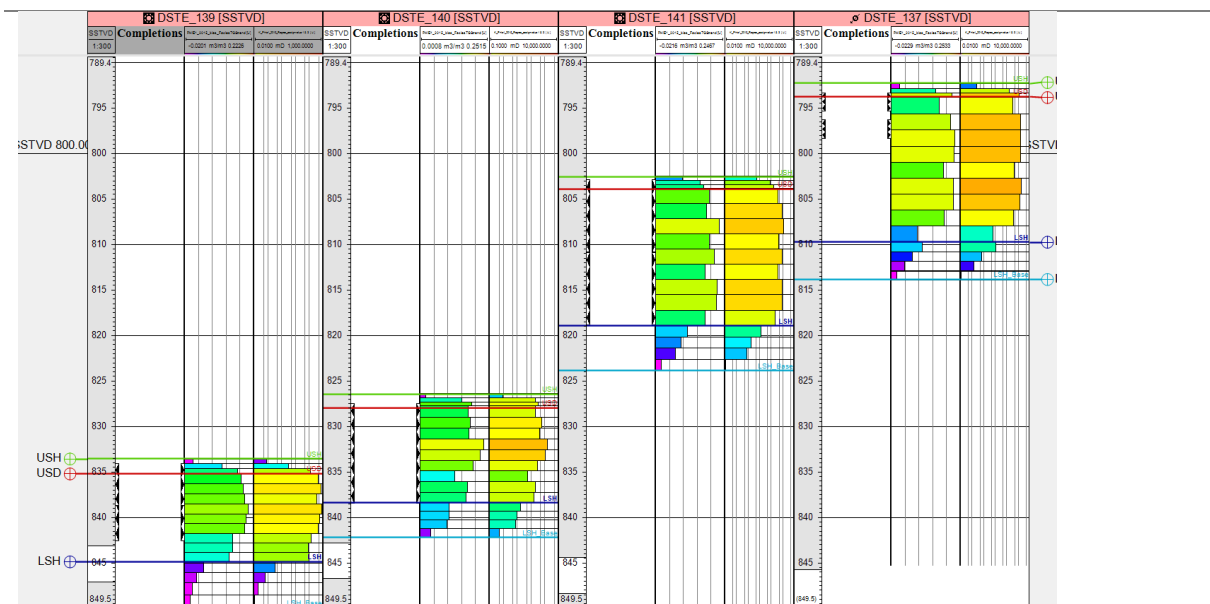
Net pay [m]	16.2	11.8	11.6
NTG [-]	0.75	0.65	-
k [mD]	994.6	566.7	250
φ [-]	0.16	0.14	-



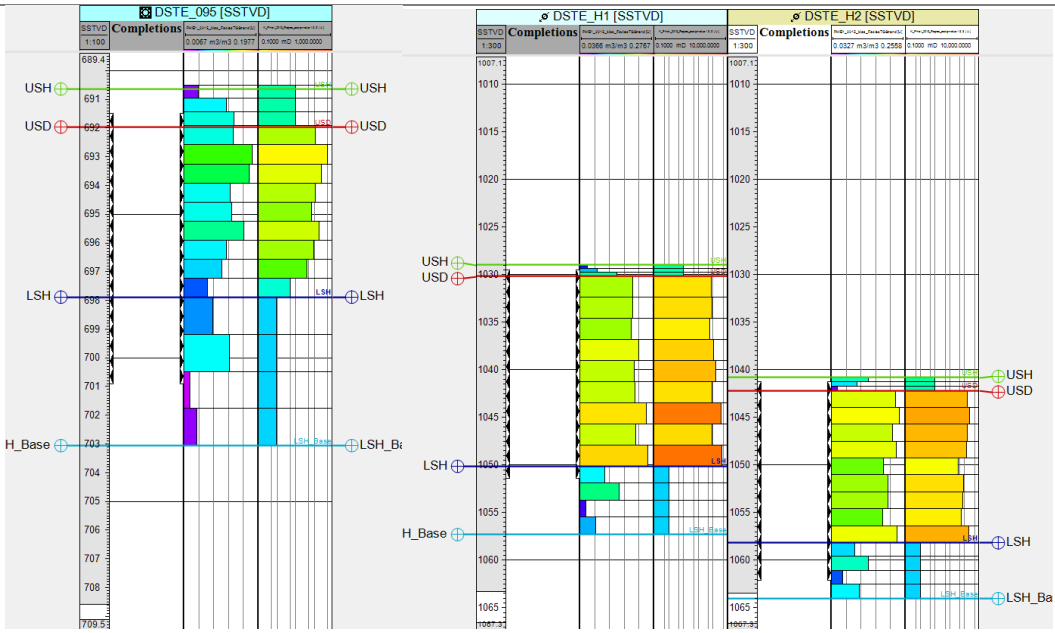
Net pay [m]	12	3.4	12.8
NTG [-]	-	0.75	0.63
k [mD]	250	187.5	446.9
φ [-]	-	0.12	0.13



Net pay [m]	14.4	16	7.6
NTG [-]	-	-	0.56
k [mD]	250	250	123.7
φ [-]	-	-	0.10



Net pay [m]	8.5	10.6	16.11	4.28
NTG [-]	-	-	-	-
k [mD]	200	200	270	200
Φ [-]	-	-	-	-



Net pay [m]	8.7	22	20.5
NTG [-]	-	0.81	0.88
k [mD]	200	866.2	693.3
Φ [-]	-	0.17	0.17

28.1.3 PVT Matching in PROSPER field Dueste

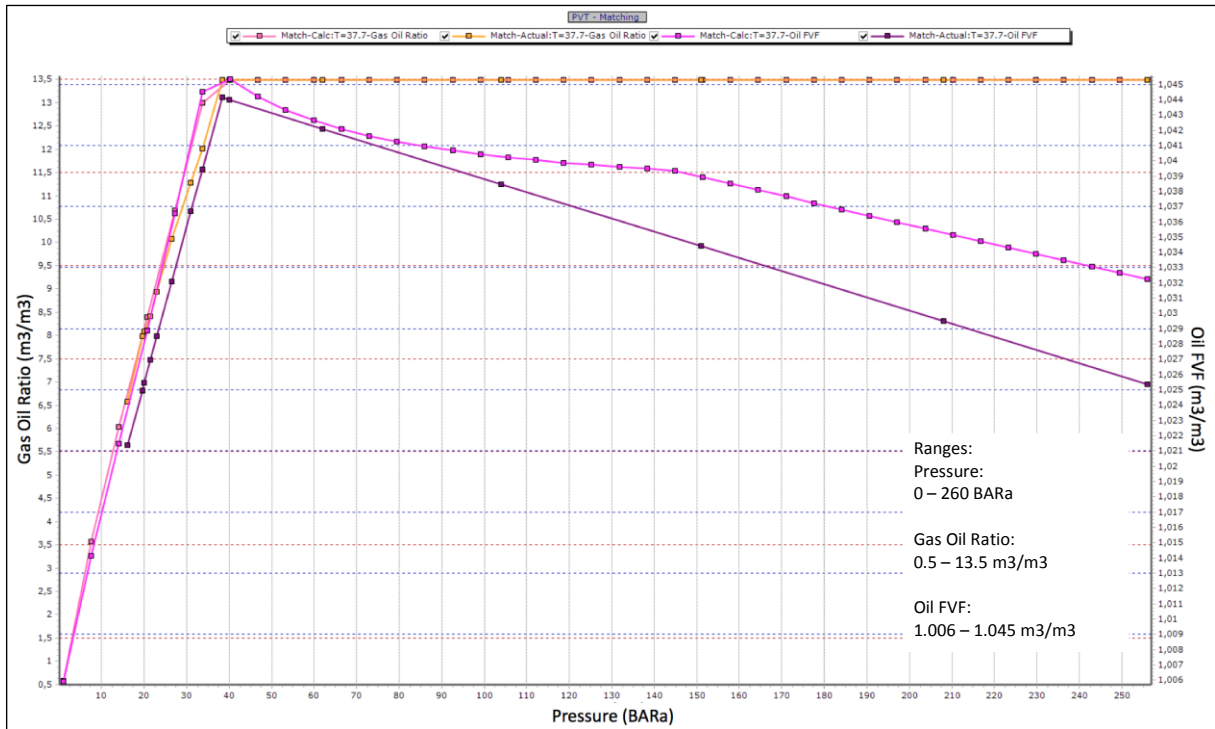


Figure 67 shows the R_s and B_o for the Dueste PROSPER files, which were correlated with Glasø

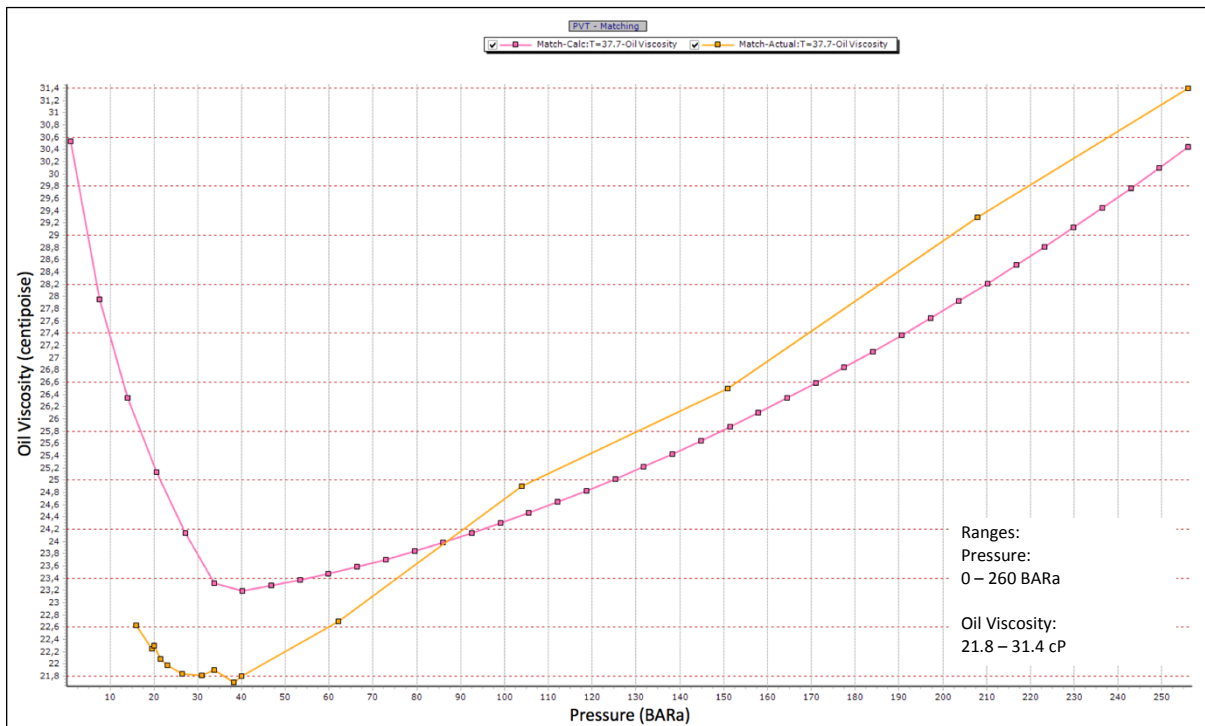


Figure 68 shows the μ_o for the Dueste PROSPER files, which was correlated with Beggs et al.

29 Appendix C

29.1.1 PVT Cell Experiment from Bockstedt 035 on the 15.03.1961

Depth	990	m		
Initial pressure	300	kg/cm ²	294.3	bar
Temperature	50	°C	122	°F
Bubble point	36	kg/cm ²	36.48	bar
γ_o @50 °C	0.86	-	33.99	°API
γ_g	0.75	-		
γ_o (dead oil)	0.88			

Pressure	R_s	Viscosity	Bo
<i>[bar]</i>	<i>[m³/m³]</i>	<i>[cP]</i>	<i>[bbl/stb]</i>
294.3	13.5		1.032
269.8	13.5		1.034
245.3	13.5	35.9	1.035
220.7	13.5		1.037
196.2	13.5	33.0	1.039
171.7	13.5		1.041
147.2	13.5	30.5	1.043
122.6	13.5		1.045
98.1	13.5	27.7	1.047
73.6	13.5		1.049
49.1	13.5	25.6	1.051
35.3	12.08	23.3	1.052
22.6	9.18		1.046
17.0	6.44		1.040
13.7		23.9	
8.8	3.61		1.034
3.9		26.0	

29.1.2 PVT Matching in PROSPER field Bockstedt

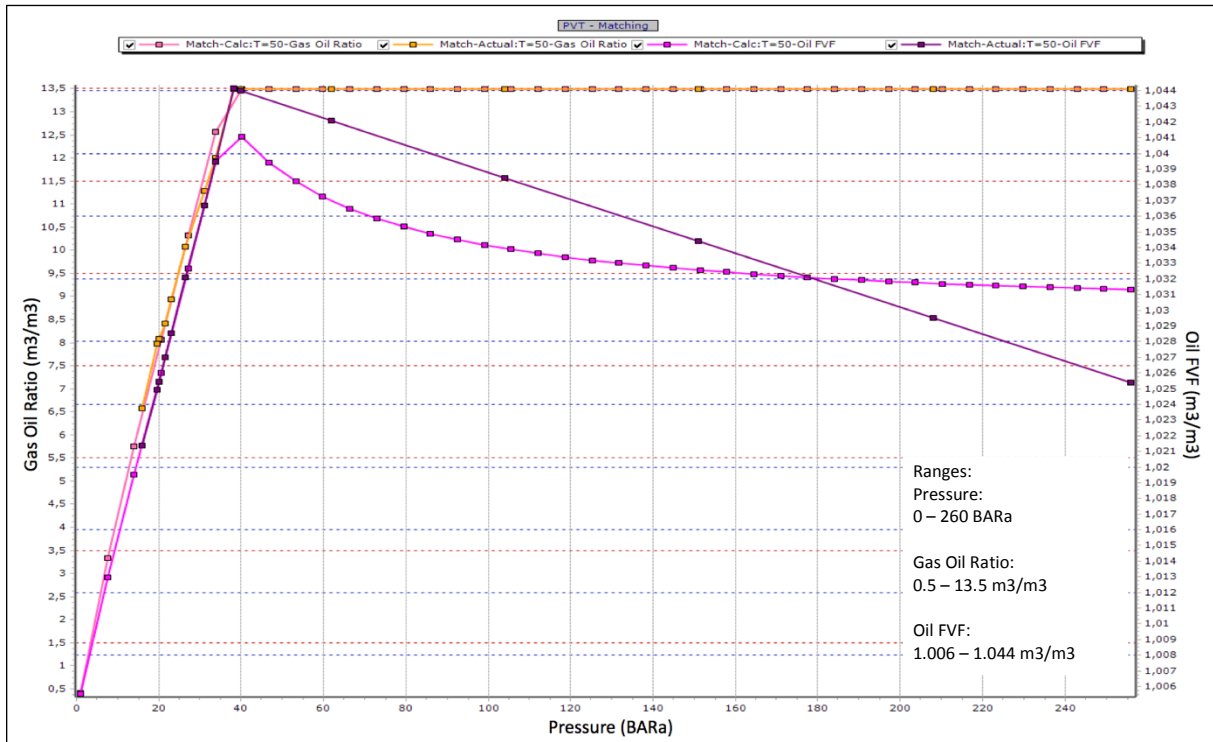


Figure 69 shows the R_s and B_o for the Bockstedt PROSPER files, which were correlated with Glasø.

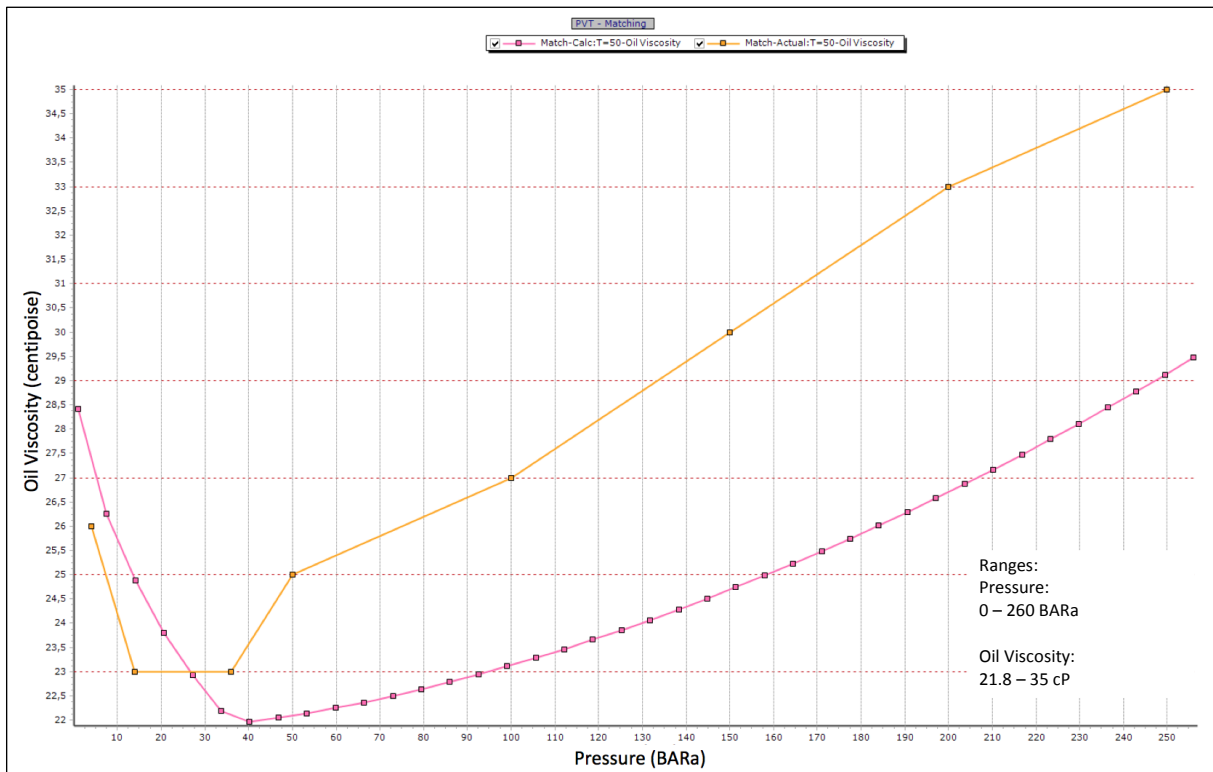


Figure 70 shows the μ_o for the Bockstedt PROSPER files, which was correlated with Beggs et al.

29.1.3 Parameters for IPR generation in Bockstedt

The IPR generation in PROSPER for the Bockstedt field differs in that way that there already existed PROSPER files from a previous study. It was able to use parameters such as the permeability and net pay as can be seen in Table 34, from the previously generated files.

Table 34 shows the initial input values for the net pay and permeability for the IPR models of the Bockstedt field in PROSPER

Well	Net Pay	Permeability
	<i>[m]</i>	<i>[mD]</i>
Bockstedt 068	10.1	1,148
Bockstedt 028	10.1	1,148
Bockstedt 069	20.8	400
Bockstedt 009	15	1,500
Bockstedt 045	20.5	430.7
Bockstedt 035	15	1,000
Bockstedt 039	20	1,000
Bockstedt 037	15	1,000
Bockstedt 036	20	1,500
Bockstedt 031	10.7	1,632
Bockstedt 035	10	1,000
Bockstedt 081	13.2	2,900
Bockstedt 056	10	151
Bockstedt 084	14.9	1,000
Bockstedt 086	10	1,000
Bockstedt 082	10	150
Bockstedt H3	33.3	1,032

30 Appendix D

30.1 Simplified Water Saturation Over Time Derivation (Dake, 1978)

Starting from the definition of the fractional flow

$$f_w = \frac{1 + \frac{k \cdot k_{ro} \cdot A}{q_t \cdot \mu_o} \cdot \left(\frac{\partial P_c}{\partial x} - \frac{\Delta \rho \cdot g \cdot \sin \theta}{1.0133 \cdot 10^6} \right)}{1 + \frac{\mu_w}{\mu_o} \cdot \frac{k_{ro}}{k_{rw}}}$$

, and assuming the reservoir to be nearly horizontal, it can be reduced to, by neglecting the gravity term

$$f_w = \frac{1 + \frac{k \cdot k_{ro} \cdot A}{q_t \cdot \mu_o} \cdot \left(\frac{\partial P_c}{\partial x} \right)}{1 + \frac{\mu_w}{\mu_o} \cdot \frac{k_{ro}}{k_{rw}}}$$

The effect of capillary pressure can be split up to the following gradients

$$\frac{\partial P_c}{\partial x} = \frac{dP_c}{dS_w} \cdot \frac{\partial S_w}{\partial x}$$

, where it can be assumed that the gradient of the water distribution function $\frac{\partial S_w}{\partial x}$ as well as the capillary pressure function $\frac{dP_c}{dS_w}$ are negligible, because of the low viscosity of the oil and similar relative permeability endpoints, which results in a low mobility ratio. The low mobility ratio is an indication for a stable displacement front and therefore a less steep slope behind the front saturation. Moreover, because of the long production time the slope is assumed to very shallow. These assumptions further reduce the fractional flow function to the following

$$f_w = \frac{1}{1 + \frac{\mu_w}{\mu_o} \cdot \frac{k_{ro}}{k_{rw}}}$$

Introducing the equation of Buckley-Leverett (Buckley & Leverett, 1942)

$$v_{S_w} = \frac{dx}{dt} \Big|_{S_w} = \frac{q_t}{A \cdot \phi} \cdot \frac{df_w}{dS_w} \Big|_{S_w}$$

, it shows that the velocity of the water saturation plane v_{S_w} is directly proportional to the derivative of the derivative of the fractional flow with regard to the water saturation. Moreover, if the capillary pressure is neglected – as in this case, then the fractional flow of water is just a function of the water saturation.

Integration of the BL equation over the total time since the start of the production leads to

$$x_{S_w} = \frac{W_i}{A \cdot \phi} \cdot \frac{df_w}{dS_w} \Big|_{S_w}$$

Furthermore, introducing Welge (Welge, 1952) method for obtaining the average water saturation behind the front \bar{S}_w

$$W_i = x_2 \cdot A \cdot \phi \cdot (\bar{S}_w - S_{wc})$$

, where W_i is the amount of water injection, which is assumed, because of the assumption of incompressibility, to be equal to the cumulative oil production. The fact that the current case is at a fixed time requires the saturation front to be at a certain location, which is estimated to be x_2 . Rearranging the above Welge definition and assuming that the front reached the breakthrough $x_2 = L$ leads to

$$\frac{W_i}{L \cdot A \cdot \phi} = (\bar{S}_w - S_{wc})$$

The definition of pore volume (or OIP) is then the following

$$OIP = L \cdot A \cdot \phi \cdot (1 - S_{wc})$$

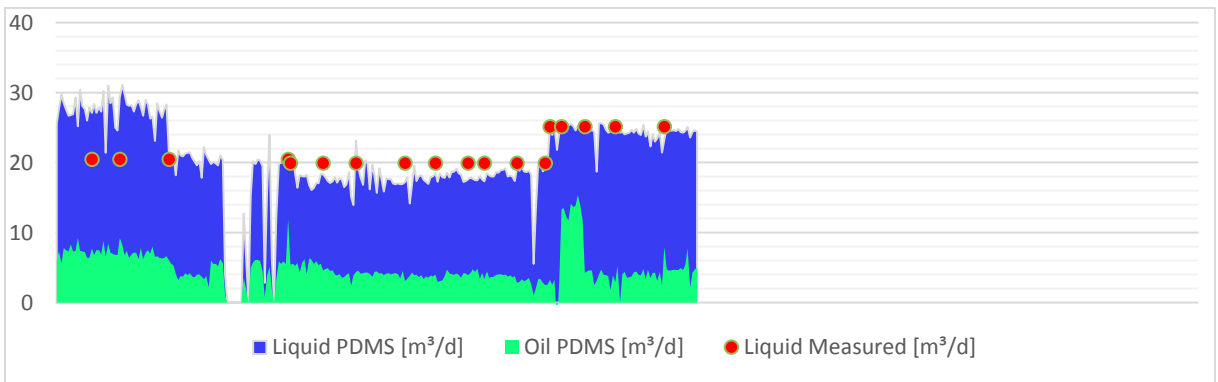
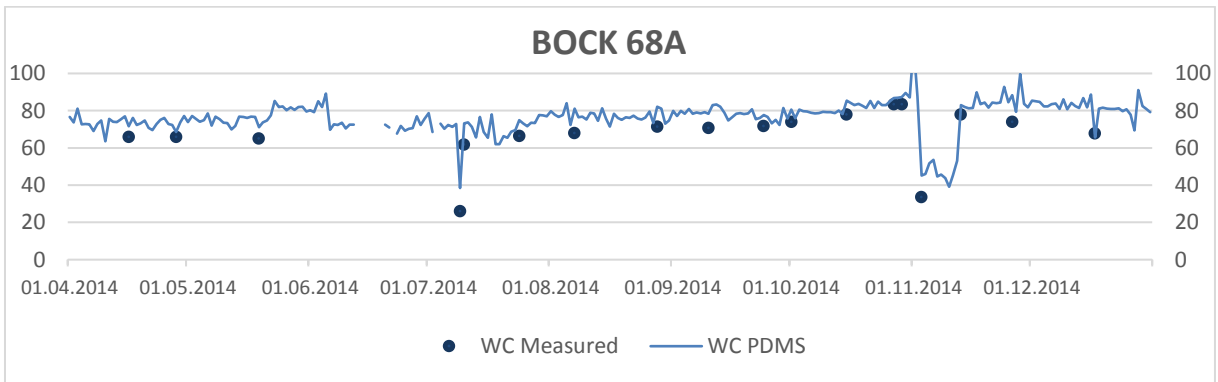
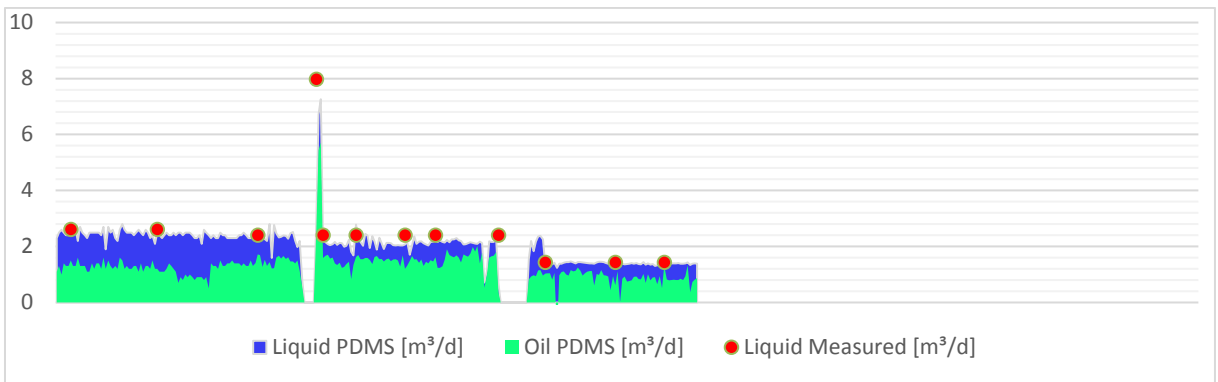
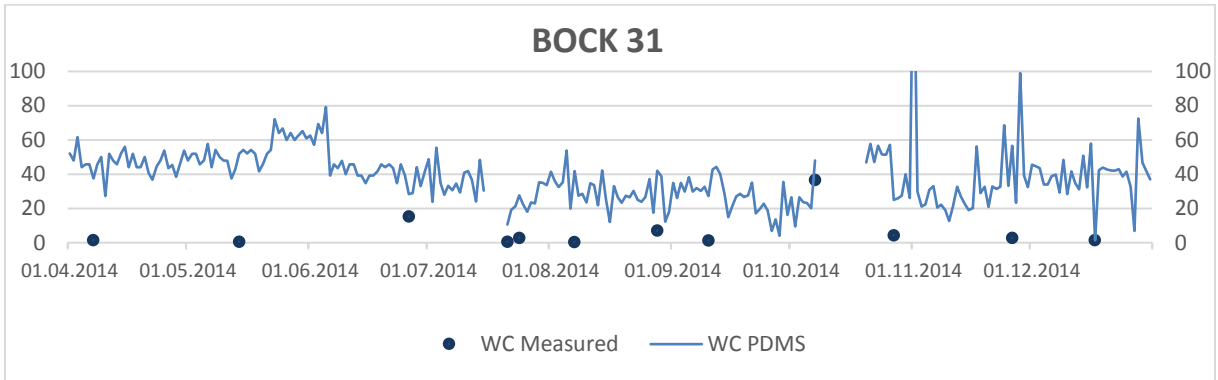
Inserting the definition of OIP to the above formulation as well as replacing the W_i with the cumulative oil production leads to the simplified definition of saturation over time as a function of oil production:

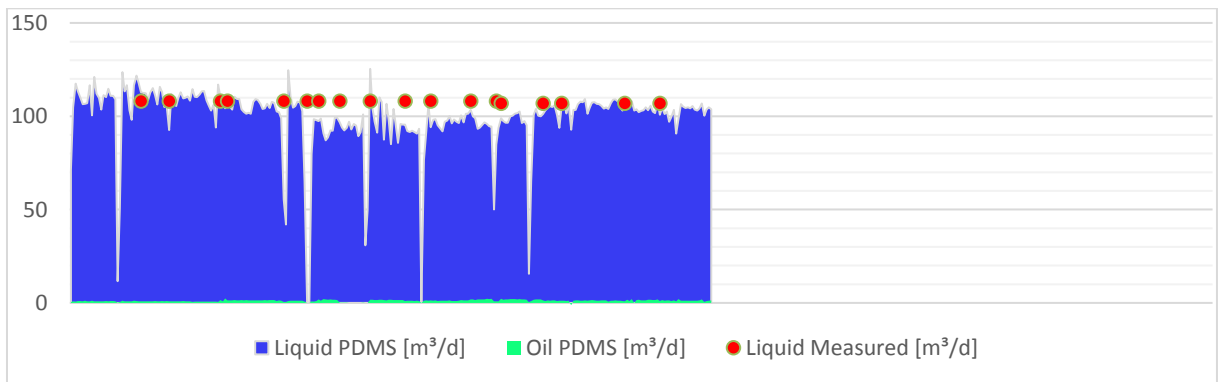
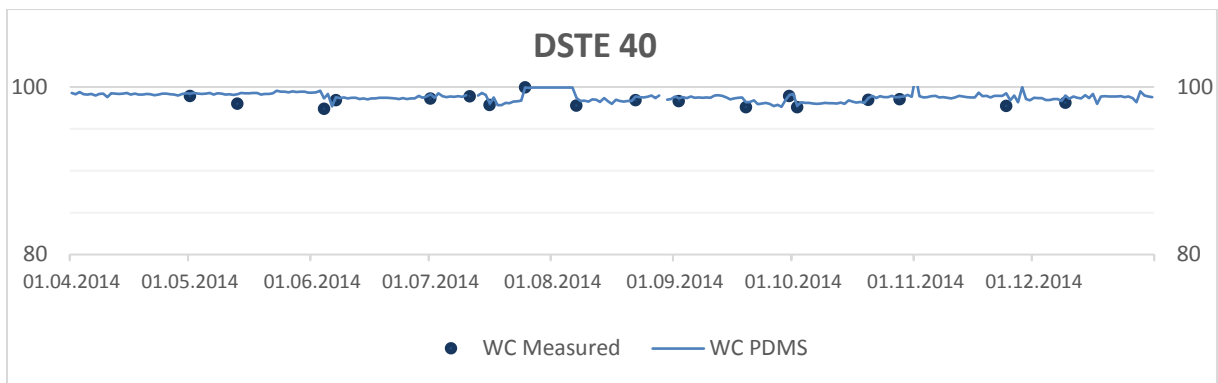
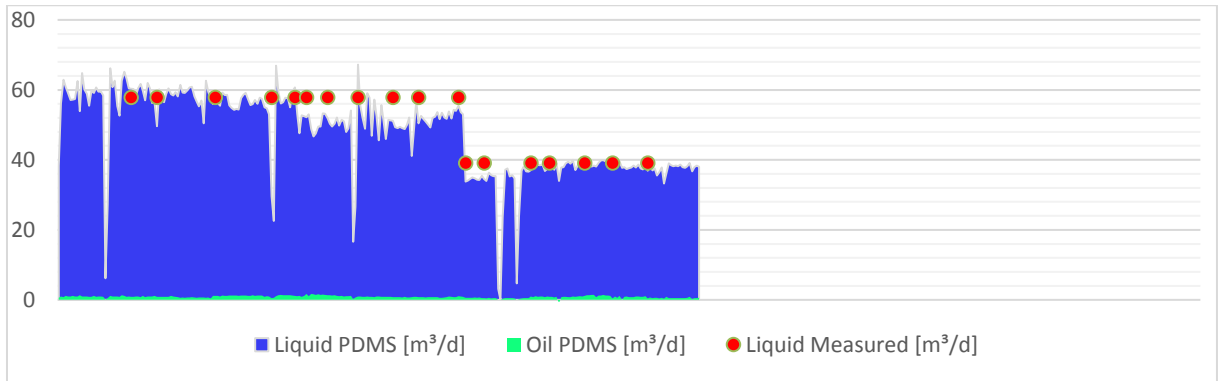
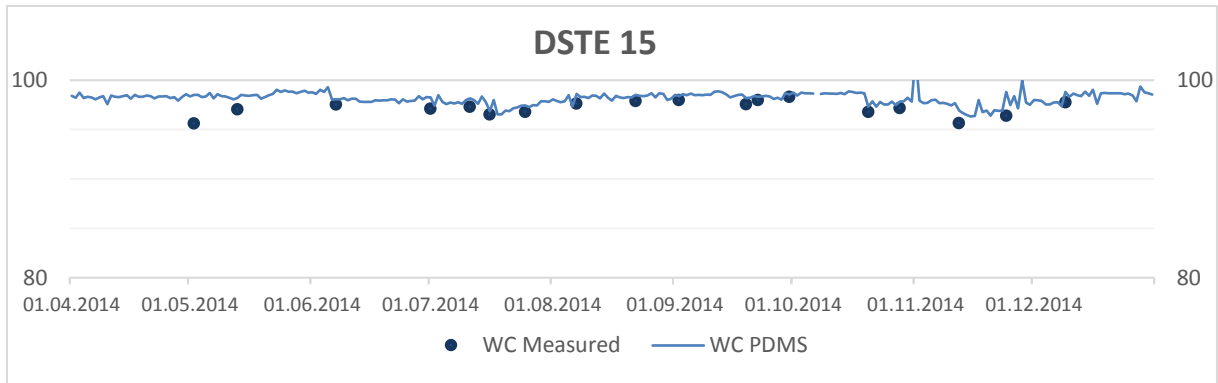
$$\frac{\sum Q_o}{OIP} \cdot (1 - S_{wc}) = \bar{S}_w(t) - S_{wc}$$

Further rearranging the equation finally leads to

$$\bar{S}_w(t) = S_{wc} + (1 - S_{wc}) \cdot \frac{\sum Q_o}{OIP}$$

31 Appendix E





32 Appendix F

This shows the VBA code for the Microsoft Excel to GAP connection and output. The first module describes the parameter updating for the injection as well as production system and the latter module illustrates the code for the parameter output for the verification runs. Both modules are for structural purposes separated into 'Subs', whereas the first and second 'Sub' in each module is almost the same. The first Sub DoAll() gives the trigger to run all other Subs and the second Sub Initialise() is necessary to build the connection between Microsoft Excel and the correct GAP file. All further Subs mainly consist of loops and IPM OpenServer statements to transfer data.

32.1 Module for Pipeline Parameter Update

```
Option Explicit
```

```
Dim Server As Object
```

```
Sub DoAll()
```

```
    Initialise
```

```
    PipelineProperties_Aldorf
```

```
    PipelineProperties_Bockstedt
```

```
    PipelineProperties_Dueste
```

```
End Sub
```

```
Sub Initialise()
```

```
    Set Server = CreateObject("PX32.OpenServer.1")
```

```
    DoCmd "GAP.Start()"
```

```
    DoCmd "GAP.Openfile(""" + Application.Worksheets("Overview").Range("B2") + """)"
```

```
    Set Server = Nothing
```

```
End Sub
```

```
Sub PipelineProperties_Aldorf()
```

```
    Set Server = CreateObject("PX32.OpenServer.1")
```

```
    Dim pipelineLabel, cLength, cID, cTVD, cRoughness As String
```

```
    Dim row As Integer
```

```
    row = 2
```

```
    Do
```

```
        pipelineLabel = Range("B" + CStr(row))
```

```
        DoSet "GAP.MOD[{{PROD}}].PIPE[{" + pipelineLabel + "}.Desc[1].Length", Application.Worksheets("Pipelines_Production").Range("C" + CStr(row))
```

```
        DoSet "GAP.MOD[{{PROD}}].PIPE[{" + pipelineLabel + "}.Desc[1].TVD", Application.Worksheets("Pipelines_Production").Range("D" + CStr(row))
```

```

    DoSet "GAP.MOD[{{PROD}}].PIPE[{" + pipelineLabel + "}.Desc[0].TVD", Application.Work-
sheets("Pipelines_Production").Range("D" + CStr(row))
    DoSet "GAP.MOD[{{PROD}}].PIPE[{" + pipelineLabel + "}.Desc[1].ID", Application.Work-
sheets("Pipelines_Production").Range("E" + CStr(row))
    DoSet "GAP.MOD[{{PROD}}].PIPE[{" + pipelineLabel + "}.Desc[1].Roughness", Applica-
tion.Worksheets("Pipelines_Production").Range("F" + CStr(row))

    row = row + 1

    Loop Until row = 21
End Sub

```

```

Sub PipelineProperties_Bockstedt()
    Set Server = CreateObject("PX32.OpenServer.1")
    Dim pipelineLabel, cLength, cID, cTVD, cRoughness As String
    Dim row As Integer

    row = 21

    Do

        pipelineLabel = Range("B" + CStr(row))

        DoSet "GAP.MOD[{{PROD}}].PIPE[{" + pipelineLabel + "}.Desc[1].Length", Application.Work-
sheets("Pipelines_Production").Range("C" + CStr(row))
        DoSet "GAP.MOD[{{PROD}}].PIPE[{" + pipelineLabel + "}.Desc[1].TVD", Application.Work-
sheets("Pipelines_Production").Range("D" + CStr(row))
        DoSet "GAP.MOD[{{PROD}}].PIPE[{" + pipelineLabel + "}.Desc[0].TVD", Application.Work-
sheets("Pipelines_Production").Range("D" + CStr(row))
        DoSet "GAP.MOD[{{PROD}}].PIPE[{" + pipelineLabel + "}.Desc[1].ID", Application.Work-
sheets("Pipelines_Production").Range("E" + CStr(row))
        DoSet "GAP.MOD[{{PROD}}].PIPE[{" + pipelineLabel + "}.Desc[1].Roughness", Applica-
tion.Worksheets("Pipelines_Production").Range("F" + CStr(row))

        row = row + 1

        Loop Until row = 45
End Sub

```

```

Sub PipelineProperties_Dueste()
    Set Server = CreateObject("PX32.OpenServer.1")
    Dim pipelineLabel, cLength, cID, cTVD, cRoughness As String

```

```

Dim row As Integer

row = 45

Do

pipelineLabel = Range("B" + CStr(row))

DoSet "GAP.MOD[{{PROD}}].PIPE[{" + pipelineLabel + "}.Desc[1].Length", Application.Work-
sheets("Pipelines_Production").Range("C" + CStr(row))
DoSet "GAP.MOD[{{PROD}}].PIPE[{" + pipelineLabel + "}.Desc[1].TVD", Application.Work-
sheets("Pipelines_Production").Range("D" + CStr(row))
DoSet "GAP.MOD[{{PROD}}].PIPE[{" + pipelineLabel + "}.Desc[0].TVD", Application.Work-
sheets("Pipelines_Production").Range("D" + CStr(row))
DoSet "GAP.MOD[{{PROD}}].PIPE[{" + pipelineLabel + "}.Desc[1].ID", Application.Work-
sheets("Pipelines_Production").Range("E" + CStr(row))
DoSet "GAP.MOD[{{PROD}}].PIPE[{" + pipelineLabel + "}.Desc[1].Roughness", Applica-
tion.Worksheets("Pipelines_Production").Range("F" + CStr(row))

row = row + 1

Loop Until row = 71
End Sub

```

32.2 Module for Full Field Validation Run Output

```

Option Explicit
Dim Server As Object

```

```

Sub DoAll()
    Initialise
    Pumps
End Sub

```

```

Sub Initialise()
    Set Server = CreateObject("PX32.OpenServer.1")
    DoCmd "GAP.Start()"
    DoCmd "GAP.Openfile( "" + Application.Worksheets("Overview").Range("B2") + "" )"
    Set Server = Nothing
End Sub

```

```

Sub Pumps()

```

```

Set Server = CreateObject("PX32.OpenServer.1")
Dim pumpLabel, datumende As String
Dim row As Integer

row = 4

Range("A1") = DoGet("GAP.PREDINFO.END.DATESTR")
datumende = DoGet("GAP.PREDINFO.END.DATESTR")

Do
pumpLabel = Cells(row, 2)
If DoGet("GAP.MOD[{PROD}].WELL[{ " + pumpLabel + " }].ISDISABLED") = 1 Then
Cells(row, 9) = "YES"
Else
Application.Worksheets("Validation_Production").Cells(row, 3) = Do-
Get("GAP.MOD[{PROD}].WELL[{ " + pumpLabel + " }].PREDRES[{31.12.2015}].RESPRES")
'Reservoir Pressure
Application.Worksheets("Validation_Production").Cells(row, 4) = Do-
Get("GAP.MOD[{PROD}].WELL[{ " + pumpLabel + " }].PREDRES[{31.12.2015}].LIQRATE")
'Liquid rate
Application.Worksheets("Validation_Production").Cells(row, 5) = Do-
Get("GAP.MOD[{PROD}].WELL[{ " + pumpLabel + " }].PREDRES[{31.12.2015}].OILRATE")
'Oil rate
Application.Worksheets("Validation_Production").Cells(row, 6) = Do-
Get("GAP.MOD[{PROD}].WELL[{ " + pumpLabel + " }].PREDRES[{31.12.2015}].WCT")      'Wa-
ter cut
Application.Worksheets("Validation_Production").Cells(row, 7) = Do-
Get("GAP.MOD[{PROD}].WELL[{ " + pumpLabel + " }].PREDRES[{31.12.2015}].WATRATE")
'Water rate
Application.Worksheets("Validation_Production").Cells(row, 8) = Do-
Get("GAP.MOD[{PROD}].WELL[{ " + pumpLabel + " }].PREDRES[{31.12.2015}].GOR")      'Gas
oil ratio
End If

row = row + 1

Loop Until Cells(row, 2) = ""
End Sub

```